# Journal of Architectural Research and Development



BIO-BYWORD SCIENTIFIC PUBLISHING PTY LTD
(619 649 400)
Level 10
50 Clarence Street
SYDNEY NSW 2000


BIO-BYWORD
SCIENTIFIC PUBLISHING PTY LTD

ISSN (ONLINE): 2208-3537
ISSN (PRINT): 2208-3529

# Journal of Architectural Research and Development

## Focus and Scope

*Journal of Architectural Research and Development* is an international peer-reviewed and open access journal which is devoted to establishing a bridge between theory and practice in the fields of architectural and design research, urban planning and built environment research.

Topics covered but not limited to:

- Architectural design
- Architectural technology, including new technologies and energy saving technologies
- Architectural practice
- Urban planning
- Impacts of architecture on environment

## About Publisher

Bio-Byword Scientific Publishing is a fast-growing, peer-reviewed and open access journal publisher, which is located in Sydney, Australia. As a dependable and credible corporation, it promotes and serves a broad range of subject areas for the benefit of humanity. By informing and educating a global community of scholars, practitioners, researchers and students, it endeavors to be the world's leading independent academic and professional publisher. To realize it, it keeps creative and innovative to meet the range of the authors' needs and publish the best of their work.

By cooperating with University of Sydney, University of New South Wales and other world-famous universities, Bio-Byword Scientific Publishing has established a huge publishing system based on hundreds of academic programs, and with a variety of journals in the subjects of medicine, construction, education and electronics.

## Publisher Headquarter

BIO-BYWORD SCIENTIFIC PUBLISHING PTY LTD
Level 10
50 Clarence Street
Sydney NSW 2000
Website: www.bbwpublisher.com
Email: info@bbwpublisher.com

2025, Volume 9, Issue 1

# Table of Contents

Journal of Architectural Research and Development, 2025, Volume 9, Issue 1
https://ojs.bbwpublisher.com/index.php/JARD
Online ISSN: 2208-3537
Print ISSN: 2208-3529

# Analysis of Reinforcement Techniques for Newly Built Tunnel Defects

**Yike Wei***

China Merchants Chongqing Highway Engineering Testing Center Co., Ltd., Chongqing 400067, China

***Corresponding author:** Yike Wei, 258522747@qq.com



**Abstract:** Newly built tunnels often encounter a series of defects within the first few years of operation. If not promptly addressed and reinforced, these defects threaten the tunnel's durability and stability and bring severe challenges to its safe operation. This study aims to explore reinforcement techniques for addressing defects in newly built tunnels. The research begins with an analysis of common defects found in newly built tunnels, followed by a case study of the Jinfeng Tunnel in Chongqing, examining the post-construction defects. The actual reinforcement strategies and methods employed for the tunnel are then discussed. Finally, based on the research findings, this study provides insights and references for tunnel operation and construction units in China, aiming to enhance the overall quality of tunnel engineering in the country, align with sustainable development goals, and promote further improvements at a macro level.

**Keywords:** Newly built tunnels; Defect treatment and reinforcement; Initial support deformation; Lining cracking

**Online publication:** February 10, 2025

## 1. Introduction

Reinforcement and treatment of defects in newly built tunnels are crucial for their long-term safety and stable operation. Effective reinforcement measures can maintain the stability and safety of the tunnel structure, preventing major accidents caused by the long-term accumulation of defects and irreversible damage to the tunnel structure. Furthermore, timely reinforcement and repair of newly built tunnels are important means to ensure their service life, improve durability, and reduce high costs caused by frequent maintenance in the later stages. Additionally, prompt treatment and reinforcement of defects in newly built tunnels can significantly enhance the comfort and sense of security for tunnel users, creating the first line of defense for the long-term sustainable operation of tunnels.

## 2. Analysis of common defects in newly built tunnels

### 2.1. Support deformation

Support deformation is a common defect in newly built tunnels. The fundamental mechanisms leading to this defect include changes in geological pressure, rock layer movement, or deviations during the construction phase. Once support deformation occurs in a newly built tunnel, it may cause the tunnel section to narrow, posing safety hazards to normal vehicle traffic and increasing stress concentration, which has a certain probability of triggering more severe structural problems.

### 2.2. Lining erosion and degradation

Lining erosion and degradation in newly built tunnels are usually caused by chemical erosion from groundwater, climatic factors, or inadequate material quality. Chemical erosion can significantly weaken the strength and durability of the tunnel lining, while the freeze-thaw cycles in winter can accelerate the process of deterioration. As time passes, changes in the physical and chemical properties of the lining material may damage the structural integrity.

### 2.3. Spalling and chipping

The causes of lining spalling and chipping in tunnels typically include material degradation, structural stress concentration, or defects left during the construction phase. Once the lining area is subjected to environmental changes or vibrations caused by frequent vehicle traffic, it is prone to small chipping or even large-scale spalling. This type of defect not only causes damage to the lining itself but also poses a safety threat to vehicles and pedestrians passing through the tunnel.

### 2.4. Structural cracking

Structural cracking in newly built tunnels is often caused by stress concentration, load fluctuations, or uneven foundation settlement. On the one hand, structural cracking can damage the integrity of the tunnel structure. On the other hand, the cracks formed by cracking provide channels for water and aggressive substances around the tunnel to invade, thereby accelerating the aging of the lining.

### 2.5. Water leakage

Water leakage, as a major defect in the field of tunnel engineering, is mostly caused by the failure of the waterproofing system, changes in groundwater levels, or structural cracking. Water leakage not only erodes the internal structure of the tunnel lining, causing a decrease in material strength but may also lead to foundation softening, resulting in uneven settlement and lining spalling. If water leakage persists, it will exacerbate defects in other structures over time, threatening the overall safe operation of the tunnel [1].

## 3. Project overview

To objectively understand the strategies for reinforcing and treating defects in newly built tunnels, this article takes the Jinfeng Tunnel in Chongqing, which was officially opened to the public in 2024, as an example. The Jinfeng Tunnel starts at Daishan Avenue in Bishan District and ends at Gaoxin Avenue in the High-tech Zone, with a total length of 9.20 km. It includes four casing interchanges, one tunnel, and comprehensive pipeline network ancillary projects. In 2018, the feasibility study report for the Jinfeng Tunnel was approved by the National Development and Reform Commission, and construction officially began on December 29, 2019. In September 2022, the Jinfeng Tunnel entered the construction scope of the ramp for the beltway. In May 2023, the main structure of the tunnel was completed, and in April 2024, the Jinfeng Tunnel was officially opened to the public. The designed speed of the Jinfeng Tunnel is 60 km/h, with a two-way six-lane design, and the total project investment is 5,170,368,500 yuan [2].

## 4. Analysis of project defects

### 4.1. Initial support deformation

The starting point of the Jinfeng Tunnel is located in a landslide group area. After completion of construction, before opening to the public, in October 2023, under the influence of a series of natural factors such as continuous rainfall, displacement of the sliding surface and deformation of the front stage occurred. Cracking and deformation appeared on the back of the completed anti-slide piles. Subsequently, the cracks continued to develop backward, causing many cracks to appear on the slope. According to investigations, the initial support at the entrance section of the Jinfeng Tunnel from KL0+806 to KL0+860 is deformed and intrusive, with a maximum deformation of 28 cm invading into the secondary lining.

### 4.2. Concrete lining cracking

Besides the initial support deformation, under the influence of the landslide, the completed secondary lining exhibited varying degrees of cracking [3]. Specifically, the cracking range of the secondary lining in the left tunnel of the Jinfeng Tunnel reached 161 m in length. Some sections showed diagonal and circumferential cracks in the secondary lining, with crack lengths concentrated between 3 m and 6 m and widths typically ranging from 1 mm to 2 mm. The cracking range of the secondary lining in the right tunnel extended up to 215 m, and some sections presented a reticulated pattern of cracks (see **Figure 1**).

**Figure 1.** Reticulated cracks in the secondary lining

Meanwhile, upon observation, there is a noticeable problem of staggered platforms in the secondary lining. The maximum crack width in some tunnels can reach up to 18 mm, accompanied by a 12 mm wide transverse displacement of the staggered platforms. The cracks have penetrated the entire ring from the secondary lining to the inverted arch. As shown in **Figure 2**.

**Figure 2.** Secondary lining cracking in Jinfeng Tunnel

### 4.3. Water leakage

Along with the cracking of the secondary lining in both the left and right tunnels of the Jinfeng Tunnel, water leakage has occurred in some areas. The cracks in the secondary lining have directly allowed groundwater to enter the interior of the Jinfeng Tunnel through the lining, resulting in the formation of distinct leakage zones. As shown in **Figure 3**.

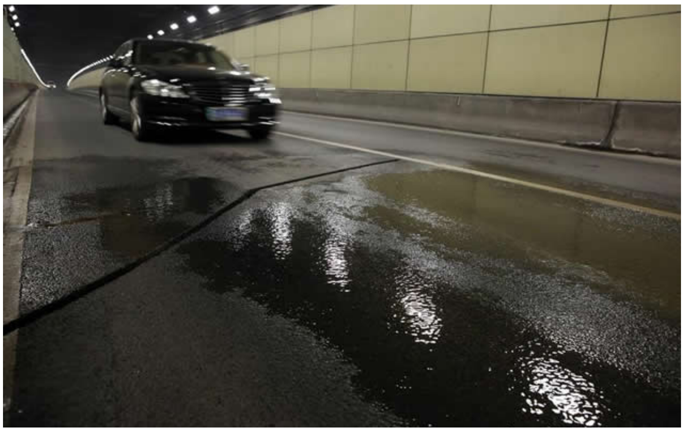

**Figure 3.** Water leakage in Jinfeng Tunnel. This defect not only causes erosion to the lining material, leading to a decrease in structural strength but also poses a threat to the overall stability of the Jinfeng Tunnel in the long run

## 5. Technical strategies for reinforcement and treatment of defects

### 5.1. Technical strategy for circular grouting reinforcement

#### 5.1.1. Technical solution

In response to the initial support deformation defect in the Jinfeng Tunnel, the project team, along with the construction unit, conducted a repair meeting analysis and decided to adopt a technical solution combining the addition of temporary arch supports with circular grouting reinforcement. Specifically, the length of the initial support arch was set to 6 m. After completing the arch construction, repair work on the secondary lining was carried out using 4φ25 steel bars, and the concrete grade was increased from C25 used in previous construction to C30. Circular grouting reinforcement is a construction technique that involves injecting grout around the perimeter of the initial support structure to form a continuous and dense grout ring, thereby enhancing the overall bearing capacity and stability of the support structure.

#### 5.1.2. Reinforcement construction treatment

The specific implementation strategy includes preliminary preparation, drilling, grouting, and inspection.

(1) Step 1: Preliminary preparation. In this phase, investigations and assessments of the defect problems are carried out to confirm the specific construction plan. The construction unit arranges technical personnel to conduct a detailed investigation and technical evaluation of the initial support deformation in the tunnel, covering the detection of deformation location, deformation range, and deformation degree. Simultaneously, a detailed analysis of the quality conditions of the Jinfeng Tunnel and the stress situation of the support is performed. Based on the investigation results, the grouting reinforcement scheme is confirmed, including the arrangement of grouting holes, grout materials, performance parameters, grouting volume, grouting pressure, and a series of other technical parameters. Finally, the construction unit confirms the construction plan, arranging grouting holes around the initial support structure circularly, with a main monitoring interval of 1.5 m, forming a circle of grouting hole networks.

Longitudinally, a row of grouting holes is arranged every 2 m, and the hole depth is designed to be 3.5 m. In terms of grouting methods, vertical drilling is adopted for shallow deformation areas, and inclined drilling (15° ~ 30°) is adopted for deeper areas to ensure a wider coverage of the grout. For cement grout, ordinary portland cement is used, configured into a cement slurry with a water-cement ratio of 0.5. Water-reducing agents and stabilizers are added to the cement slurry, and the initial grouting pressure is set at 0.3 MPa ~ 0.5 MPa, gradually increasing to 0.5 MPa ~ 1.0 MPa based on the specific diffusion of the slurry. For high-permeability areas, the grouting pressure is increased to 1.5 MPa.

(2) Step 2: Grouting drilling based on the design plan. During the operation phase, construction workers are required to strictly control the hole depth and angle. After completing the drilling, high-pressure air is used to clean the holes to ensure that there are no residuals inside [4].

(3) Step 3: Grouting. During the construction operation, high-pressure grouting equipment is used to inject the slurry into the drilled holes according to the preset grouting pressure. It is required to ensure that the slurry fully penetrates and fills the gaps and cracks in the support structure. Professional personnel are arranged to conduct real-time monitoring, strictly recording the grouting pressure, flow rate, and slurry consumption. The grouting strategy is flexibly adjusted based on the grouting effect. After completing the grouting, the grouting effect is inspected using geological radar to confirm that the support structure has been adequately reinforced [5].

## 5.2. Technical strategy for repairing lining cracks

### 5.2.1. Technical solution

In response to the cracking problems in the secondary lining of the left and right tunnels of the Jinfeng Tunnel, the project department and the construction unit have studied and decided to adopt steel strips combined with shotcrete reinforcement for cracks with a width of less than 5 mm in the plain concrete lining. During the construction, steel strips are arranged longitudinally along the outer edge of the lining contour, and C25 concrete is used as the spraying material. For cracks with a width greater than 5 mm and areas with dense networks of cracks in the secondary lining, a three-limb grating combined with shotcrete reinforcement is adopted. Grooves are cut into the original secondary lining surface, followed by the installation of three-limb gratings in a longitudinal direction and the application of 13 cm thick C25 concrete.

### 5.2.2. Repair and reinforcement construction

(1) Repair of cracks less than 5 mm: Repair of cracks less than 5 mm in the left and right tunnels of the Jinfeng Tunnel [6].

(i) Step 1: Preparation. Comprehensively clean the construction area to ensure that the surface is free of loose materials, impurities, and harmful substances, providing a good bonding interface for the repair work.

(ii) Step 2: Arrange steel strips. Construction workers are arranged to place W280 steel strips along the longitudinal contour of the lining, with a longitudinal spacing accurately controlled at 0.8 m. Before construction, measurements are taken to confirm the positions of the steel strips and mark them to ensure accurate placement.

(iii) Step 3: Shotcrete construction. C25 concrete is used for spraying and reinforcement. During construction, strict control of the concrete spraying thickness is required to ensure that it meets the structural strength and durability requirements. Workers are instructed to pay close attention to the uniformity and surface flatness of the concrete during the spraying operation, minimizing unevenness and irregularities on the structural surface. After completing the construction, necessary curing measures are strictly implemented to ensure complete solidification of the concrete and maximize its performance [7].

(2) Repair of cracks greater than 5 mm: Repair construction is organized for cracks greater than 5 mm in the secondary lining of the left and right tunnels of the Jinfeng Tunnel.

(i) Step 1: Surface treatment. Construction workers are arranged to chisel grooves on the surface of the secondary lining, with the width and depth of the grooves flexibly adjusted based on the specific conditions of the cracks, to ensure the smooth embedding of the three-limb grid [8].

(ii) Step 2: Installation of the three-limb grid. The three-limb grid is arranged longitudinally along the cracks, with strict control of the longitudinal spacing at 1.0 m. During installation, it is necessary to ensure that the grid fits tightly with the chiseled groove and is fixed securely. After installation, steel mesh is hung, ensuring that the steel bars are tightly bonded to the grid.

(iii) Step 3: Concrete spraying. C25 concrete is used for basin concrete spraying, with strict control of the thickness at 13 cm. During the spraying operation, construction workers are required to pay strict attention to the uniformity of concrete distribution, and no pores or weakened areas should appear. After spraying, technical personnel are arranged to carry out concrete curing strictly following standards.

(3) Technical strategy for groove cutting and pipe burying: Technical plan to address the leakage problem caused by cracks in the secondary lining of the Jinfeng Tunnel. For areas where the water leakage is only at the water outlet point, construction workers are arranged to clean up the concrete around the water outlet, then chisel a groove (length × width × depth = 50 mm × 50 mm × 40 mm) at the water outlet point, and finally use instant leakage stopper to block the water outlet. For areas with severe water leakage, pipe-burying technology is adopted to divert groundwater to the side of the ditch.

(4) Reinforcement construction for treatment during the repair phase of water leakage areas.

(i) Step 1: Preparation. Construction workers are arranged to carefully clean the concrete surface around the water outlet, and then chisel a square groove of 50 mm × 50 mm × 40 mm as a space to accommodate the sealing material, ensuring that the material can fully block the leakage point. After grooving, the sealing material is selected and quickly filled into the groove. Because the material hardens very quickly, the filling operation needs to be completed rapidly. After filling, the leakage-stopping material is compacted to ensure it has a good sealing effect [9].

(5) For areas with severe leakage, pipe-burying technology is adopted to solve the leakage problem in the form of drainage.

(i) Step 1: Preparation. Before construction, a comprehensive analysis of the source of leakage is conducted to determine the path and pressure conditions of the water flow, facilitating reasonable design of the drainage pipe network layout.

(ii) Step 2: Confirm technical parameters. Based on the investigation results, the number and location of pipes to be buried at each leakage point are determined.

(iii) Step 3: Bury the drainage pipes. The leaking water in the cracks is drained to the side of the tunnel ditch. This process requires ensuring the tightness of pipe connections and the smoothness of drainage. Concurrently, a collection and drainage system is built on the side of the ditch to properly dispose of the discharged water and prevent it from reverse infiltration or penetration into other structures, causing impact.

(iv) Step 4: Inspection. After the completion of pipe installation, a systematic water flow test is conducted to confirm the effectiveness and reliability of the drainage system. Additionally, the operating unit needs to regularly inspect and maintain the drainage system to ensure its long-term normal operation [10].

## 6. Conclusion

In summary, this article takes the newly built tunnel, the Jinfeng Tunnel in Chongqing as an example to analyze the diseases that occurred after the tunnel was completed, including initial support deformation, secondary lining cracking, and water leakage problems. Subsequently, the construction unit's treatment and reinforcement plans and construction processes for various issues of the Jinfeng Tunnel are discussed in detail. Tunnel operation and construction units in China can learn from the practical construction methods of the Jinfeng Tunnel discussed in this article to effectively control the further deterioration of newly built tunnel issues. This can create the first line of defense for the long-term safe and stable operation of newly built tunnels, protecting the lives and property safety of tunnel users while improving the comfort of tunnel traffic.

## Disclosure statement

The author declares no conflict of interest.

## References


[1] Liu F, 2023, Finite Element Analysis of Highway Tunnel Disease Treatment and Steel Strip Reinforcement Technology. Engineering Construction and Design, 2023(1): 96–98.

[2] Yuan H, 2022, Study on the Mechanism of Water Leakage Disease in Tunnel Secondary Lining and Reinforcement Treatment Technology. Heilongjiang Transportation Science and Technology, 45(8): 118–121.

[3] Xiao C, Jia Y, Li K, et al., 2022, Research on Comprehensive Treatment Technology for Leakage Diseases in Active Tunnels—Taking Corrugated Steel Lining Reinforcement as an Example. Sichuan Building Materials, 48(9): 154–156.

[4] Wang Y, 2024, Design of Disease Treatment for the Civil Engineering Structure of Huilongwan Tunnel. Science and Technology Information, 22(16): 235–238, 243.

[5] Zhang C, Wu H, 2024, Analysis and Treatment Scheme of Highway Tunnel Lining Diseases. Anhui Architecture, 31(2): 150–153.

[6] Cao Y, 2024, Analysis of Highway Tunnel Disease Detection and Treatment Technology. Sichuan Building Materials, 50(7): 172–174.

[7] Deng J, Chen R, Yan D, 2024, Reinforcement Technology for Cracking of Side and Upslope at the Entrance Section of Shallow-buried and Unbalanced Tunnel. Western China Communication Science and Technology, 2024(5): 101–102.

[8] Yang Z, Xu Y, Wang X, et al., 2024, Discussion on the Treatment Construction of Cracking Diseases in the Middle Wall of Thin-walled Arch Tunnels. China Highway, 657(5): 118–120.

[9] Liu P, 2023, Research on New Temporary Support Technology for the Treatment of Inverted Arch Diseases in Tunnel Construction in Complex Geological Environments. Shandong Transportation Science and Technology, 2023(4): 100–104.

[10] Zhang L, Weng X, Xiong X, et al., 2022, Evaluation Analysis and Treatment Technology of Secondary Lining Diseases in Tunnel Entrance Section. Journal of Shandong Jiaotong University, 30(2): 72–80.

Journal of Architectural Research and Development, 2025, Volume 9, Issue 1
https://ojs.bbwpublisher.com/index.php/JARD
Online ISSN: 2208-3537
Print ISSN: 2208-3529

# Research on the Performance and Diffusion Behavior of Geopolymer Grouting Material Made from Coal Roof Bottom Ash

**Xinxin Yu*, Haibo Zhang, Yu Liu, Fengshun Zhang**

School of Materials Science and Engineering, Henan Polytechnic University, Jiaozuo 454003, China

***Corresponding author:*** Xinxin Yu, yxyyds68@163.com



**Abstract:** As the cost of grouting treatment for water control in coal roofs during underground coal mining continues to rise, coupled with the accumulation of industrial solid waste resulting from rapid economic development in China, the ecological environment is facing severe challenges. To address these issues, this study, based on a high water-to-cement ratio, uses mine overburden (OB) and furnace bottom ash (FBA) as the primary raw materials, with sodium silicate as the modifier, to develop a new type of geopolymer grouting material with high stability and compressive strength for coal roof water control. Additionally, COMSOL software was used to numerically simulate the diffusion process of the grout slurry in fractures under dynamic water flow. The results indicate that, with a sodium silicate modulus of 1.5 and a dosage of 4%, the stability of the slurry increased by 26.2%, and the 28-day compressive strength improved by 130.98%. Numerical simulations further show that the diffusion process of the slurry is closely related to slurry viscosity, grouting pressure, and grouting time and that the diffusion pattern in the fractures is similar to that of ultra-fine cement slurry. This study provides a theoretical basis for coal mine roof grouting water control projects.

**Keywords:** Coal mine top grouting; Regional management; Numerical simulation; Comprehensive utilization; Solid waste

**Online publication:** February 10, 2025

## 1. Introduction

In underground engineering and mining, fissure water entering the excavation zone through rock pores and faults presents significant safety hazards. With the increase in excavation depth, water leakage from the coal seam roof not only corrodes equipment but also potentially causes harm to personnel [1–3]. Ground grouting technology (as shown in **Figure 1**) has become a critical method for controlling water leakage from the coal seam roof [4,5]. The performance of grouting materials directly impacts the quality of the grouting effect and the longevity of the project. Currently, there is a wide variety of grouting materials for the coal seam roof, with traditional materials such as cement grout and chemical grouts having good slurry properties, but they are expensive and have significant environmental impacts [6–8]. According to incomplete statistics, the cement used in grouting releases approximately 4 × $10^4$ tons of carbon dioxide ($CO_2$) annually [9]. Therefore, reducing the demand for cement in grouting material production and using solid waste to replace cement in large quantities is of great significance for achieving the "peak carbon emissions by 2023, carbon neutrality by 2060" goals [10,11].

Currently, solid waste grouting materials mainly include slag, fly ash, or combinations of both. Yang et al. studied the properties of composite grouting materials based on cement, fly ash, and slag [12]. Wang et al. developed a mortar using blast furnace slag for roadbed reinforcement, aiming to optimize the material's rheological properties and mechanical strength [13]. Li et al. explored the application of new calcium-based activators in coal bottom ash-based cementitious materials through orthogonal tests and range analysis [14]. Bakhrakh et al. used coal ash and furnace slag as cement additives to increase the calcium, silicate, hydrate (C-S-H) gel content and the cement's hydration degree [15]. Fernandez et al. pointed out that the activity of fly ash is influenced by its silica and alumina content, exhibiting high late strength in geopolymers [16].

However, existing research mostly focuses on improving a single property of the grout slurry under low water-to-cement ratios. However, applying solid waste in grouting water control requires a comprehensive evaluation of multiple properties of the slurry, including fluidity, stability, and compressive strength. Furthermore, the feasibility of using new materials in practical applications should be further investigated.

Mine overburden (OB) is the waste generated during coal mining, mainly consisting of useless minerals and rock fragments [17]. Furnace bottom ash (FBA), a common industrial by-product, contains a certain amount of silicate and aluminate components [18]. Incorporating OB into furnace bottom ash geopolymer not only facilitates the resource utilization of mine waste, reducing its environmental pollution and accumulation pressure but also provides new raw materials for construction [19,20].

Based on the aforementioned background, this study, after extensive preliminary experiments, selected FBA, desulfurization gypsum (DSG), ordinary portland cement (OPC), and OB as the base materials. The research, under the premise of a high water-to-cement ratio, aims to improve the stability and compressive strength of the slurry and to develop a new type of grouting material with high stability and strength using solid waste resources. Finally, the diffusion characteristics of the new grouting material were simulated and evaluated using COMSOL numerical simulation software, providing a reference for the practical application of geopolymer grouting materials in coal mine roofs.

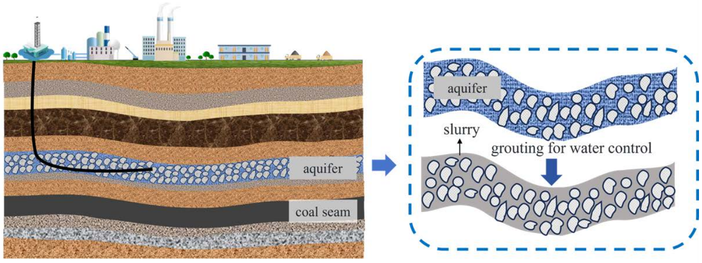


**Figure 1.** Schematic diagram of water control in the ground area

## 2. Experiment

### 2.1. Experimental materials

The FBA, DSG, and OPC used in the experiment were provided by Jiaozuo Qianye Cement Co., Ltd. The chemical composition of the main raw materials, FBA and OB, is shown in **Table 1**. OB was sourced from a mining area in Jiulishan, Jiaozuo City, naturally air-dried in its original state, and then ball-milled, with a specific surface area of 3261 $m^2$/kg. The calcium carbonate ($CaCO_3$) in OB mainly exists in the form of a calcite mineral structure, which exhibits water absorption, water retention, and slight expansion properties. These characteristics help reduce the shrinkage of the stone body and improve overall moisture retention [21].

**Table 1.** Chemical composition of **FBA** and OB (%)

| Component | CaO | $SiO_2$ | $Al_2O_3$ | MgO | $Fe_2O_3$ | $K_2O$ | $P_2O_5$ | Burning loss |
|---|---|---|---|---|---|---|---|---|
| FBA | 12.24 | 48.30 | 21.54 | 0.87 | 4.76 | 2.44 | 0.12 | 1.41 |
| OB | 46.18 | 28.16 | 10.72 | 7.85 | 3.56 | 2.58 | 0.52 | 5.36 |

Note: calcium oxide (CaO), silicon dioxide ($SiO_2$), aluminum oxide ($Al_2O_3$), magnesium oxide (MgO), iron oxide ($Fe_2O_3$), potassium oxide ($K_2O$), potassium pentoxide ($P_2O_5$)

## 2.2. Test and method

### 2.2.1. Experimental plan

Different amounts of sodium hydroxide (NaOH) solid were added to the sodium silicate solution to prepare sodium silicate with varying moduli. Through extensive preliminary experiments, it was determined that the geopolymer base was FBA: DSG: OPC: OB in a ratio of 45:2:3:50. For the stability test, a water-to-cement ratio of 1.8 was used, with sodium silicate of different moduli (1.3, 1.5, 2.4, 3.2) and addition amounts (2%, 4%, 6%, 8%) incorporated. For the geopolymer grouting material, the compressive strength test was conducted with a water-to-cement ratio of 0.4, and the curing age was set to 28 days. Three parallel samples were prepared for each group to minimize experimental errors. The specific experimental plan is shown in **Table 2**.

**Table 2.** Test scheme

| Level | Modulus | Percentage (%) |
|---|---|---|
| 1 | 1.3 | 2 |
| 2 | | 4 |
| 3 | | 6 |
| 4 | | 8 |
| 5 | 1.5 | 2 |
| 6 | | 4 |
| 7 | | 6 |
| 8 | | 8 |
| 9 | 2.4 | 2 |
| 10 | | 4 |
| 11 | | 6 |
| 12 | | 8 |
| 13 | 3.2 | 2 |
| 14 | | 4 |
| 15 | | 6 |
| 16 | | 8 |

### 2.2.2. Testing methods

(1) Fluidity: The fluidity of the slurry was tested according to the Marsh funnel viscosity test method (SY/T 6864-2020, China).

(2) Determination of water precipitation rate: The test was conducted according to the calculation method for

the water separation rate of concrete admixtures (GB 8076-2008, China).

(3) Compressive strength: The compressive strength of the test specimens at 3 d, 7 d, and 28 d curing ages was tested according to the Cement Mortar Strength standard (GB/T17671-199, China) using a WHY-300/10 microcomputer-controlled pressure testing machine with a loading rate of 100 N/s.

(4) X-ray diffraction (XRD): X-ray diffraction analysis was performed using a Smart X X-ray diffractometer (Japan). The testing conditions were set to 45 kV voltage, 200 mA current, a scanning speed of 10°/min, and a scanning range of 5° to 70°.

(5) Scanning electron microscopy (SEM): The morphology of the hydration products was observed using a scanning electron microscope (SEM) from Zeiss (Germany), model Merlin Compact. The test specimens were cut and gold-coated before the SEM analysis.

# 3. Analysis of test results

## 3.1. Fluidity

The flowability of the geopolymer slurry under different modulus and dosages of sodium silicate shows varying trends, as illustrated in **Figure 2**. The flowability increases with the increase in the modulus of sodium silicate. This is primarily due to the higher sodium silicate modulus, which leads to a relatively higher content of sodium ($Na^+$) ions in the solution. A higher $Na^+$ concentration promotes the release of water from the geopolymer slurry, enhancing the interactions between water and other components. As a result, the friction and adhesion between the particles in the slurry are reduced, lowering the viscosity and improving the flowability of the slurry [22].

As shown in **Figure 2**, the outflow time of the slurry under different dosages of sodium silicate exhibits a pattern of initially decreasing and then increasing. When the dosage of sodium silicate reaches a certain level, the concentration of sodium silicate in the geopolymer slurry becomes too high, which may lead to the formation of excessive gel-like or over-hydrated products between the sodium silicate and FBA geopolymer particles. These gel-like substances and hydrated products significantly increase the viscosity of the slurry, resulting in reduced flowability.

Moreover, excessive sodium silicate may also lead to the over-adsorption of free water in the system, causing the structure of the slurry to become more compact. This further restricts its flowability, leading to an increase in outflow time. Therefore, the change in flowability shows a trend of initially decreasing and then increasing, which is closely related to the gelation and accumulation of hydrated products caused by the excessive dosage of sodium silicate.

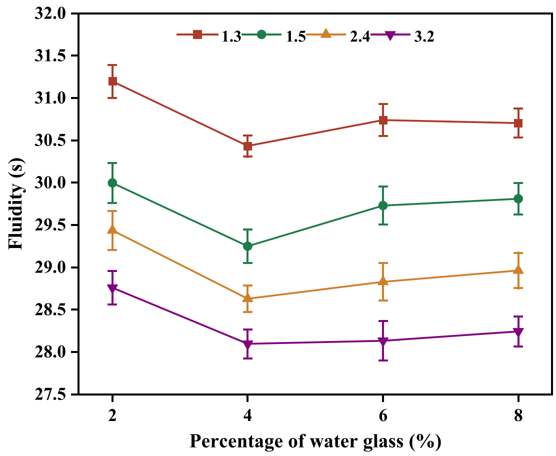


**Figure 2.** Influence of different sodium silicate modulus and dosage on slurry fluidity of geopolymer

### 3.2. Stability

The water separation rate of the geopolymer slurry under different sodium silicate moduli and dosages is shown in **Figure 3**. The stability of the geopolymer slurry changes with variations in the sodium silicate modulus and dosage. As illustrated in **Figure 3**, the water separation rate of the slurry with added sodium silicate is lower than that of the control group (12.05%), indicating an improvement in stability. The slurry's stability increases with a higher sodium silicate modulus. Specifically, within the modulus range of 1.5 to 2.4, the improvement in stability is more pronounced compared to the ranges of 1.3 to 1.5 and 2.4 to 3.2.

Under the same modulus, the water separation rate of the slurry first decreases and then increases as the sodium silicate dosage increases. For example, at a modulus of 1.5, as the dosage increases from 2% to 8%, the water separation rate of the slurry is 10.13%, 9.17%, 9.73%, and 9.88%, respectively. When the dosage exceeds 4%, the water separation rate rises significantly.

This behavior is due to the strong gelling properties of sodium silicate, which promote the formation of C-S-H or C-A-S-H gels in the geopolymer slurry. These hydration products help to form a more stable network structure, reducing the water separation rate and enhancing stability. However, excessive sodium silicate content may suppress the polymerization reaction, reducing the slurry's stability. Therefore, when preparing geopolymer grouting slurry, avoid excessive sodium silicate dosages that could adversely affect the slurry's stability[23].

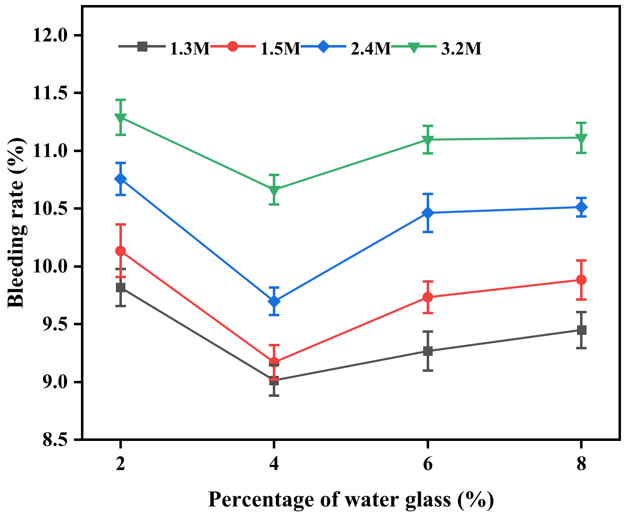


**Figure 3.** Influence of different sodium silicate modulus and dosage on the stability of geopolymer slurry

### 3.3. Compressive strength

The 28-day compressive strength of the geopolymer grouting material specimens with different sodium silicate moduli and dosages is shown in **Figure 4**. The compressive strength of the specimens at 28 days varies with different sodium silicate moduli and dosages. Under all sodium silicate moduli, the compressive strength of the geopolymer specimens is higher than that of the control group, which has a compressive strength of 3.27 MPa without sodium silicate. When the sodium silicate modulus is 1.3 and 1.5, the activation effect is more pronounced. At moduli of 2.4 and 3.2, the increase in compressive strength is relatively lower but still higher than that of the control group without sodium silicate.

At lower sodium silicate moduli, the concentration of silicate ions in the sodium silicate is higher, which can more effectively promote the reaction between the minerals in the mine tailings and the sodium silicate, generating more sulfoaluminate hydrate gels. This helps to enhance the compressive strength of the geopolymer. On the other hand, at higher moduli, the sodium silicate may produce fewer gels during hydration, leading to a less significant improvement in compressive strength compared to lower moduli.

Under the same sodium silicate modulus, when the dosage exceeds 4%, the compressive strength of the geopolymer material starts to decline. This indicates that increasing the sodium silicate dosage can improve the compressive strength within a certain range. An appropriate amount of sodium silicate promotes the formation of more hydration products and enhances the network structure of the geopolymer. However, when the dosage is too high, it may lead to excessive hydration, causing an overly high concentration of sodium silicate in the system. This could negatively affect the reaction uniformity, resulting in the formation of excess hydration products and pores, which may reduce the compressive strength. Therefore, in practical applications, the sodium silicate dosage needs to be optimized to enhance the strength while avoiding excessive reactions.

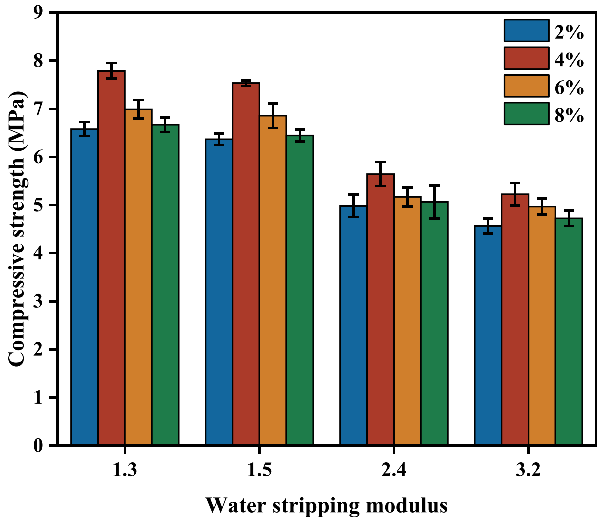


**Figure 4.** Influence of different sodium silicate modulus and dosage on 28 d compressive strength of geopolymer test block

In summary, the addition of water glass promotes the reaction between the mining waste and the components in the water glass, resulting in the formation of a denser hydration gel structure, thereby improving the stability and compressive strength of the furnace bottom ash geopolymer. The modulus and dosage of water glass are key factors influencing the enhancement of stability and strength. A moderate modulus and dosage can optimize the generation of hydration products, improving the stability and strength of the geopolymer material. Conversely, excessive dosage or an inappropriate modulus may lead to limited strength improvement or even a reduction in performance. Therefore, selecting the appropriate modulus and dosage of water glass is crucial to ensuring the performance of the geopolymer. Considering the flowability, stability, and compressive strength of the geopolymer grout material, as well as the economic cost, a water glass modulus of 1.5 and a dosage of 4% are determined for the furnace bottom ash geopolymer grout material.

## 3.4. Microscopic morphology

### 3.4.1. XRD analysis

XRD analysis was performed on geopolymer samples with the optimal water glass dosage and modulus, as well as representative samples without water glass after 28 d of curing (see **Figure 5**). The following conclusions can be drawn. After the optimal amount of water glass was added, the content of $CaCO_3$, $Al_2O_3$, and $SiO_2$ in the geopolymer decreased, while the C-A-S-H phase was generated. The XRD pattern indicates that the addition of water glass caused the dissolution of $Al_2O_3$ and $SiO_2$ in the alkaline environment, resulting in the formation of $SiO_4^{4-}$ and $AlO_4^{5-}$ ions. These ions are then combined with $Ca^{2+}$ ions in the reaction system to form C-S-H and C-A-

S-H gels. These gel substances interconnect and bond, forming a denser mesh structure that effectively increases the cohesion between soil particles, significantly enhancing the strength of the sample. Therefore, under the optimal water glass dosage, the compressive strength of the geopolymer is significantly higher than that of the sample without water glass. This result indicates that the addition of water glass can improve the hydration reaction of the geopolymer, promote the formation of favorable gel phases, and thereby enhance its mechanical properties.

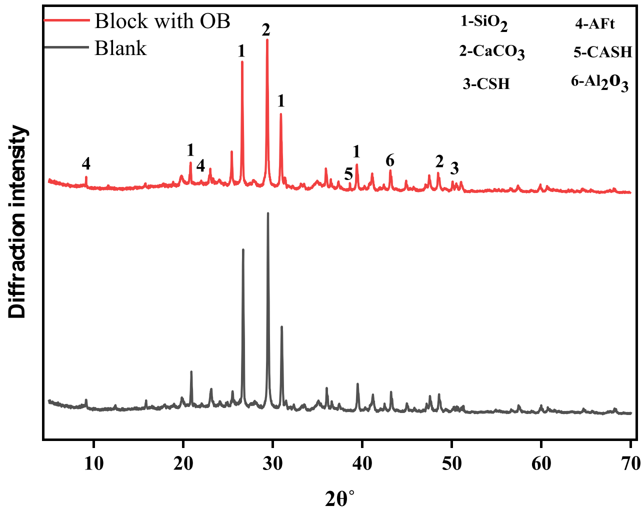


**Figure 5**. XRD spectra of optimum sodium silicate modulus and dosage and control group

### 3.4.2. SEM analysis

To investigate the effect of water glass on the internal microstructure of blast furnace slag-based geopolymer, SEM observations were conducted on samples cured for 28 d with and without water glass at the optimal dosage. Typical results are shown in **Figure 6**. As seen in **Figure 6**, it can be seen that the hydration products of the bottom ash geopolymer primarily consist of flaky and flocculent C-S-H gels, as well as needle-like ettringite. Compared to **Figure 6(a)**, the hydration products in **Figure 6(b)** have formed larger particle aggregates, which effectively fill the pores between the blast furnace slag and OB particles, as well as between particle clusters, forming a continuous structural network. This significantly improves the structure of the geopolymer, giving it a stacked and denser appearance [24]. Such structural changes greatly enhance the compressive strength of the blast furnace slag-based geopolymer.

The above changes indicate that sodium silicate, as an effective admixture, plays an important role in promoting the hydration reaction, improving the morphology of hydration products, and enhancing the mechanical properties of FBA-based geopolymers, thereby proving its key role in the application of geopolymers.

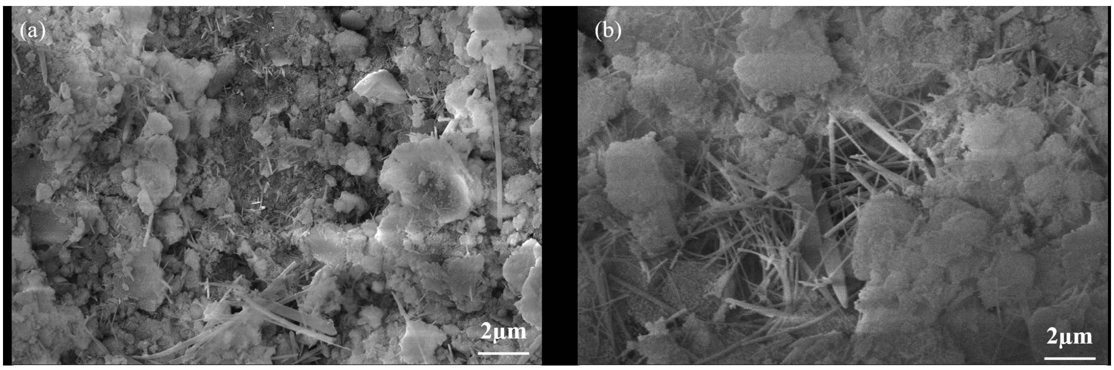


**Figure 6.** SEM comparison diagram: (a) control group, (b) optimal sodium silicate modulus and dosage

# 4. Crack diffusion simulation analysis

## 4.1. Governing equations

The diffusion of the slurry in the water-saturated fractures under dynamic water conditions conforms to the two-phase Darcy's law physical field in the Porous Media and Groundwater Flow module of COMSOL Multiphysics. Considering both water and slurry as incompressible, isotropic fluids, the generalized Darcy's law formula is as follows:

$$v = \frac{k}{\mu}\nabla p$$

$$v = s_o v$$

$$v = s_w v$$

$$s_o + s_w = 1$$

In the equations,  indicates the volume fraction of water within the fractures of the rock mass. The term refers to the seepage velocity field, whereas  and  represent the flow rates of the slurry and water, respectively. The parameter μ is the viscosity of the slurry. Additionally, k signifies the permeability of the medium, and p is the pressure within the seepage field.

## 4.2. Fracture model

The three-dimensional single-fracture grouting model and the corresponding mesh division results are shown in **Figure 7**. It is assumed that the boundaries of the model are the rock mass boundaries, and the simulation considers only the slurry diffusion part. The fracture model is set to 2 m × 1 m × 2 m, the diameter of the grouting pipe is 0.053 m, and its length is 0.5 m. The left boundary of the model is the water inflow, the right boundary is the outflow, and the remaining boundaries are set to no flow.

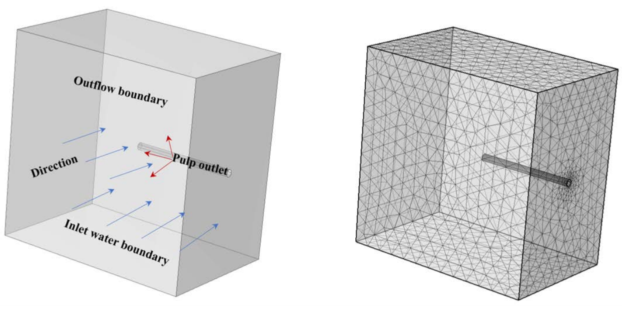


(a) grouting model (b) meshing

**Figure 7.** 3D single crack grouting model and mesh generation

To further investigate the performance of the furnace bottom ash geopolymers used as grouting materials, simulations were conducted using the research data of Zheng, which focused on ultra-fine cement slurry and slag-water glass as a control group for analysis [25]. The specific properties of the slurry are provided in **Table 3**. The rock mass has a porosity of 0.35 and a permeability of $1 \times 10^{-12}$ $m^2$. The applied dynamic water pressure is 2 MPa, while the initial pressure for the grouting is also set to 2 MPa.

**Table 3.** Parameters related to numerical simulation

| Fluids | Water | FBA solid waste slurry | Ultra-fine cement paste | Slag- water glass slurry |
|---|---|---|---|---|
| p (kg·m$^{-3}$) | 1,000 | 1,680 | 1,500 | 1,100 |
| μ (Pa·s) | 0.001 | 0.0378 | 0.012 | 0.003 |

## 4.3. Analysis of simulation results

### 4.3.1. Slurry volume fraction diffusion analysis

Taking a diffusion time of 5 seconds as an example, the volume fraction contour maps of different slurries are shown in **Figure 8**, and the volume fractions of the slurries at the same cross-section are shown in **Figure 9**. As seen in **Figure 9**, under dynamic water conditions, the volume fraction of the three slurries is significantly influenced by the direction of the water flow.

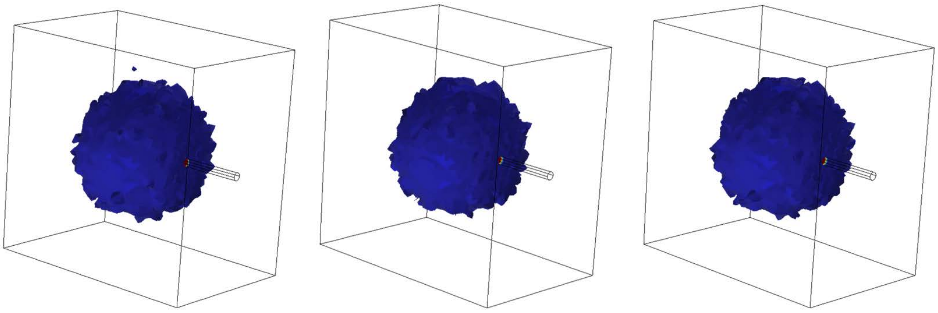

(a) superfine cement slurry (b) geopolymer slurry (c) slag-water glass slurry

**Figure 8.** Cloud image of volume fraction of different slurries

As shown in **Figure 9**, under dynamic water conditions, the slurry exhibits reverse diffusion, with the highest slurry concentration and volume fraction around the grouting pipe. The volume fraction and diffusion distance vary differently for each grouting material. Due to the higher density and viscosity of ultra-fine cement and geopolymer slurries compared to the slag-water glass slurry, the resistance during the diffusion process is greater, resulting in slower diffusion. Additionally, **Figure 8** and **Figure 9** show that the volume fraction and diffusion range of the geopolymer and ultra-fine cement slurries are similar, but the volume fraction of all three slurries does not increase with the expansion of the grouting diffusion range. This indicates that the viscosity of the slurry is non-linearly related to the grouting sealing effect, and the impact of dynamic water erosion on the grouting performance is significant.

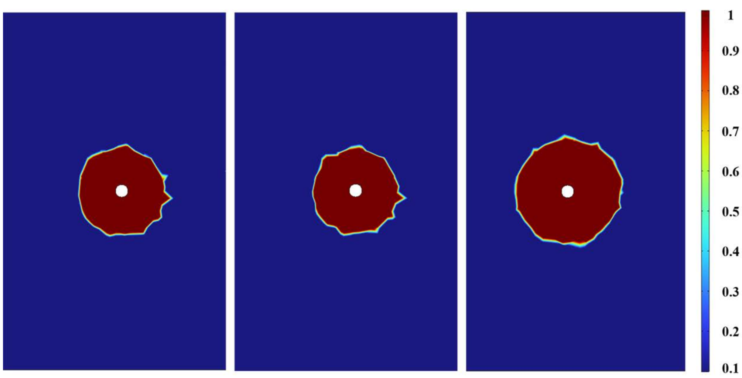


(a) Superfine cement slurry (b) terpolymer slurry (c) silica-sodium silicate slurry

**Figure 9.** Changes in volume fraction of different grout under dynamic water environment

### 4.3.2. Slurry diffusion distance analysis

**Figure 10** displays the forward and reverse diffusion distances of various grouting materials in dynamic water circumstances. The viscosity of the slurry increases with time, and the reverse diffusion resistance progressively increases as well, stabilizing at a constant diffusion distance, as can be seen by comparing the diffusion distances of various slurries in the dynamic water environment depicted in **Figure 10**. Under the effect of water flow, the slag-water glass slurry has the lowest viscosity and the highest diffusion distance, the ultrafine cement slurry comes second, and the geopolymer slurry has the smallest diffusion distance. Subsequent investigation shows that the slurry's viscosity and diffusion distance have a negative correlation, confirming that all three slurries display specific regularities during reverse flow diffusion. Diffusion distance is greater in the slurry with lower viscosity and vice versa.

The maximum diffusion distances of the geopolymer and ultrafine cement slurries were compared, and it was discovered that there is an 8.16% difference in the forward diffusion distance and a 2.38% difference in the reverse diffusion distance. This finding implies that geopolymer slurry can partially substitute ultrafine cement grout components, lowering expenses without sacrificing grouting reinforcing efficacy.

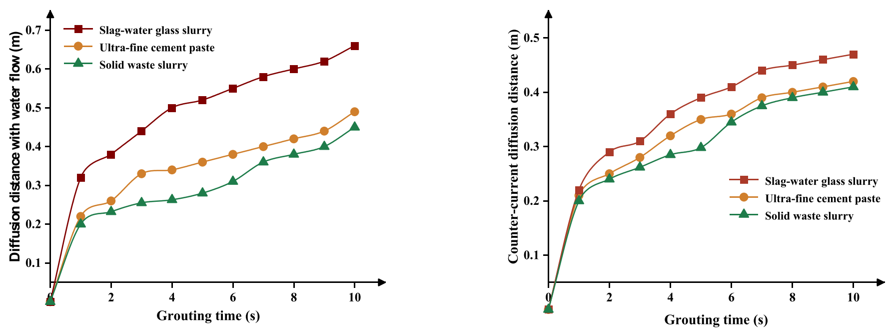


(a) down-flow grout diffusion distance (b) down-flow grout diffusion distance

**Figure 10.** Different serious diffusion distances along and back

### 4.3.3. Analysis of the influence of grouting pressure on slurry diffusion distance

In dynamic water pressure environments, the diffusion distance of grouting materials is significantly influenced by grouting pressure. Taking geopolymer slurry as an example, different grouting pressures (2 MPa, 4 MPa, 6 MPa, 8 MPa, and 12 MPa) were applied for analysis to explore the reverse flow diffusion distance of the slurry under varying grouting pressures.

Using a diffusion time of 5 seconds as an example, the maximum reverse and forward diffusion distances under varying grouting pressures are shown in **Figure 11**. The diffusion behavior of geopolymer grouting materials at different grouting pressures is depicted in **Figure 12**. From **Figure 11**, it is clear that grouting pressure has a considerable effect on the diffusion extent of the slurry. Specifically, as the grouting pressure increases, there is a marked expansion in the diffusion range of the slurry.

As seen from **Figure 11** and **Figure 12**, with the continuous increase in grouting pressure, the reverse diffusion distance of the slurry in the water flow gradually increases. This suggests that in actual grouting engineering applications, appropriately increasing the grouting pressure can effectively enhance the diffusion effect of the slurry, thereby improving the reinforcement effect of the grouting, especially in complex water environments.

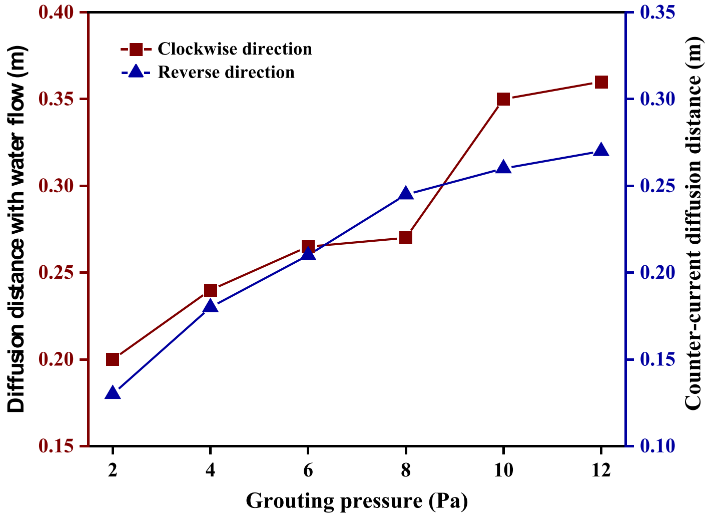


**Figure 11.** Diffusion distance of different mud in a dynamic water environment

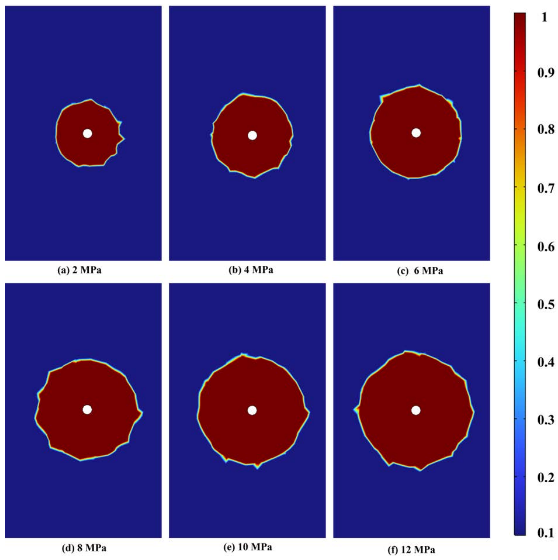


**Figure 12.** Diffusion law of polymer grouting materials under different grouting pressures

## 5. Conclusion

Based on the experimental results and numerical simulation analysis in this study, the following key conclusions are drawn.

(1) Enhancement of geopolymer grouting material performance by sodium silicate: The addition of sodium silicate significantly improved the stability and compressive strength of the geopolymer grouting material. With a sodium silicate modulus of 1.5 and an addition rate of 4%, the stability of the slurry increased by 26.2%, and the 28-day compressive strength increased by 130.98%. As an important additive, sodium silicate enhances the gel structure of the geopolymer grout, thereby improving its stability and mechanical properties.

(2) COMSOL numerical simulation analysis: The numerical simulation results indicate that the diffusion behavior of geopolymer slurry shows a trend similar to that of ultra-fine cement slurry. The slurry's resistance to scouring in dynamic water environments is closely related to its viscosity, with higher viscosity helping to improve the slurry's durability in cracks. Furthermore, appropriately increasing the

grouting pressure can promote the diffusion of the slurry in both downstream and upstream directions, improving its permeability and sealing effect.

(3) Economic analysis: The production cost of geopolymer grouting materials is significantly lower than that of ultra-fine cement, demonstrating its significant economic advantage in practical applications. This cost advantage further confirms the superiority of geopolymer grouting materials in crack grouting and provides strong support for their wide application in fields such as water sealing in coal seam roofs and solid waste resource utilization.

### Disclosure statement

The authors declare no conflict of interest

## Funding

Enterprise entrusted funding Project (Project No. H23-467).

## References

[1] Tian S, Wang Y, Li H, et al., 2024, Analysis of the Causes and Safety Countermeasures of Coal Mine Accidents: A Case Study of Coal Mine Accidents in China from 2018 to 2022. Process Safety and Environmental Protection, 187: 864–875.

[2] Lacoue-Labarthe T, Nunes PALD, Ziveri P, et al., 2016, Impacts of Ocean Acidification in a Warming Mediterranean Sea: An Overview. Regional Studies in Marine Science, 5: 1–11.

[3] Han S, Chen H, Long R, et al., 2017, Evaluation of the Derivative Environment in Coal Mine Safety Production Systems: Case Study in China. Journal of Cleaner Production, 143: 377–387.

[4] Yang R, Li Y, Guo D, et al., 2017, Failure Mechanism and Control Technology of Water-Immersed Roadway in High-Stress and Soft Rock in a Deep Mine. International Journal of Mining Science and Technology, 27(2): 245–252.

[5] Yang W, He S, 2022, Coal Mine Safety Management Index System and Environmental Risk Model Based on Sustainable Operation. Sustainable Energy Technologies and Assessments, 53(C): 102721.

[6] Liu Q, Dou F, Meng X, et al., 2021, Building Risk Precontrol Management Systems for Safety in China's Underground Coal Mines. Resources Policy, 74(C): 101631.

[7] Li X, Zhang S, Ren R, et al., 2024, Comprehensive Evaluation and Spatial-Temporal Evolution Characteristics of Urban Resilience in Chengdu-Chongqing Economic Circle. Chinese Journal of Population, Resources and Environment, 22(1): 58–67.

[8] Zhang J, Guan X, Li H, et al., 2017, Performance and Hydration Study of Ultra-Fine Sulfoaluminate Cement-Based Double Liquid Grouting Material. Construction and Building Materials, 132: 262–270.

[9] Tang L, Wang Z, Zhang X, et al., 2023, Influence of Rheological Parameters on Cement Slurry Penetration Characteristics of Novel Oscillating Grouting Technology. Construction and Building Materials, 2023: 409.

[10] Li Y, Chen M, Shi Q, et al., 2024, Biomass Fractionation Techniques Impact on the Structure and Antioxidant Properties of Isolated Lignins. Separation and Purification Technology, 330: 125499.

[11] Wang J, Wang Y, Yu J, et al., 2022, Effects of Sodium Sulfate and Potassium Sulfate on the Properties of Calcium Sulfoaluminate (CSA) Cement Based Grouting Materials. Construction and Building Materials, 353: 129045.

[12] Yang Y, Wang J, Dou H, 2014, Mechanical Properties of Anti-Seepage Grouting Materials for Heavy Metal Contaminated Soil. Transactions of Nonferrous Metals Society of China, 24(10): 3316–3323.

[13] Wang M, Wang C, Yu J, et al., 2021, Investigation of the Grouting Effect of Blast Furnace Slag-Based Mortar on Void Road Bases Based on the Grouting Simulation Test. Construction and Building Materials, 282(4): 122567.

[14] Li M, Bao S, Zhang Y, et al., 2024, Preparation and Characterization of Low-Activity Coal Bottom Ash-Based Cementitious Materials via Orthogonal Experiment. Journal of Building Engineering, 2024: 96.

[15] Bakhrakh A, Solodov A, Naruts V, et al., 2017, High-Performance Self-Compacting Concrete with the Use of Coal Burning Waste. IOP Conference Series: Earth and Environmental Science, 90: 12213.

[16] Pawluczuk E, Kalinowska-Wichrowska K, Jimenez JR, et al., 2021, Geopolymer Concrete with Treated Recycled Aggregates: Macro and Microstructural Behavior. Journal of Building Engineering, 2021: 44.

[17] Fan G, Zhang D, Wang X, 2014, Reduction and Utilization of Coal Mine Waste Rock in China: A Case Study in Tiefa Coalfield. Resources Conservation & Recycling, 83: 24–33.

[18] Yatsenko EA, Ryabova AV, Vil'Bitskaya NA, et al., 2022, Eco-Geopolymers Based on CHP Plant Ash-Slag Waste: Promising Materials for Road Construction in the Arctic Zone. Glass and Ceramics, 78(11–12): 490–493.

[19] Buch-Hansen M, 1997, Environment—A Liability and an Asset for Economic Development: Some Views on Environmental Protection with Economic Development in Bhutan. International Journal of Sustainable Development & World Ecology, 4: 17–27.

[20] Buchdahl JM, Raper D, 2015, Environmental Ethics and Sustainable Development. Sustainable Development, 2015: 6.

[21] Ren C, Li KQ, Wang Y, et al., 2023, Preparation and Hydration Mechanisms of Low Carbon Ferrochrome Slag-Granulated Blast Furnace Slag Composite Cementitious Materials. Materials, 2023: 16.

[22] Rao AP, Rao AV, Pajonk GM, 2007, Hydrophobic and Physical Properties of the Ambient Pressure Dried Silica Aerogels with Sodium Silicate Precursor Using Various Surface Modification Agents. Applied Surface Science, 253(14): 6032–6040.

[23] Bilondi MP, Toufigh MM, Toufigh V, 2018, Experimental Investigation of Using a Recycled Glass Powder-Based Geopolymer to Improve the Mechanical Behavior of Clay Soils. Construction and Building Materials, 170: 302–313.

[24] Wang C, Zhao L, Guo Z, et al., 2024, Mechanistic Study of Fly Ash Activity Enhanced by High Temperature to Strengthen Cementitious Materials. Construction and Building Materials, 2024: 416.

[25] Dong-Zhu Z, Qing-Song Z, Peng LI, et al., 2017, Numerical Simulation of Dynamic Grouting in Drift Sand Strata. Computer Simulation, 34(1): 241–244 + 309.

**Publisher's note**

Bio-Byword Scientific Publishing remains neutral with regard to jurisdictional claims in published maps and institutional affiliations.

Journal of Architectural Research and Development, 2025, Volume 9, Issue 1
https://ojs.bbwpublisher.com/index.php/JARD
Online ISSN: 2208-3537
Print ISSN: 2208-3529

# A Review of Research Trends in Public-Private Partnership based on CiteSpace: Bibliometrics and Visualization

**Huijie Jiang**[1], **Lihong Li**[2], **Hang Yin**[3], **Yuanzhi Wang**[4]*

[1]Shenzhen Polytechnic University, Shenzhen 518055, China
[2]College of Management, Shenyang Jianzhu University, Shenyang 110168, China
[3]TY Intelligent Science and Technology (Chongqing) Co., Ltd., Chongqing 401100, China
[4]Shenzhen Dongsen Construction Project Management Co., Ltd., Shenzhen 518024, China

***Corresponding author:*** Yuanzhi Wang, 243513830@qq.com



**Abstract:** Applying the Public-Private Partnership (PPP) model is indispensable in creating new economic growth points in the public service sector. However, there is still a lack of research on mapping the application of the PPP model in the new era and context. Therefore, based on reviewing the characteristics and development concepts of the PPP model, this paper uses CiteSpace software to analyze the sample authors, journals, and regions in the Scopus database. This paper aims to explore the current development status, research paradigms, and research gap as well as future trends of the PPP model. The results show that (1) The focus of PPP research has shifted from traditional models such as Build-Operate-Transfer (BOT) and Private Finance Initiatives (PFI) to contemporary themes such as risk management, policy analysis, and project governance. Subsequent research (2014–2018) has emphasized the importance of governance and regulatory frameworks to improve PPP outcomes. (2) The growing academic interest in PPP development in China accounts for 28.78% of the total publications. This surge reflects China's rapid economic growth and highlights the interplay between government regulation and private financing. Key research themes include risk management, performance evaluation, contractual flexibility, and financing mechanisms, particularly concerning the BOT model. (3) Effective risk management, relationship dynamics, and innovative financing strategies are key components of a strong PPP knowledge framework. Collaborative risk sharing and strong relationships between public and private entities are key to project success, and strategic financing partnerships are necessary to cope with the complexity of large infrastructure projects.

**Keywords:** CiteSpace; Public-Private Partnership (PPP); Bibliometrics and visualization

**Online publication:** February 10, 2025

## 1. Introduction

As early as the 17th century, the United Kingdom began utilizing the Public-Private Partnership (PPP) model for public projects, effectively addressing funding shortages and inefficiencies while enhancing the overall benefits of infrastructure development. The completion of the Shenzhen Shajiao B power plant in 1984, executed under the

Build-Operate-Transfer (BOT) model, marked a significant milestone in China's adoption of the PPP framework for infrastructure initiatives. Recently, there has been a growing emphasis on the PPP model across various sectors, attracting increasing academic interest and yielding valuable research contributions. In the realm of statistical analysis of the PPP model, scholars such as Al Sharif, Ke, Dimas, and Tang have primarily concentrated on author distribution and research trajectories [1–4]. Their findings regarding the volume of publications, regional distribution, and highly cited literature predominantly highlight external project development aspects and the internal knowledge structure characteristics inherent to PPP projects. Furthermore, the majority of empirical studies have examined issues related to project risk, public-private relationships, and project financing. In contrast, non-empirical research has largely focused on project financing, critical success factors, project risk, and concession agreements.

The PPP model, characterized by its collaborative dynamics, benefit-sharing, and risk-sharing attributes, has emerged as a pivotal reform initiative aimed at fostering new avenues for economic growth. This model facilitates the efficient allocation of resources, encourages innovation, and enhances the quality of public services through the strategic involvement of both public and private sectors. Recent research on the PPP model has produced significant findings, contributing to its evolution into a well-established domain within management science. Scholars have explored various facets of the PPP framework, including its operational mechanisms, effectiveness in different sectors, and its role in achieving sustainable development goals. Despite these advancements, a comprehensive review of the existing literature reveals a predominant reliance on qualitative inductive analyses. This methodological bias highlights a notable scarcity of quantitative approaches and visual analyses, which can provide deeper insights into the dynamics and performance of PPP projects. Moreover, there is a dearth of studies that critically examine citation patterns, which are essential for understanding the intellectual structure and influence of research within this field. To address these gaps and to gain a more holistic understanding of the current landscape and future trends of the PPP model, it is imperative to adopt a multifaceted research approach. This approach should prioritize quantitative methodologies while integrating qualitative analyses to enrich the findings. Additionally, employing visualization techniques will facilitate a clearer interpretation of complex data and enhance the overall understanding of the interactions and outcomes associated with the PPP model. By embracing a comprehensive research framework, scholars can not only advance the theoretical foundations of the PPP model but also provide practical insights that inform policy decisions and implementation strategies in various contexts.

To address the identified research gaps, this study employs bibliometric analysis as the primary analytical method, utilizing CiteSpace software to visualize and analyze sample data while clarifying the characteristics and concepts of the PPP model. The study encompasses various elements, including sample data, relevant journals, authors' geographical regions, institutional affiliations, and citation references. Based on the findings, this research provides a comprehensive overview of the current state of PPP model development and anticipates future research priorities and trends. Firstly, in contrast to purely textual theoretical research, this study aims to present the current status and future directions of PPP model development through data visualization, charts, and other illustrative forms, thereby offering scholars a more intuitive understanding of the subject. Secondly, the application of CiteSpace software facilitates visual analysis that not only organizes and summarizes fundamental information from the publications within the sample data sources but also employs co-citation analysis to examine the relationships among authors, institutions, geographical regions, and references. This approach culminates in a comprehensive and systematic perspective of the research landscape. Finally, this study explores the future developmental trends of the PPP model from an all-encompassing and multi-faceted standpoint, aiming to provide researchers across various fields with a clearer understanding of the PPP model and its implications. By integrating quantitative analysis with qualitative insights, this research contributes to the advancement of knowledge in the field and informs practical applications in PPP initiatives.

## 2. Characteristics of the PPP model

To enhance the practical application of the Public-Private Partnership (PPP) model in engineering projects, both domestic and international experts and scholars have conducted extensive studies on its definition, leading to a preliminary consensus. However, the unique economic conditions, policy contexts, and operational focuses of different countries and regions, along with the varying priorities of industries, financial institutions, and regulatory committees, contribute to a diverse theoretical framework surrounding the PPP model in practice. The characteristics and definitions of the PPP model are presented in **Table 1**.

**Table 1.** Characteristics and definitions of PPP

| Institutions | Definition |
|---|---|
| United Nations Development Program | A cooperative relationship between a government, a for-profit enterprise, and a nonprofit organization based on a project. |
| World Bank | Long-term contracts between the private sector and government agencies for the provision of public assets or services, in which the private sector bears significant risk and management responsibility for projects and is paid for performance. |
| Asian Development Bank | A range of possible partnerships between public and private sector entities for infrastructure and other services. |
| The Canadian Council for Public-Private Partnerships | A business relationship established by the public and private sectors based on their respective professional work experience to meet public needs through appropriate resource allocation, risk sharing, and benefit sharing. |
| PPP National Committee of the United States | A contractual arrangement between a public sector agency and a for-profit private sector developer in which resources and risks are used to provide public services or develop public infrastructure. |
| Hong Kong Efficiency Unit | The provision of public services or the implementation of projects by the public and private sectors, with varying degrees of involvement and commitment depending on their respective professional expertise. |
| European Commission | A partnership between the public and private sectors in which both parties share risks and responsibilities based on their respective strengths and weaknesses to provide public services for which the public sector is responsible. |

Savas, in Privatization and Public-Private Partnerships, defines “Public-Private Partnership” as a type of action that relies primarily on non-governmental organizations (NGOs) to meet people’s needs [5]. The PPP model relies less on government action than formal projects and also points out that the key to success is competition among private institutions. Based on the perspective of the relationship between public and private define, Sagalyn from all the involved departments of PPP projects in different periods of work [6], its development process is divided into three stages: in the first stage, because of the lack of work experience, can be drawn lessons from mature division of labor unclear boundaries between public, private and consultant, in the process of project implementation cope with many problems of unknown; In the second stage, to improve the professionalism of PPP project implementation, professional planners are often employed to assist in the implementation of PPP projects; In the third stage, relevant theories and policies have achieved initial results. The implementation of PPP projects is mostly carried out by taking the initiative to seek the way of the private sector. Public and private sectors give full play to the advantages of each department in terms of working resources and environment to provide coordinated and optimized convenience for the efficient operation of projects. The commercialization concept of the worldwide revolution in infrastructure provision and project finance, which was written in Public Private Partnerships by Grimsey [7], made an important contribution to the privatization of infrastructure in Australia. The book not only discussed the essence of the PPP model and its transformative impact on infrastructure construction but also profoundly analyzed the key points for the successful implementation of the PPP model with the help of abundant cases.

The implementation of the PPP mode not only requires the public and private to make full use of their respective advantages in resources and environment but also requires them to bear corresponding risks within their respective capabilities, to achieve the goal of saving resources while completing projects with high quality and efficiency [8–10]. The active participation of private entities not only gives full play to their professional skills in the process of project implementation, experience, technology, and innovation advantage but also to their own working experience in advance forecast project development prospects in the market. At the same time, the positive interaction of public and private enlarged the public understanding of the project, based on the public focus on its own core competency [11] supported project on the policies and procedures [12]. As a result, the coordination and cooperation between public and private will greatly improve the output quality of public facilities and services and deliver satisfactory work results to owners [13].

## 3. Method and data

The specific process of this study is illustrated in **Figure 1**. Bibliometrics, which emerged in the early 20th century, has gained popularity in academic research due to its capacity for quantitatively analyzing publications within specialized fields and presenting the results visually. This methodology allows researchers to analyze key aspects such as literature content, keywords, reference documents, journals, geographical distribution, institutions, and trends within a particular area. In contrast to traditional qualitative research methods, bibliometrics, grounded in the principles of total lead analysis and visualization, offers a more detailed and comprehensive understanding of a field. It not only aids researchers in identifying the latest developments but also helps predict future directions within the discipline.

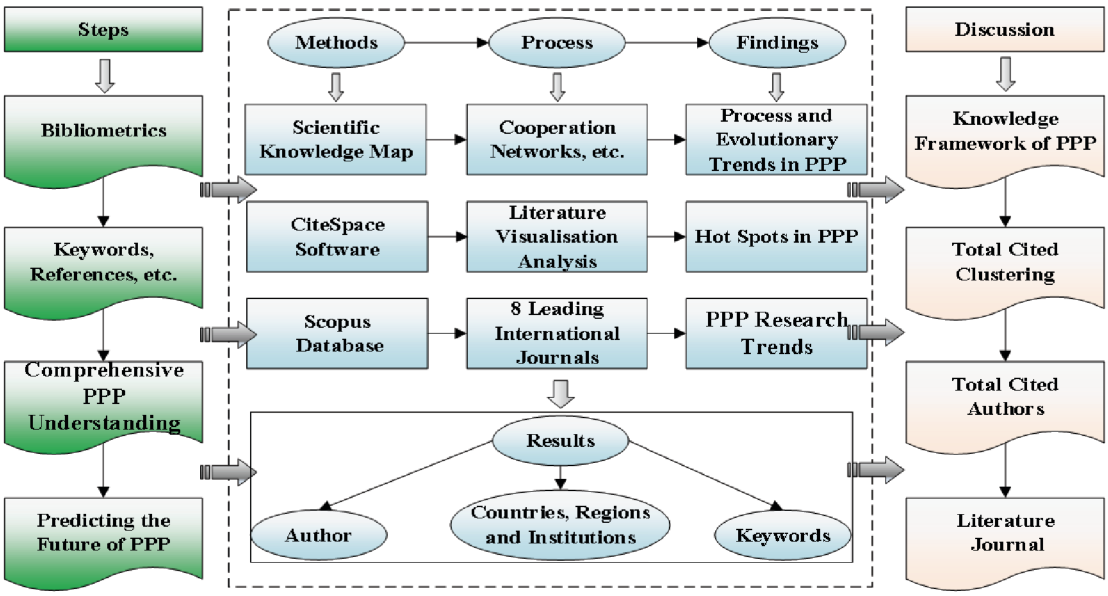


**Figure 1**. Study framework

Scientific knowledge mapping is a visual tool that employs various analytical methods, including citation analysis, co-occurrence analysis, clustering analysis, frequency analysis, social network analysis, and multidimensional scaling. This approach is essential for literature data analysis, producing knowledge maps that include cooperation networks, co-occurrence networks, citation networks, and cited networks. Such quantitative analyses and visualizations intuitively reflect the processes and evolutionary trends in the development of disciplinary knowledge. CiteSpace is an advanced information visualization software developed by Professor Chen's research team at Drexel University in the United States. It is recognized as a leading tool among similar open-access software for identifying and displaying emerging trends and developments in scientific literature. CiteSpace generates network visualizations based on knowledge structures, subjects, periods, and the evolutionary trends of various information. It offers different analytical views, including cluster views, timelines, and time zones, enabling researchers to quickly identify subject areas, locate reference hotspots, and discern collaborative geographical patterns and unique collaborative domains. In this study, CiteSpace software was employed to conduct a visualization analysis of literature sourced from the Scopus database. By analyzing the results from cluster views, timelines, and time zone analyses, the research aims to highlight hotspots in PPP studies. The findings are expected to assist researchers in expanding both the scope and depth of PPP research in China, fostering a more profound integration of PPP theory and practice.

The accuracy of the dataset, which plays an important role in literature analysis, is contingent upon the selection of academic databases and the design of search strategies. Scopus, developed by Elsevier, is the world's largest database of abstracts and citations. This comprehensive database not only includes citation information for collected articles but also integrates network and patent retrieval data within a user-friendly interface, offering researchers a convenient one-stop resource for accessing scientific and technological literature. To ensure that the collected literature is of high quality and influence within the professional field, this study utilized the Scopus database as the primary data source. It employed specific criteria based on source journals, keywords, and document types, conducting keyword searches across eight leading international journals in the selected field (see **Table 2** for search information). The analysis focused on research trends related to the PPP model, utilizing all papers published in the Web of Science (WOS) Core Collection database from 1999 to 2018, spanning approximately 20 years, as input data for CiteSpace. All keywords utilized in the search strategy were compared with related terms, leading to the adoption of a broad definition of PPP, with a focus on the construction sector. This process yielded a total of 1,494 citations, in contrast to 34,696 citations across all identified documents.

**Table 2.** Summary of search details

| Labels | Contents | Labels | Contents |
|---|---|---|---|
| Visual analysis software | CiteSpace | keywords | "PPP" |
| Literature database | Scopus | Number of citations | 1,494 |
| Time range | 1999–2018(20 years) | Number of cited references | 34,696 |
| Professional field | Construction Management | | |

## 4. Results and discussion of citation analysis

This section could provide a concise and precise description of the citation analysis results, their interpretation, as well as the analysis conclusions that can be drawn.

### 4.1. Author analysis

This study is limited to journal articles published in English. The eight international top journals selected are: the International Journal of Project Management, Journal of Construction Engineering and Management, Construction Management and Economics, Journal of Management in Engineering, Engineering Construction and Architectural

Management, Construction Innovation, Automation in Construction, and the Tumu Gongcheng Xuebao China Civil Engineering Journal. By analyzing the authorship information obtained from the dataset, it is possible to scientifically reveal and identify the main researchers, institutions, and countries of the PPP research. By analyzing the co-authors, a network of co-authors and a network of institutions and countries of co-authors were generated as described below. According to the statistical results of CiteSpace on the authors of 1,494 papers (1999–2018), 203 authors contributed more than two papers per capita. Among them, the top 30 authors with five or more papers contributed are listed in **Table 3**. The top 30 authors from the data are ranked based on their contribution amount and their collaborative relationships, as illustrated in **Figure 2**. In this figure, the curve represents the author, the edges between nodes represent collaborations, and the node size reflects the author's contribution to the papers. Among these, there are seven representative collaborative groups. The top three authors with the highest contribution amounts are Chan APC, Yuan JF, and Marques RS, who serve as central nodes in the collaboration network. Additionally, several independent collaborations are distributed around these core contributors.

**Table 3.** The top 30 authors and their contribution

| Author | Contribution | Author | Contribution | Author | Contribution |
|---|---|---|---|---|---|
| Chan APC | 42 | Chen C | 9 | Smith J | 6 |
| Yuan JF | 19 | Cheung E | 9 | Petersen OH | 6 |
| Marques RC | 17 | Song JB | 9 | Jin XH | 6 |
| Zhang XQ | 14 | Chou JS | 8 | Van Den Hurk M | 5 |
| Skibniewski MJ | 14 | Girmscheid G | 7 | Regan M | 5 |
| Li QM | 14 | Yeung JFY | 7 | Hellowell M | 5 |
| Xiong W | 12 | Lam PTI | 7 | Verhoest K | 5 |
| Ke YJ | 12 | Osei-kyei R | 7 | Wang Y | 5 |
| Wang SQ | 11 | Xu YL | 7 | Deng XP | 5 |
| Cruz CO | 10 | Carpintero S | 6 | Feng Z | 5 |

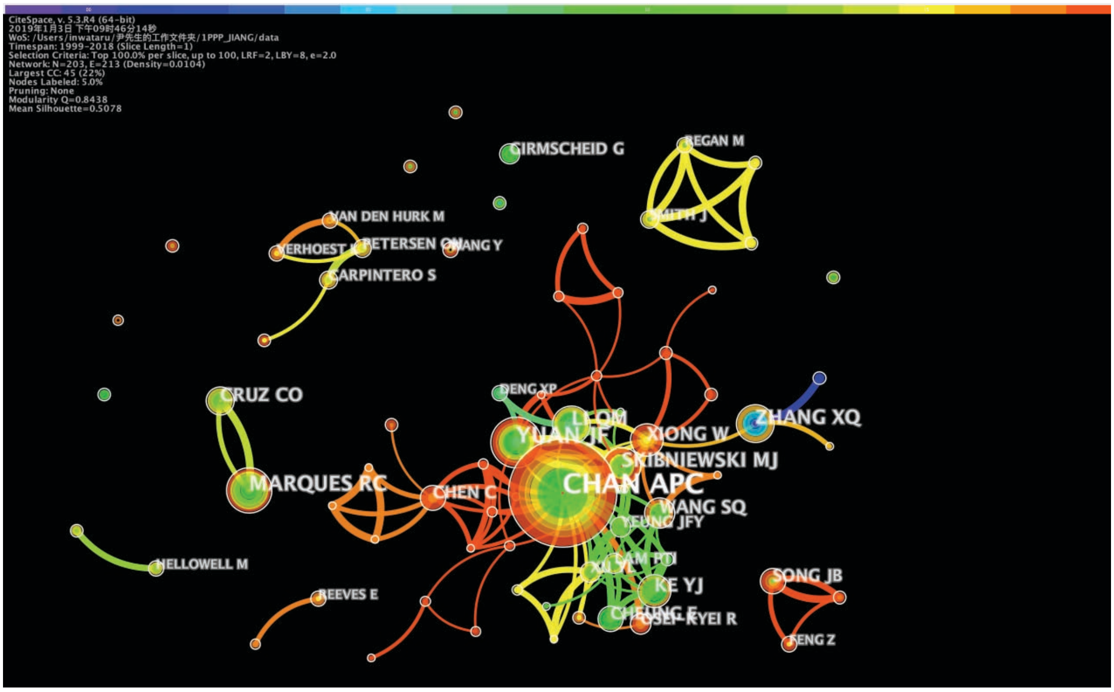


**Figure 2.** Paper contributing author between network diagram

Statistics show that more and more researchers' attention is graduating to the development of China's PPP, combined with the author's collaboration network diagram there are a large number of independent cooperation networks to forecast, the future there will be a lot for China's situation and the independent existence of subject research trend of combination, such as the Chinese government regulations and private financing analysis of PPP. Since 2009, Chan APC as the main author cooperation team has done key research on the risk allocation of PPP, covered the project potential elements [14], China's PPP risk sharing model [15], the PPP success factors [16], etc. In addition, some partners also separately studied the project satisfaction [17,18], a renegotiation [19,20]. The cooperative network of Smith J and Regan M focuses on performance evaluation from the perspective of the whole life cycle [21–23]. Cooperation network between Song JB and Feng Z, BOT mode in PPP [24–27]. To study the restraining factors and government support of various PPP projects, Petersen OH et al. made a comparative analysis of PPP in several countries [28–30]. Cruz CO author cooperation network, such as more focus on the problem of flexibility of the PPP contract, emphasizing the capital value of flexible implementation projects to maximize [31,32]. The cooperative network of Hellowell M analyzes the role of government decision-making in PPP and the purpose of private investment, especially in hospital projects [33–35]. Reeves E et al. paid more attention to the private financing methods of PPP [36,37].

## 4.2. Countries, regions, and institutions analysis

To further investigate the contributions of different regions to research on the Public-Private Partnership (PPP) model, this study compiles statistics on the geographical distribution of published papers, as presented in **Table 4**. The contributions from these countries and regions account for 75.10% of the total number of papers. Notably, the leading contributor is the People's Republic of China, which accounts for 28.78% of the total publications, representing nearly one-third of the overall output. Although the origin of the PPP model is not China, the steady increase in the country's economic growth rate since 1990 and the rapid development of its infrastructure have positioned China at the forefront of global infrastructure initiatives [38]. Consequently, the demands of China's economic and infrastructural development have significantly accelerated domestic scholarly research on PPP in a relatively short timeframe. Furthermore, the statistical results underscore the critical role of policy orientation in advancing PPP development. For instance, the introduction of related planning for new-type urbanization utilizing the PPP model by the Chinese government from 2013 to 2017 has catalyzed a research boom, making new-type urbanization a prominent topic within the field.

**Table 4.** Countries and regions with the top 10 paper contributions

| Region | Contribution | Region | Contribution |
|---|---|---|---|
| People's Republic of China | 430 | Germany | 39 |
| United States of America (U.S.A.) | 206 | Spain | 38 |
| England | 158 | Netherlands | 37 |
| Australia | 104 | Taiwan | 35 |
| Italy | 41 | India | 34 |

The contributions of the top 10 regions are illustrated in conjunction with the cooperative relationships among countries and regions, as depicted in the network diagram in **Figure 3**. In this diagram, the curves represent collaborative ties between countries and regions, while the nodes signify the literature associated with each location. Nodes of the same color indicate that they belong to the same cluster, highlighting a specific or primary research focus. If a state within a cluster is connected to another cluster, it suggests that the country is also engaged in additional research areas. The analysis primarily highlights the core contributions from China, the U.S.A., and England, which are central to the diffusion of research. This is accompanied by various independent collaborations among other countries and regions. Notably, the relationships illustrated by the curves indicate that almost all countries and regions maintain cooperative ties with China, suggesting that there is considerable global interest in the development of the PPP model in China. Currently, China's PPP market development, along with its policy and institutional framework, is regarded as leading globally. China has emerged as the largest PPP market in the world, contributing significantly to the evolution of global PPP practices [39]. This development enhances the ability of countries along the Belt and Road Initiative to effectively implement PPP projects, and it reflects the inevitable outcomes of China's rapid economic growth and infrastructure expansion.

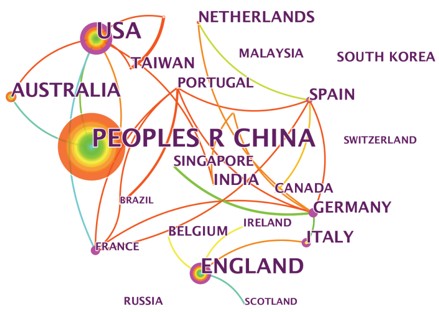


**Figure 3.** Network diagram of countries and regions contributing papers

The distribution of research organizations affiliated with the PPP-related papers collected in this study is illustrated in **Figure 4**. The analysis indicates that institutions from China occupy a central position within the institutional cooperation network. The network diagram reveals that Hong Kong Polytechnic University serves as the hub, with numerous organizations interconnected, highlighting its pivotal role in collaborative efforts. **Table 5** presents the top 10 research institutions based on paper contributions. Among these, six institutions are from China, while the remaining four are from Belgium, Singapore, the U.S.A., and Portugal, respectively. Notably, the top three contributing institutions are all Chinese: Hong Kong Polytechnic University, with 56 papers; Southeast University, with 23 papers; and Tsinghua University, with 16 papers. This indicates that the research outputs from China's PPP institutions hold significant value on a global scale.


**Figure 4.** Network diagram of the institutions contributing papers

**Table 5.** Paper contribution amount in the top 10 research institutions

| Institution | Contribution | Institution | Contribution |
|---|---|---|---|
| Hong Kong Polytech University | 56 | Dalian University Technology | 12 |
| Southeast University | 23 | University of Maryland | 10 |
| Tsinghua University | 16 | Sichuan University | 10 |
| University of Antwerp | 13 | University of Lisbon | 9 |
| National University of Singapore | 12 | Tianjin University | 9 |

## 4.3. Keywords analysis

This study employs quantitative visual analysis of keywords to explore the distribution of research hotspots in the field of PPP, with the results presented in **Figure 5**. After excluding the keywords "PPP" and "public-private partnership" the leading keywords in the statistical ranking are "management," "China," and "performance," The quantitative visualization analysis conducted on 1,494 papers from 1999 to 2018, using CiteSpace software, reveals these prominent keywords. In addition to the top keywords, over nearly two decades of research, other frequently used terms include "infrastructure," "partnership," "risk allocation," "model," "BOT," and "policy." A classification and analysis of these keywords indicate that the types of projects involved in infrastructure research predominantly encompass highway projects [40], water treatment projects [41], waste recycling projects [42], and urban transportation projects [43]. Research about PPP models primarily includes the revenue-sharing model [44], price model [45], value-for-money (VFM) model [46], risk management model [47], and cooperative game model [48]. Additionally, significant areas of inquiry involve risk sharing between partners [49], government policy guidance [50], and the BOT model [51].

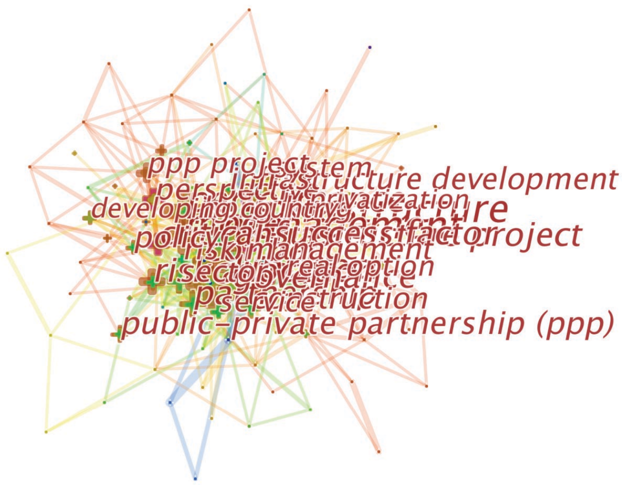


**Figure 5.** Network diagram of keywords in the paper

To comprehensively and clearly observe the evolving trends in PPP research, this study divides the period from 1999 to 2018 into three distinct phases: the first phase from 1999 to 2008, the second from 2009 to 2013, and the third from 2014 to 2018.

### 4.3.1. Session 1: 1999–2008

According to the results of quantitative visualization analysis of keywords by CiteSpace from 1999 to 2008 (as shown in **Figure 6** and **Table 6**), PPP research focuses on topics related to BOT mode, private financing institutions, project management, and risk management during this period. Among them, the hot research on BOT mode mainly involves the analysis of the BOT procurement mode [52], the setting of cooperation terms in BOT contracts [53], and the success factors in the construction and operation stage [54]. The hot spots of private financing institutions mainly involve performance supervision of Private Finance Initiative (PFI) implementation [55], key success factors of PFI project implementation [56], and relationship management of PFI partnership [57].

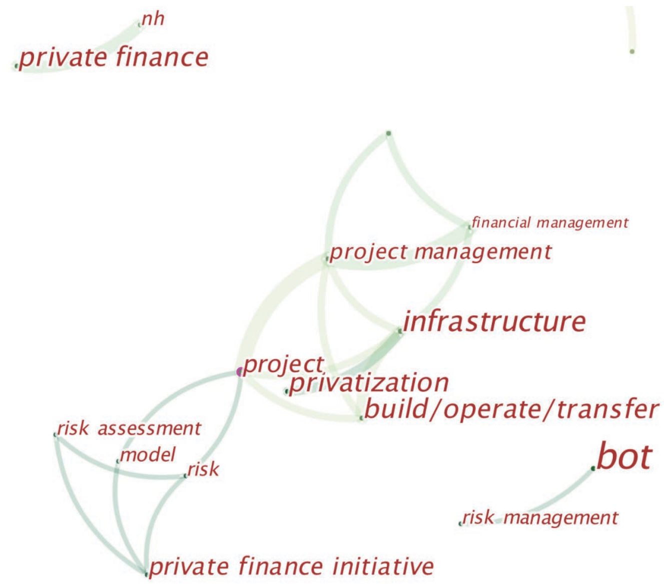


**Figure 6.** Keyword network diagram from 1999 to 2008

**Table 6.** The top 20 keywords between 1999 and 2008

| Keywords | Contribution | Centrality | Keywords | Contribution | Centrality |
|---|---|---|---|---|---|
| Bot | 26 | 0.00 | Risk management | 3 | 0.09 |
| Infrastructure | 7 | 0.10 | Risk | 3 | 0.06 |
| PFI | 11 | 0.00 | Trust | 3 | 0.00 |
| Private finance | 6 | 0.00 | Model | 3 | 0.01 |
| Privatization | 6 | 0.09 | Risk assessment | 3 | 0.02 |
| Project | 5 | 0.25 | Game theory | 2 | 0.00 |
| Project Management | 4 | 0.10 | Financial management | 2 | 0.01 |

### 4.3.2. Session 2: 2009–2013

Many hotspots involved in PPP policy analysis include the effectiveness and risk of policy implementation. The quantitative visualization analysis of keywords performed by CiteSpace for the period from 2009 to 2013 (as shown in **Table 7** and **Figure 7**) indicates that the research scope of PPP hotspots is gradually expanding. The focus is no longer limited to traditional frameworks such as the Private Finance Initiative (PFI) and the Build-Operate-Transfer (BOT) model. Instead, there is a noticeable increase in studies addressing risk sharing, risk management, modeling, and policy-related issues. Specifically, the pathway for PPP risk management typically involves two key components: risk identification and risk assessment [58]. Moreover, several significant research hotspots during this period have centered on the analysis of PPP policies, particularly regarding the effectiveness and risks associated with policy implementation [59].

**Table 7.** The Top 20 keywords between 2009 and 2013

| Keywords | Contribution | Centrality | Keywords | Contribution | Centrality |
|---|---|---|---|---|---|
| Infrastructure | 39 | 0.12 | Policy | 18 | 0.04 |
| Management | 32 | 0.07 | Construction | 18 | 0.04 |
| Performance | 28 | 0.09 | Project | 16 | 0.04 |
| Partnership | 26 | 0.10 | Service | 16 | 0.04 |
| China | 25 | 0.10 | Private finance initiative | 15 | 0.14 |
| Risk allocation | 24 | 0.05 | Governance | 14 | 0.05 |
| Model | 24 | 0.10 | Infrastructure project | 14 | 0.04 |
| Risk management | 22 | 0.06 | Critical success factor | 14 | 0.04 |
| Bot | 21 | 0.01 | Procurement | 13 | 0.03 |
| Risk | 20 | 0.04 | Network | 12 | 0.05 |

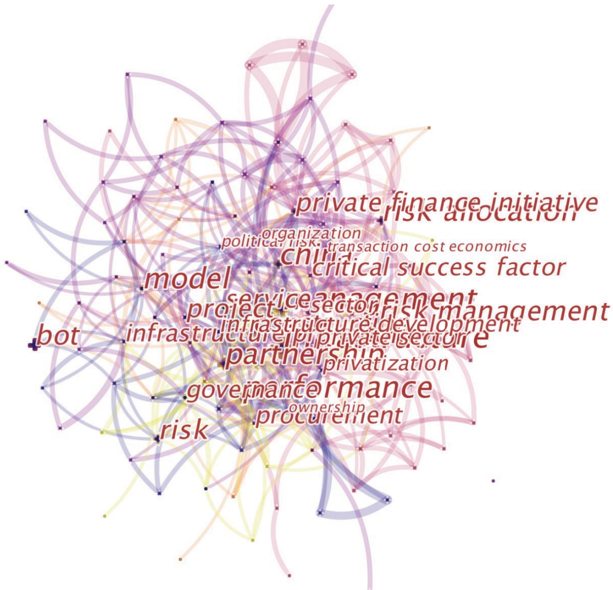


**Figure 7.** Keyword network diagram from 2009 to 2013

### 4.3.3. Session 3: 2014–2018

The keywords visualization analysis conducted by CiteSpace for the period from 2014 to 2018 (as illustrated in **Table 8** and **Figure 8**) indicates a more diversified trend in research topics. In addition to key themes such as project management, project performance, success factors, and risk management, the issue of project governance has garnered significant attention during this period. Among the primary topics within project governance are government regulation [60] and the legal framework governing contracts [61].

**Table 8.** The Top 20 keywords between 2014 and 2018

| Keywords | Contribution | Centrality | Keywords | Contribution | Centrality |
|---|---|---|---|---|---|
| Management | 83 | 0.03 | Risk | 43 | 0.02 |
| Infrastructure | 77 | 0.02 | Perspective | 42 | 0.07 |
| China | 73 | 0.04 | Risk Allocation | 35 | 0.02 |
| Performance | 59 | 0.03 | Partnership | 35 | 0.04 |

**Table 8 (Continued)**

| Keywords | Contribution | Centrality | Keywords | Contribution | Centrality |
|---|---|---|---|---|---|
| Project | 59 | 0.07 | Sector | 34 | 0.01 |
| Model | 57 | 0.01 | System | 29 | 0.02 |
| Governance | 50 | 0.05 | Infrastructure Development | 29 | 0.02 |
| Infrastructure Project | 47 | 0.04 | Developing Country | 27 | 0.02 |
| Contract | 46 | 0.01 | Hong Kong | 27 | 0.10 |
| Critical Success Factor | 45 | 0.06 | Concession Period | 24 | 0.05 |

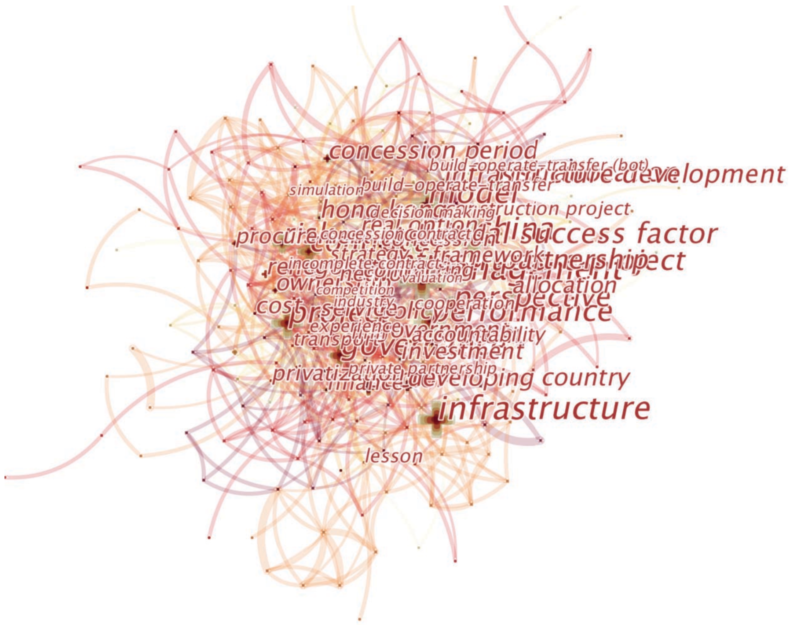


**Figure 8.** Keyword network diagram from 2014 to 2018

# 5. Discussion

## 5.1. Knowledge framework of PPP

Through the analysis of data sources using CiteSpace, a total of approximately 34,696 references were identified across 1,494 papers published from 1999 to 2018. The top 10 references ranked by citation frequency are presented in **Table 9.** The most frequently cited work by Ke YJ examines reasonable risk-sharing methods in China's PPP projects, while the second most cited reference focuses on the key factors contributing to the success of these projects. The third significant reference addresses risk assessment practices within China's PPP framework.

These findings suggest that the context of the PPP model, particularly about China, is a primary focus for researchers in the field. Moreover, the areas of risk assessment, risk sharing, financing methods, foundational frameworks, key success factors, and overall project viability represent the fundamental themes of discussion in PPP research. This underscores the importance of understanding how these elements interact within the Chinese context, providing valuable insights for practitioners and policymakers involved in the implementation of PPP projects. As the field continues to evolve, addressing these core areas will be crucial for enhancing the effectiveness and sustainability of PPP initiatives both in China and globally.

The analysis of highly cited references from a co-citation perspective reveals a diverse methodological landscape within the field of PPP research. Some of these references are based on empirical research, while others adopt a non-empirical approach. Despite this methodological diversity, the predominant themes across these studies consistently center on three key areas: risk management, relational dynamics, and financing strategies. This indicates that, regardless of the research approach employed, scholars are primarily focused on understanding how these elements interact within the PPP framework. The emphasis on risk underscores its critical role in project success and sustainability, while the exploration of relationships highlights the importance of collaboration between public and private entities. Additionally, financing remains a pivotal concern, as securing adequate funding is essential for the effective implementation of PPP projects. Overall, these findings suggest that further exploration of these interconnected themes is vital for advancing knowledge in the field and enhancing the practical application of the PPP model.

**Table 9.** Information of references in the top 10 cited frequency statistics

| Author | Year | Frequency | Literature resources | Research perspectives |
|---|---|---|---|---|
| Ke YJ [62] | 2010 | 62 | INT J PROJ MANAG | China's PPP projects and reasonable risk-sharing |
| Chan APC [63] | 2010 | 54 | J CONSTR ENG M | China perspective, key success factors |
| Tang LY [64] | 2010 | 53 | INT J PROJ MANAG | Risk, financing, contract agreement |
| Chan APC | 2011 | 47 | J MANAGE ENG | China's PPP projects, risk assessment, and risk sharing |
| Hodge GA | 2007 | 45 | PUBLIC ADMIN REV | The performance evaluation |
| Xu YL | 2010 | 43 | AUTOMAT CONSTR | The risk assessment |
| Yescombe ER | 2007 | 43 | PUBLIC PRIVATE PARTN | Policy, financing |
| Kwak YH | 2009 | 42 | CALIF MANAGE REV | Development framework |
| Hwang BG | 2013 | 39 | INT J PROJ MANAG | Key factors, risks |
| Marques RC | 2011 | 35 | J CONSTR ENG M ASCE | Risks, contracts |

### 5.1.1. Risk management

Risk management in Public-Private Partnership (PPP) projects encompasses several critical components, including risk factor identification, risk assessment, and the analysis of risk-sharing frameworks. For instance, Bing et al. utilized the value judgment method to analyze the risks associated with the entire life cycle of PPP projects [65]. They highlighted the significance of recognizing various risk factors and categorized them into three levels: micro risks, medium risks, and macro risks. This classification aids in developing targeted risk management strategies appropriate for different scales and contexts. Grimsey and Lewis contributed to this discourse by evaluating risk factors specifically within the context of infrastructure projects employing the PPP model [7]. They proposed a comprehensive risk assessment framework that facilitates systematic analysis and understanding of the inherent risks involved in such partnerships. Building on this foundational work, Ke et al. employed the Delphi survey method to analyze risk preferences associated with PPP projects in China [66]. Their findings revealed that government entities identified 12 specific risks, including "levy and nationalization" risks, while the private sector recognized 10 risks. Notably, there were 12 risks deemed to be shared among stakeholders, illustrating the collaborative nature of risk management in PPP projects. These studies collectively underscore the complexity of risk management in PPP, emphasizing the need for robust frameworks that accommodate the diverse interests of stakeholders. Moreover, the emphasis on collaboration in risk-sharing highlights the importance of effective communication and negotiation between public and private entities. Future research should further explore the dynamics of risk perception among different stakeholders, as well as the effectiveness of various risk-sharing mechanisms in enhancing project outcomes. By advancing this understanding, researchers can contribute to the development of more resilient and successful PPP models.

### 5.1.2. Relational dynamics

The organizational relationship between the public and private sectors is a critical determinant of the success of Public-Private Partnership (PPP) projects. Ineffective relationships can lead to misunderstandings, conflicts, and ultimately project failure. Research on relationships within PPP projects primarily focuses on topics such as relationship improvement, relationship management, and relationship contracts. For instance, Iossa and Martimort examined the impact of the relationship between the public sector and private capital from a micro-economic perspective [67]. Their analysis highlights the significance of incentive structures and flexibility in PPP contracts, which can enhance organizational relationships and foster cooperation between stakeholders. Soomro and Zhang (2015) evaluated the key factors contributing to relationship failures in 35 PPP projects, identifying critical issues such as communication breakdowns and misaligned objectives [68]. They proposed an improvement mechanism for partnerships that emphasizes the importance of establishing clear communication channels and aligning the interests of both parties. Liu et al. utilized principal-agent theory to analyze the relationship dynamics within PPP contracts, specifically focusing on incentive mechanisms designed to reduce opportunistic behavior [69]. Their findings suggest that well-structured incentive mechanisms are essential for minimizing conflicts of interest and ensuring that both parties remain committed to the project's success. Overall, these studies collectively highlight the complexity of organizational relationships in PPP projects and the necessity of adopting a multifaceted approach to relationship management. Future research should further explore the interplay between relationship quality and project outcomes, investigating how different management strategies can enhance collaboration and reduce the risk of conflicts.

### 5.1.3. Financing strategies

Research on financing within the PPP framework encompasses several key areas, including financing sources, financing strategies, and financing risk assessments. Wang et al. investigated the primary financing sources utilized in the construction of sponge city projects in China, highlighting the importance of innovative financing mechanisms that leverage both public and private resources [70]. The findings illustrate how local governments can collaborate with private entities to secure funding, which is crucial for the successful implementation of large-scale infrastructure projects. Liu and Wilkinson conducted a comparative analysis of PPP projects in Hong Kong and New Zealand, identifying effective financing strategies that include robust business development, streamlined financing arrangements, comprehensive tender documentation, and an effective governance structure for PPP consortia [71]. This comparative approach provides valuable insights into how different regulatory environments and market conditions influence financing strategies, ultimately impacting the success of PPP projects. Additionally, Li et al. analyzed the risk implications associated with various parameters in PPP project financing, including capital structure, asset income, and volatility [72]. The study emphasizes the critical need for thorough risk assessments to understand how these factors can affect the overall financial viability of PPP initiatives. In summary, the evolving landscape of PPP financing underscores the importance of strategic collaboration between public and private sectors. Future research should focus on further delineating the relationships between financing strategies and project outcomes, as well as exploring the effectiveness of different risk assessment methodologies. By advancing this understanding, stakeholders can better navigate the complexities of financing within PPP frameworks, ultimately leading to more successful project delivery.

## 5.2. Discussion of total cited clustering

Using CiteSpace, we conduct a comprehensive analysis of copolymerization types within the Web of Science

(WOS) core journals, focusing on 1,494 published papers from 1999 to 2018. The analysis employs a time slice of one year, with three key thresholds set at default values: reference frequency (c) at 2, resonant frequency (cc) at 2, and coefficient (CCV) set at 20 for the initial period, (5, 4, 20) for the second, and (4, 3, 20) for the third. The results, illustrated in the timeline view shown in **Figure 9** and **Table 10**, reveal that nodes #0, #2, and #3 represent the three core matrices within the field of PPP research, demonstrating sustained relevance over time. These matrices encapsulate critical areas of inquiry and persist throughout the analysis period. Given their prominence, this study focuses on the research content associated with these three matrices.

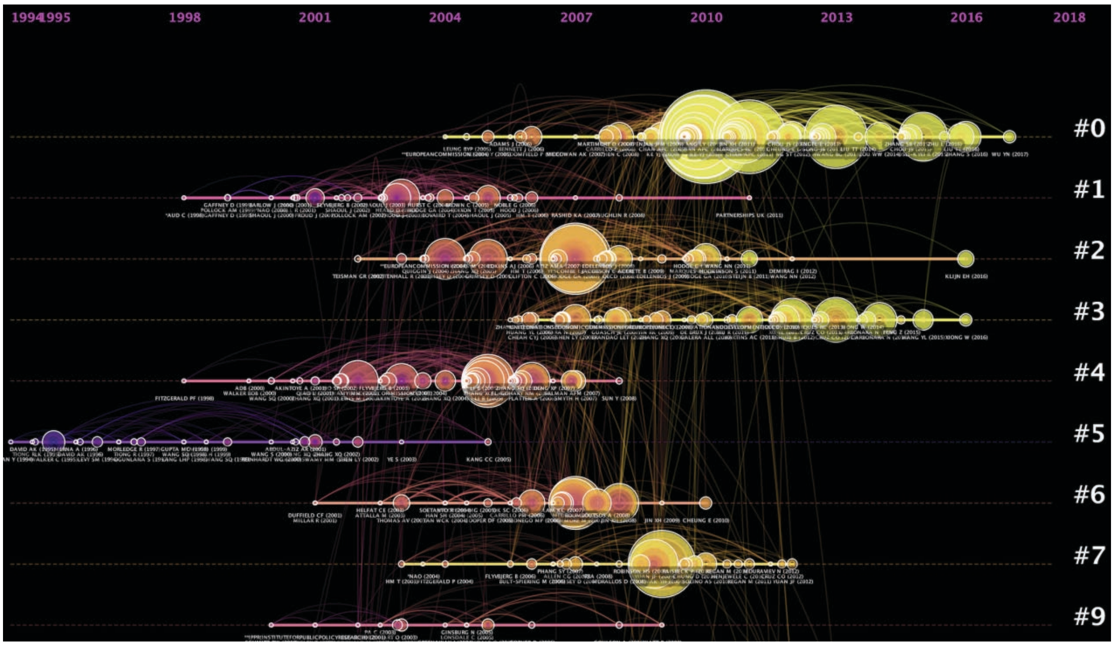


**Figure 9.** References cited clustering analysis the time line of the view

**Table 10.** Co-cited clustering matrix analysis of references

| Cluster ID | Document | Silhouette value |
|---|---|---|
| 0 | Public-private partnership | 0.719 |
| 1 | Pfi process | 0.819 |
| 2 | Harnessing market competition | 0.767 |
| 3 | PPP toll road | 0.796 |
| 4 | Construction industry | 0.7 |
| 5 | Public-private partnered project | 0.956 |
| 6 | Efficient risk allocation | 0.831 |
| 7 | Capital market collapse | 0.864 |
| 9 | Private finace initiative | 0.942 |
| 10 | Slow adoption | 0.87 |
| 11 | PFI project | 0.991 |
| 12 | UK private finance initiative | 0.994 |
| 13 | Operate-transfer scheme | 0.996 |
| 14 | Facing management choice | 0.993 |
| 18 | Ria model | 0.99 |

### 5.2.1. #0 successful factors of PPP

The clustering theme #0 centers on analyzing key factors and identifying risks associated with the success of Public-Private Partnership (PPP) projects. This analysis employs principal-agent theory to examine the relationships among PPP project partners, incorporating case studies that assess social capital capabilities and financial evaluations. These evaluations form the foundation for risk sharing within the PPP contract structure. Additionally, the client's contract framework serves as a critical basis for leveraging social capital in executing PPP projects [73]. Building on this foundation, some scholars explore the role of Special Purpose Entities (SPEs) utilized in PPP arrangements for mega projects. The integration of law, finance, and project management constitutes the fundamental elements of the contract framework in constructing SPEs [74]. Furthermore, research on project success and risk factor identification predominantly focuses on infrastructure projects related to energy, transportation, water conservancy, and healthcare. Among these, five critical success factors emerge: project feasibility, project environment, project company, project contractor, and project suppliers [14]. In energy projects, the most significant success factors include the necessity of the project, the expected debt repayment capacity, the competency of personnel from the developer, the financial capacity of the contractor, and the level of project financing management [75]. Conversely, the risks impacting PPP projects encompass various dimensions, with critical factors identified as political risk, legal risk, government credit risk, market demand fluctuations, inflation risk, and product price risk [76]. It is important to note that the risks associated with different types of projects may vary. For instance, quasi-revenue projects are exposed to additional risks such as nationalization/default, lack of supporting infrastructure, and public opposition [77]. This body of research often employs case study methodologies to provide in-depth insights into these complex dynamics [15]. By systematically identifying and analyzing these factors, researchers contribute to a more nuanced understanding of the determinants of success and the associated risks in PPP projects.

### 5.2.2. #2 financing proposal for PPP

The focal point of cluster #2 is the financing theory surrounding PPP. This encompasses a thorough examination of financing methods, risk analysis, practical evaluations of financing plans, and feasibility assessments of business investments. Such research often draws on existing PPP case studies, integrating comparable instances to analyze practical outcomes. In their analysis of social capital's role in financing, Silvestre and De Araujo compared two types of PPP projects in Portugal—highway and water supply projects—highlighting the varying degrees of enthusiasm and resistance toward social capital participation in these contexts [78]. Practical analyses of Private Finance Initiatives (PFI) frequently involve comparisons between healthcare and transportation projects. Henjewele et al. argued that the expertise of the private sector can enhance cost, time, and risk performance in public projects, although they also emphasize the persistent financing challenges faced by these initiatives [79]. Wang et al. utilized a Generalized Linear Model (GLM) to explore the impact of competitive bidding, transaction costs, contract types, and deadlines on private investment levels in PPPs [80]. The findings indicated that higher levels of asset specificity and greater surplus control rights for private investors correlate positively with the likelihood of private investment, particularly in the context of competitive bidding. Pantelias and Zhang contributed to this discourse by proposing a financing analysis framework that employs various sensitivity and scenario analyses to assess the feasibility of project financial evaluations [81]. Moreover, this body of research often investigates the financing dynamics between social capital and governmental entities. Consequently, the matrix incorporates extensive studies on the relationships inherent in PPPs. For instance, Warsen et al. conducted a multi-level analysis using survey data from 144 stakeholders involved in Dutch PPP projects, revealing that trust and effective management are closely linked to project cooperation [82]. Additionally, the matrix engages in a complex analysis of relationship governance, recognizing the inherent challenges within PPP structures. Relevant studies highlight that PPPs represent intricate infrastructure projects characterized by ambiguous responsibilities between public and private partners, leading to a complex governance framework [83]. Such insights underscore the necessity for robust governance structures to facilitate collaboration and mitigate risks within PPP projects.

#### 5.2.3. #3 franchise period

The inherent characteristics of long cycles, irreversibility, and high uncertainty in PPP projects often lead to the undervaluation of concessions in project evaluations. Consequently, cluster #3 aggregates studies that analyze the value generated during the concession period. This includes discussions on the optimal duration of the concession, flow forecasts during this period, cooperative optimization strategies, and revenue equivalence. Lv et al. proposed an alternative model designed to address the inflexibility of traditional Net Present Value (NPV) management, enabling a more effective determination of the optimal concession period for Build-Operate-Transfer (BOT) transportation projects [84]. Another significant challenge is the accurate measurement of the concession period, particularly in forecasting traffic volumes. Phong et al. utilized the Geometric Brownian Motion (GBM) process to estimate traffic volume for transportation projects, employing a Monte Carlo simulation technique to analyze various scenarios [85]. This stochastic approach allows for a systematic examination of traffic volume fluctuations, providing more reliable estimates for PPP projects. In addition to traffic forecasting, the analysis of revenue equivalence is critical for transportation projects. Repolho et al. constructed a cooperative optimization model aimed at ensuring profit for social capital while maximizing social welfare [86]. Furthermore, analyses related to the concession period also explore strategies to enhance the likelihood of social capital involvement through government decision-making, promoted the innovative capabilities of social capital via competitive gaming, and ensured long-term stability in the concession period through renegotiation mechanisms [87]. Most studies investigating the concession period of PPPs employ mathematical modeling paradigms, incorporating methods such as Bayesian analysis, Brownian motion, Monte Carlo simulations, and Nash equilibrium. These analytical frameworks provide robust tools for assessing the complexities associated with the concession period and optimizing project outcomes.

### 5.3. Discussion of total cited authors and literature journal

#### 5.3.1. Discussion of total cited authors

The analysis of total citations indicates that there are 29,938 referenced works, with the top 10 cited authors highlighted for their influence and frequency, as presented in **Table 11**. Among these, Zhang XQ from the Hong Kong University of Science and Technology emerges as the most prominent author, recognized for their pivotal contributions in identifying key success factors for the PPP model within infrastructure projects [88]. The study delineated five critical dimensions: economic viability, appropriate risk allocation through reliable contractual arrangements, sound financial packages, favorable investment environments, and the importance of a reliable concessionaire consortium with robust technical capabilities. While Zhang's classification method has provided significant insights, it has also influenced how subsequent studies categorize factors affecting PPP project performance, risk management, and regulatory challenges. Notably, recent scholarly attention has shifted towards understanding the factors that contribute to the early termination of PPP contracts. Scholars have suggested that accurately determining compensation mechanisms can mitigate the risks associated with early contract termination [89]. The second most-cited author, Li B has also made substantial contributions to the field, though his specific contributions warrant further exploration [90]. Following him, Grimsey D stands out for establishing methodologies related to PPP risk assessment and the valuation of project finance, as detailed in his seminal works [91,92]. This evolving discourse around PPP highlights the importance of adaptive frameworks that can account for the complexities of risk, performance, and contractual obligations. Further investigation into the interplay between these factors will enhance the understanding of PPP dynamics and inform best practices in project management.

**Table 11.** Influence of the top 10 co-cited authors and frequency

| Author | Centrality | Year | Frequency |
|---|---|---|---|
| Zhang XQ | 0.06 | 2002 | 241 |
| Li B | 0.15 | 2006 | 195 |
| Grimsey D | 0.15 | 2006 | 179 |
| Hodge GA | 0.05 | 2007 | 158 |
| Chan APC | 0.04 | 2010 | 143 |
| World B | 0.01 | 2006 | 138 |
| Akintoye A | 0.06 | 2005 | 134 |
| Lewis M | 0.12 | 2006 | 124 |
| Ke YJ | 0.01 | 2010 | 121 |
| Hm T | 0.06 | 2003 | 116 |

**Table 12.** Literature publications top 10

| Journals | Count |
|---|---|
| Journal of Management in Engineering | 52 |
| International Journal of Project Management | 51 |
| Journal of Construction Engineering and Management | 43 |
| Journal of Construction Engineering and Management ASCE | 38 |
| Transportation Research Record | 31 |
| Public Money Management | 30 |
| Sustainability | 27 |
| Journal of Infrastructure Systems | 23 |
| International Journal of Strategic Property Management | 18 |
| Public Management Review | 18 |

### 5.3.2. Discussion of literature journal analysis

**Table 12** presents the top 10 journals ranked by their contributions to the literature on PPP. The Journal of Management in Engineering holds the top position, emphasizing contemporary issues in civil engineering management through case studies, technical descriptions, and engineering practices. The journal's focus on PPP hotspots is primarily manifested through empirical case studies and practical engineering applications. Recent publications have highlighted critical topics such as PPP relationship governance [93], risk perception in PPP contexts [94], and specific case studies centered on PPP implementations in China [95–97]. Ranking second, the International Journal of Project Management concentrates on softer scientific issues within the realm of project management. The journal frequently addresses vital topics relevant to PPP, including risk management, project success factors, and the incentives that drive participant engagement. This emphasis reflects a growing recognition of the intricate dynamics influencing PPP outcomes. In addition to these leading journals, Transportation Research

Record, Public Money Management, and Public Money Management also demonstrate a keen interest in PPP research outside the primary domain of project management. Transportation Research Record specifically targets PPP research related to transportation projects, providing valuable insights into the unique challenges and solutions within this sector. Public Management Review explores financing issues pertinent to public management projects, while Public Money Management focuses on governmental decision-making processes, underscoring the critical role of policy frameworks in facilitating successful PPP implementations. Collectively, these journals contribute to a comprehensive understanding of the diverse aspects of PPP, ranging from theoretical explorations to practical applications, and highlight the multifaceted nature of collaboration between public and private entities.

## 6. Conclusion

In this study, based on reviewing the basic concepts of PPP, CiteSpace software is used to quantitatively visualize and analyze the papers dealing with PPP research in the selected journals during the last 20 years from 1999 to 2018, which mainly include authors, journals, countries, regions, institutions, keywords, and references. The conclusions are obtained as follows.

Firstly, the focus of research on PPP has evolved significantly from 1999 to 2018. While early studies focused on traditional models such as Build-Operate-Transfer (BOT) and Private Finance Initiative (PFI), later studies show an expansion into different areas such as risk management, policy analysis, and project governance. This transformation reflects the growing complexity and multifaceted nature of PPP projects in contemporary research. The main themes of PPP-related infrastructure research cover a wide range of projects, including road construction, water treatment, waste recycling, and urban transport. In addition, key models such as revenue sharing and risk management are at the center of the discussion. The later phase of the study (2014–2018) in particular highlights the growing emphasis on the role of project governance and government regulation in PPP, with a focus on the effectiveness of legal frameworks governing contracts and policy implementation, suggesting that governance challenges are becoming a central concern for researchers, a trend that underscores the importance of understanding the regulatory and institutional contexts that influence the outcomes of PPP.

Secondly, there is a growing academic interest in the development of PPP in China and a significant transformation in the interest in understanding the unique regulatory and financing environment that affects PPP projects, with future research increasingly exploring the interplay between government regulations and private financing in the context of China. The diversity of PPP research themes reveals a variety of key research topics within the PPP framework, including risk management, performance evaluation, contractual flexibility, and government decision-making. Notably, studies on BOT models and private financing mechanisms are prevalent, indicating that researchers are actively addressing the theoretical and practical challenges associated with the implementation of PPP in different sectors. Chinese academia is the major contributor to PPP research, accounting for 28.78% of total publications. This remarkable output reflects China's rapid economic growth and infrastructural development, which have made the country a central player in the development of PPP practice globally, and underscores the critical role of policy orientation in promoting PPP research and implementation. Between 2013 and 2017, the Chinese government's new urbanization planning and other initiatives stimulated a significant increase in academic activity, making this topic a prominent focus of the PPP field.

Finally, the PPP knowledge framework highlights the interrelated themes of risk management, relationship dynamics, and financing strategies, further reflecting the complexity and multifaceted nature of PPP projects. Effective risk management becomes the cornerstone of successful PPP implementation, but also an important process that influences the outcome of the project. Collaborative risk-sharing mechanisms are essential to enhance project sustainability and stakeholder confidence. Relationship dynamics within the PPP knowledge framework as key determinants reveal that the quality of the relationship between public and private entities is critical to the success of a PPP project. Effective communication, aligned goals, and well-designed incentives are necessary to promote trust and cooperation. Financing strategies within the PPP knowledge framework are evolving, with increasing emphasis on innovative financing mechanisms that utilize public and private resources. Comparative analyses demonstrate how different regulatory environments affect the relevant strategies, highlighting the need for robust risk assessments to measure their impact on project viability. The emphasis on strategic partnerships in financing highlights the importance of cooperation in addressing the complexity of large infrastructure projects.

## 7. Limitation

Although this study provides some guidance for future research on PPP to some extent, some objective factors in the research process may mislead future research. Therefore, to avoid this problem, here is an overview of three main constraints: first, the finiteness of data sources. Although our data cover the most important ones in the PPP field, the data source of this study firstly locates eight restricted journals in Scopus data, and some important journals may not be taken into account, resulting in a small number for research and analysis. Secondly, the limitation of software function. CiteSpace cannot directly process the content of citations, so it needs to manually analyze and explain the details of important articles. This process is time-consuming and relatively prone to errors. Finally, the limitations of information transmission. Since the information provided by the analysis results of data sources and CiteSpace is only a brief introduction to the paper, compared with obtaining all the information through full-text reading, this analysis method may cause the loss of key details in the full text. Therefore, the above three limitations remain to be further studied and solved.


## Funding

The research was supported by the following projects:

(1) Philosophy and Social Sciences Planning Leading Group of Guangdong Province (Project No. GD21CGL31).

(2) Research Projects of Department of Education of Guangdong Province (Project No. 2023WCXTD037).


## Disclosure statement

The authors declare no conflict of interest.

## References


[1] Al-Sharif F, Kaka A, 2004, PFI/PPP Topic Coverage in Construction Journals. Proc., ARCOM Conf., F. Khosrowshahi. ed., Vol, 1, Heriot-Watt Univ., Edinburgh, U.K., 2004: 711–719.

[2] Ke YJ, Wang SQ, Albert PCC, et al., 2009, Research Trend of Public-Private Partnership in Construction Journals. Journal of Construction Engineering and Management, 135(10): 1076–1086.

[3] Castro e Silva ND, Oliveira CC, Fernanda R, et al., 2016, Bibliometric Analysis of PPP and PFI Literature: Overview of 25 Years of Research. Journal of Construction Engineering and Management, 142(10).

[4] Tang L, 2010, A Review of Studies on Public-Private Partnership Projects in the Construction Industry. International Journal of Project Management, 28(7): 683–694.

[5] Savas ES, 2000, Privatization and Public-Private Partnerships. CQ Press, U.K.

[6] Sagalyn LB, 2007, Public/Private Development: Lessons From History, Research, and Practice. Journal of the American Planning Association, 73(1): 7–22.
[7] Grimsey D, Lewis MK, 2004, Public Private Partnerships: The Worldwide Revolution in Infrastructure Provision and Project Finance. Edward Elgar, U.K.
[8] Shen LY, Platten A, Deng XP, 2006, Role of Public Private Partnerships to Manage Risks in Public Sector Projects in Hong Kong. International Journal of Project Management, 24(7): 587–594.
[9] Li B, Akintoye A, Edwards PJ, et al., 2005, The Allocation of Risk in PPP/PFI Construction Projects in the UK. International Journal of Project Management, 23(1): 25–35.
[10] Ho SP, 2006, Model for Financial Renegotiation in Public–Private Partnership Projects and its Policy Implications: Game Theoretic View. Journal of Construction Engineering and Management, 132(7): 678–688.
[11] Cumming D, 2007, Government Policy Towards Entrepreneurial Finance. Innovation Investment Funds. Journal of Business Venturing, 22(2): 193–235.
[12] Algarni AM, Arditi D, Polat G, 2007, Build–Operate–Transfer in Infrastructure Projects in the United States. Journal of Construction Engineering and Management, 133(10): 28–735.
[13] Edkins AJ, Smyth HJ, 2006, Contractual Management in PPP Projects: Evaluation of Legal Versus Relational Contracting for Service Delivery. Journal of Professional Issues in Engineering Education and Practice, 132(1): 82–93.
[14] Chan APC, Lam PTI, Chan DWM, et al., 2010, Critical Success Factors for PPPs in Infrastructure Developments: Chinese Perspective. Journal of Construction Engineering and Management, 136: 484–494.
[15] Chan APC, Lam PTI, Wen Y, et al., 2015, Cross-Sectional Analysis of Critical Risk Factors for PPP Water Projects in China. Journal of Infrastructure Systems, 21: 10.
[16] Osei-kyei R, Chan APC, Javed AA, et al., 2017, Critical Success Criteria For Public-Private Partnership Projects: International Experts' Opinion. International Journal of Strategic Property Management, 21: 87–100.
[17] Teng TL, Yuan JF, Li QM, 2015, System Dynamics Balance Model to Achieve Tripartite Satisfaction in Public Private Partnership Projects, Destech Publications, Inc., Lancaster.
[18] Xiong W, Yuan JF, Li QM, et al., 2015, Performance Objective-Based Dynamic Adjustment Model to Balance the Stakeholders' Satisfaction in PPP Projects. Journal of Civil Engineering and Management, 21: 539–547.
[19] Xiong W, Zhang XQ, 2014, Concession Renegotiation Models for Projects Developed through Public-Private Partnerships. Journal of Construction Engineering and Management, 140.
[20] Xiong W, Zhang XQ, 2016, The Real Option Value of Renegotiation in Public-Private Partnerships. Journal of Construction Engineering and Management, 142.
[21] Liu JX, Love PED, Davis PR, et al., 2015, Conceptual Framework for the Performance Measurement of Public-Private Partnerships. Journal of Infrastructure Systems, 21.
[22] Liu JX, Love PED, Sing MCP, et al., 2017, PPP Social Infrastructure Procurement: Examining the Feasibility of a Lifecycle Performance Measurement Framework. Journal of Infrastructure Systems, 23.
[23] Liu JX, Love PED, Smith J, et al., 2015, Life Cycle Critical Success Factors for Public-Private Partnership Infrastructure Projects. Journal of Management in Engineering, 31.
[24] Feng Z, Zhang SB, et al., 2015, Modeling the Impact of Government Guarantees on Toll Charge, Road Quality and Capacity for Build-Operate-Transfer (BOT) Road Projects. Transportation Research Part a-Policy and Practice, 78: 54–67.
[25] Song JB, Jin LL, Zhao YP, et al., 2017, Using Bargaining-Game Model to Negotiate Compensation for the Early Termination of BOT Highway Projects. Transportation Research Part a-Policy and Practice, 105: 197–209.
[26] Song JB, Song DR, et al., 2015, Modeling the Concession Period and Subsidy for BOT Waste-to-Energy Incineration

Projects. Journal of Construction Engineering and Management, 141.

[27] Zhang YW, Feng Z, Zhang SB, 2018, The Effects of Concession Period Structures on BOT Road Contracts. Transportation Research Part a-Policy and Practice, 107: 106–125.

[28] Carpintero S, Petersen OH, 2016, Public-Private Partnerships (PPPs) in Local Services: Risk-Sharing and Private Delivery of Water Services in Spain. Local Government Studies, 42: 958–979.

[29] Van Den Hurk M, Brogaard L, Lember V, et al., 2016, National Varieties of Public-Private Partnerships (PPPs): A Comparative Analysis of PPP-Supporting Units in 19 European Countries. Journal of Comparative Policy Analysis, 18: 1–20.

[30] Verhoest K, Petersen OH, Scherrer W, et al., 2015, How Do Governments Support the Development of Public Private Partnerships? Measuring and Comparing PPP Governmental Support in 20 European Countries. Transport Reviews, 35: 118–139.

[31] Cruz CO, Marques RC, 2013, Flexible Contracts to Cope with Uncertainty in Public-Private Partnerships. International Journal of Project Management, 31: 473–483.

[32] Martins J, Marques RC, Cruz CO, 2014, Maximizing the Value for Money of PPP Arrangements through Flexibility: An Application to Airports. Journal of Air Transport Management, 39: 72–80.

[33] Colla P, Hellowell M, Vecchi V, et al., 2015, Determinants of the Cost of Capital for Privately Financed Hospital Projects in the UK. Health Policy, 119: 1442–1449.

[34] Vecchi V, Hellowell M, 2013, Securing a Better Deal From Investors in Public Infrastructure Projects Insights from Capital Budgeting. Public Management Review, 15: 109–129.

[35] Vecchi V, Hellowell M, Croce RD, et al., 2017, Government Policies to Enhance Access to Credit for Infrastructure-Based PPPs: An Approach to Classification and Appraisal. Public Money & Management, 37: 133–140.

[36] Geddes RR, Reeves E, 2017, The Favourability of US PPP Enabling Legislation and Private Investment in Transportation Infrastructure. Utilities Policy, 48: 157–165.

[37] Palcic D, Reeves E, Stafford A, 2018, Lifting the Lid: The Private Financing of Motorway PPPs in Ireland. Economic and Social Review, 49: 217–239.

[38] Wan G, Morgan PJ, Barro RJ, 2016, Economic Growth and Convergence, Applied to China. China & World Economy, 24(5): 5–19.

[39] Zhang LJ, 2017, Standardization is the Key to China Becoming the World’s Largest PPP Market. China Economic Weekly, 2017(37): 34–37.

[40] Verweij S, 2015, Producing Satisfactory Outcomes in the Implementation Phase of PPP Infrastructure Projects: A Fuzzy Set Qualitative Comparative Analysis of 27 Road Constructions in the Netherlands. International Journal of Project Management, 33: 1877–1887.

[41] Patsiadas P, Angelides DC, 2017, Negotiation System for PPP Infrastructure Contracts. International Journal of Management and Decision Making, 16: 151–171.

[42] Attarzadeh M, Chua DKH, Beer M, et al., 2017, Options-Based Negotiation Management of PPP–BOT Infrastructure Projects. Construction Management and Economics, 35: 676–692.

[43] Pradhan RP, Verma A, Dash S, et al., 2017, Critical Success Factors for PPP Infrastructure Projects in India. Wegman F, Dell’acqua G, eds, International Congress on Transport Infrastructure and Systems, TIS 2017. CRC Press/Balkema, 2017: 485–491.

[44] Wang Y, Liu J, 2015, Evaluation of the Excess Revenue Sharing Ratio in PPP Projects Using Principal-Agent Models. International Journal of Project Management, 33: 1317–1324.

[45] Xu Y, Sun C, Skibniewski MJ, et al., 2012, System Dynamics (SD)-Based Concession Pricing Model for PPP Highway Projects. International Journal of Project Management, 30: 240–251.

[46] Ameyaw C, Adjei-kumi T, Owusu-manu DG, 2015, Exploring Value for Money (VfM) Assessment Methods of Public-Private Partnership Projects in Ghana: A Theoretical Framework. Journal of Financial Management of Property and Construction, 20: 268–285.

[47] Singh LB, Kalidindi SN, 2006, Traffic Revenue Risk Management Through Annuity Model of PPP Road Projects in India. International Journal of Project Management, 24: 605–613.

[48] Zhang Y, Feng J, Yang S, 2017, Allocation of Control Rights in the PPP Project: A Cooperative Game Model. 2017 3rd International Conference on Advances in Energy, Environment and Chemical Engineering, AEECE 2017. Institute of Physics Publishing.

[49] Carbonara N, Costantino N, Pellegrino R, 2014, Concession Period for PPPs: A Win-Win Model for a Fair Risk Sharing. International Journal of Project Management, 32: 1223–1232.

[50] Jephcote C, Chen H, Ropkins K, 2016, Implementation of the Polluter-Pays Principle (PPP) in Local Transport Policy. Journal of Transport Geography, 55: 58–71.

[51] Wibowo A, Permana A, Kochendörfer B, et al., 2012, Modeling Contingent Liabilities Arising from Government Guarantees in Indonesian BOT/PPP Toll Roads. Journal of Construction Engineering and Management, 138: 1403–1410.

[52] Zhang X, 2004, Improving Concessionaire Selection Protocols in Public/ Private Partnered Infrastructure Projects. Journal of Construction Engineering and Management, 130: 670–679.

[53] Braadbaart O, Zhang M, Wang Y, 2009, Managing Urban Wastewater in China: A Survey of Build-Operate-Transfer Contracts. Water and Environment Journal, 23: 46–51.

[54] Zhang XQ, Kumaraswamy MM, 2001, Procurement Protocols for Public-Private Partnered Projects. Journal of Construction Engineering and Management, 127: 351–358.

[55] Clifton C, Duffield CF, 2006, Improved PFI/PPP Service Outcomes through the Integration of Alliance Principles. International Journal of Project Management, 24: 573–586.

[56] Eaton D, Akabiyikli R, Dickinson M, 2006, An Evaluation of the Stimulants and Impediments to Innovation within PFI/PPP Projects. Construction Innovation, 6: 63–67.

[57] Smyth H, Edkins A, 2007, Relationship Management in the Management of PFI/PPP Projects in the UK. International Journal of Project Management, 25: 232–240.

[58] Fischer K, Leidel K, Riemann A, et al., 2010, An Integrated Risk Management System (IRMS) for PPP Projects. Journal of Financial Management of Property and Construction, 15: 260–282.

[59] Chou JS, Tserng HP, Lin C, et al., 2012, Critical Factors and Risk Allocation for PPP Policy: Comparison between HSR and General Infrastructure Projects. Transport Policy, 22: 36–48.

[60] Sabry MI, 2015, Good Governance, Institutions and Performance of Public Private Partnerships. International Journal of Public Sector Management, 28: 566–582.

[61] Umar AA, Zawawi NAWA, Abdul-aziz AR, 2018, Exploratory Factor Analysis of Skills Requirement for PPP Contract Governance. Built Environment Project and Asset Management.

[62] Ke YJ, Wang SQ, Albert PCC, et al., 2010, Preferred Risk Allocation in China's Public-Private Partnership (PPP) Projects. International Journal of Project Management, 28(5): 482–492.

[63] Chan APC, Lam PTI, Chan DWM, et al., 2010, Potential Obstacles to Successful Implementation of Public-Private Partnerships in Beijing and the Hong Kong Special Administrative Region. Journal of Management in Engineering, 26: 30–40.

[64] Tang LY, 2010, A Review of Studies on Public-Private Partnership Projects in the Construction Industry. International Journal of Project Management, 28(7): 683–694.

[65] Bing L, Akintoye A, Edwards PJ, et al., 2005, The Allocation of Risk in PPP/PFI Construction Projects in the UK.

International Journal of Project Management, 23: 25–35.

[66] Ke Y, Wang S, Chan APC, et al., 2010, Preferred Risk Allocation in China's Public-Private Partnership (PPP) Projects. International Journal of Project Management, 28: 482–492.

[67] Iossa E, Martimort D, 2015, The Simple Microeconomics of Public-Private Partnerships. Journal of Public Economic Theory, 17: 4–48.

[68] Soomro MA, Zhang X, 2015, Roles of Private-Sector Partners in Transportation Public-Private Partnership Failures. Journal of Management in Engineering, 31.

[69] Liu J, Gao R, Cheah CYJ, et al., 2016, Incentive Mechanism for Inhibiting Investors' Opportunistic Behavior in PPP Projects. International Journal of Project Management, 34: 1102–1111.

[70] Wang Y, Sun M, Song B, 2017, Public Perceptions of and Willingness to Pay for Sponge City Initiatives in China. Resources, Conservation and Recycling, 122: 11–20.

[71] Liu T, Wilkinson S, 2014, Large-Scale Public Venue Development and the Application of Public-Private Partnerships (PPPs). International Journal of Project Management, 32: 88–100.

[72] Li S, Abraham D, Cai H, 2017, Infrastructure financing with Project Bond and Credit Default Swap under Public-Private Partnerships. International Journal of Project Management, 35: 406–419.

[73] Hellowell M, Vecchi V, 2015, The Non-Incremental Road to disaster? A Comparative Policy Analysis of Agency Problems in the Commissioning of Infrastructure Projects in the UK and Italy. Journal of Comparative Policy Analysis: Research and Practice, 17: 519–532.

[74] Sainati T, Brookes N, Locatelli G, 2017, Special Purpose Entities in Megaprojects: Empty Boxes or Real Companies? Project Management Journal, 48: 55–73.

[75] Zhao ZY, Zuo J, Zillante G, et al., 2010, Critical Success Factors for BOT Electric Power Projects in China: Thermal Power Versus Wind Power. Renewable Energy, 35: 1283–1291.

[76] Xu Y, Yang Y, Chan AP, et al., 2011, Identification and Allocation of Risks Associated with PPP Water Projects in China. International Journal of Strategic Property Management, 15: 275–294.

[77] Xu YL, Chan APC, Xia B, et al., 2015, Critical Risk Factors Affecting the Implementation of PPP Waste-to-Energy Projects in China. Applied Energy, 158: 403–411.

[78] Silvestre HC, De Araujo J, 2012, Public-Private Partnerships/Private Finance Initiatives. Portugal Theory, Practice, and Results. Public Performance & Management Review, 36: 316–339.

[79] Henjewele C, Sun M, Fewings P, 2014, Comparative Performance Of Healthcare and Transport PFI Projects: Empirical Study on the Influence of Key Factors. International Journal of Project Management, 32: 77–87.

[80] Wang HM, Chen B, Xiong W, et al., 2018, Commercial Investment in Public-Private Partnerships: The Impact of Contract Characteristics. Policy and Politics, 46: 589–606.

[81] Pantelias A, Zhang ZM, 2010, Methodological Framework for Evaluation of Financial Viability of Public-Private Partnerships: Investment Risk Approach. Journal of Infrastructure Systems, 16: 241–250.

[82] Warsen R, Nederhand J, Klijn EH, et al., 2018, What Makes Public-Private Partnerships Work? Survey Research into Ill Outcomes and the Quality of Cooperation in PPPs. Public Management Review, 20: 1165–1185.

[83] Van Gestel K, Willems T, Verhoest K, et al., 2014, Public-Private Partnerships in Flemish Schools: A Complex Governance Structure in a Complex Context. Public Money & Management, 34: 363–370.

[84] Lv JN, Ye G, Liu W, et al., 2015, Alternative Model for Determining the Optimal Concession Period in Managing BOT Transportation Projects. Journal of Management in Engineering, 31: 7.

[85] Phong NT, Likhitruangsilp V, Onishi M, 2017, Developing a Stochastic Traffic Volume Prediction Model for Public-Private Partnership Projects. Saloma, Borgan WR, Buntoro F, et al., (eds.) 3rd International Conference on Construction and Building Engineering. Melville: Amer Inst Physics.

[86] Repolho HM, Antunes AP, Church RL, 2016, PPP Motorway Ventures—An Optimization Model to Locate Interchanges with Social Welfare and Private Profit Objectives. Transportmetrica a-Transport Science, 12: 832–852.
[87] De Clerck D, Demeulemeester E, 2016, An Ex Ante Bidding Model to Assess the Incentive Creation Capability of a Public-Private Partnership Pipeline. International Journal of Project Management, 34: 117–131.
[88] Zhang XQ, 2005, Critical Success Factors for Public-Private Partnerships in Infrastructure Development. Journal of Construction Engineering and Management, 131: 3–14.
[89] Wei X, Zhang X, 2014, Compensation Approaches for Early Termination of PPP Projects.
[90] Li B, Akintoye A, Edwards PJ, et al., 2005, Critical Success Factors for PPP/PFI Projects in the UK Construction Industry. Construction Management and Economics, 23(5): 459–471.
[91] Grimsey D, Lewis MK, 2002, Evaluating the Risks of Public Private Partnerships for Infrastructure Projects. International Journal of Project Management, 20: 107–118.
[92] Grimsey D, Lewis MK, 2005, Are Public Private Partnerships Value for Money?: Evaluating Alternative Approaches and Comparing Academic and Practitioner Views. Accounting Forum, 29: 345–378.
[93] Carrillo de Albornoz VA, Millan JM, Solino AS, 2018, Managing a Portfolio of Public-Private Partnerships: Concessionaire Perspective. Journal of Management in Engineering, 34.
[94] Khallaf R, Naderpajouh N, Hastak M, 2018, Modeling Three-Party Interactional Risks in the Governance of Public-Private Partnerships. Journal of Management in Engineering, 34.
[95] Song J, Hu Y, Feng Z, 2018, Factors Influencing Early Termination of PPP Projects in China. Journal of Management in Engineering, 34.
[96] Wang L, Zhang X, 2018, Bayesian Analytics for Estimating Risk Probability in PPP Waste-to-Energy Projects. Journal of Management in Engineering, 34.
[97] Yuan J, Li W, Zheng X, et al., 2018, Improving Operation Performance of Public Rental Housing Delivery by PPPs in China. Journal of Management in Engineering, 34.

**Publisher's note**

Bio-Byword Scientific Publishing remains neutral with regard to jurisdictional claims in published maps and institutional affiliations.

Journal of Architectural Research and Development, 2025, Volume 9, Issue 1
https://ojs.bbwpublisher.com/index.php/JARD
Online ISSN: 2208-3537
Print ISSN: 2208-3529

# Application of Deep Foundation Pit Construction Technology in Civil Engineering Construction

**Nan Jiang***

Zhejiang University of Science & Technology, Hangzhou 310023, Zhejiang Province, China

***Corresponding author:*** Nan Jiang, JJ57586627@163.com



**Abstract:** As one of the commonly used technologies in modern civil engineering, the construction technology is becoming more and more widely used with the continuous growth of building height. In the construction process of high-rise buildings, the deep foundation pit support provides the necessary stability for the foundation structure of the building project, and more effectively guarantees the quality of the project. Through the reasonable supporting structure, the deep foundation pit technology can effectively prevent the risk of soil collapse, foundation pit deformation and other risks, and improve the safety factor of the whole construction project. Especially in the high-rise buildings, the deep foundation pit support technology can consolidate the foundation for the long-term stability of the project, and significantly prolong the service life of the building. The continuous development of deep foundation pit construction technology is the inevitable demand of high-rise building construction, and also provides a powerful help for the development of civil engineering industry. Based on this, this paper focuses on the application of deep foundation pit construction technology in civil engineering construction.

**Keywords:** Civil engineering; Deep foundation pit construction technology; Application

**Online publication:** February 13, 2025

## 1. Foreword

Deep foundation pit construction technology is widely used in the construction of high-rise buildings and other projects. With the advancement of urbanization process, land resources are increasingly tight, and the demand for deep foundation pit project is increasing. In order to ensure the safety and stability in the construction process of deep foundation pit, the reasonable application of support technology is particularly important. Deep foundation pit support technology aims to prevent soil collapse, foundation pit deformation and other safety risks, and ensure the smooth construction through the effective support structure.

## 2. Analysis of the importance of deep foundation pit support construction

With the acceleration of the urbanization process, more and more building projects have begun to expand to the underground space, and deep foundation pit engineering has gradually become a common demand in modern building construction. However, the soil environment of the construction site is usually complex and changeable, and the geological conditions are quite different, which makes some soil layers cannot directly meet the requirements of the construction of high-rise buildings, and there may even be a risk of instability [1–5]. Therefore, the construction technology of deep foundation pit support arises at a historic moment. Strengthening the soil to avoid soil collapse, deformation, and other problems, provides a safe working environment for the subsequent construction. Common supporting technologies include concrete pile plates, steel sheet piles, concrete mixing piles, etc., which can effectively support the soil layer, prevent the surrounding ground subsidence, ensure the stability of the foundation pit, and prevent the penetration of groundwater and the movement of the soil. The choice of each support method needs to be formulated according to the specific geological conditions of the construction site, the surrounding environment, and the project scale.

In modern civil engineering projects, especially in the construction of deep foundation pit and large-diameter projects, the requirements of deep foundation pit support are getting higher and higher. With the continuous expansion of the project scale, the design and construction of the supporting structure often face greater challenges. The stability of deep foundation pit support is directly related to the safety of the whole project. Once the problem occurs in the foundation pit support structure, it may lead to soil collapse, affect the construction progress, and even bring serious safety accidents. Therefore, the construction team must calculate the carrying capacity of the supporting structure according to the actual situation of the site, and scientifically design the supporting system to ensure the safety and reliability of every step in the construction process. To solve the problem of soil layer stability, deep foundation pit support is more necessary to consider seepage prevention and waterproofing, to avoid the damage of groundwater infiltration to the foundation pit. Seepage prevention and reinforcement play an important role in this process. Commonly used technologies include wellpoint dewatering, dewatering well, and other methods, which can effectively reduce the risk of water accumulation in the foundation pit and reduce the influence of the hydrological environment on the supporting structure in the construction process [6–9].

However, the deep foundation pit support is not only designed to provide a temporary safety guarantee in the construction process but also plays an important role in the whole life cycle of the project. After the completion of the project, the foundation pit supporting structure usually needs to be removed. How to carry out the demolition operation and make reasonable use of the demolition materials has become a new topic. In the process of demolition, the recycling of materials directly affects the economic benefits of the project. The construction team needs to pay attention to how to reduce the waste of resources and improve the reuse rate of demolition materials, to achieve the goal of saving cost and reducing environmental pollution. In general, the construction team should reasonably select the support methods according to the needs of the specific project, to ensure the safety and stability of the project, and to maximize the overall benefit of the project. Under the condition of limited resources, through the scientific construction of the supporting structure, we can realize the maximum benefit of the project construction, and promote the development of modern civil engineering towards a safer, more efficient, and environmental protection direction.

## 3. Application of deep foundation pit construction technology in civil engineering construction

### 3.1. Construction technology of reverse arch wall support

The construction technology of reverse arch wall supports is constructed through various structural forms such as round or oval, which have high stability and can effectively resist the soil lateral pressure in the process of foundation pit excavation [10–15]. During the construction, the principle of layered construction from top to bottom must be followed, and the supporting structure of each layer needs to be accurately constructed to ensure the stability of the overall structure. However, in the construction process, if the arch cannot be successfully formed, the construction team should check the site situation in time, adjust the support scheme, and use the composite support system to provide additional support, to ensure the construction safety. Designers need to pay special attention to the water level change when determining the vector span ratio of the axis of the arch wall. If the water level in the foundation pit is too high, it may cause adverse effects on the bottom structure of the foundation pit, and even endanger the safety of the whole project in a serious case. Therefore, the construction team should implement effective water level control measures according to the precipitation situation, timely flow closure, prevent the occurrence of water accumulation phenomenon, and ensure the smooth construction of the reverse arch wall support.

### 3.2. Construction technology of concrete pouring pile

Concrete cast-in-place pile construction plays an important role in civil engineering, especially in deep foundation pit construction. The construction technology of concrete cast-in-place piles can effectively improve the underground seepage problem, effectively protect the pit wall of the foundation pit, reduce soil erosion, and ensure the safety of the construction process. Through the high-strength cement wall of the cast-in-place pile, the safety risks such as settlement and collapse can be significantly reduced, making the whole foundation pit structure more stable [16–19]. Compared with other supporting technologies, a significant advantage of concrete pile construction is rarely hole collapses in the construction process. To ensure smooth construction, the construction team needs to accurately calculate the pile spacing to avoid the problem of too dense or too thin piles. In the specific operation process, the construction personnel should focus on the analysis of the difficulties in the project, especially the slope protection problems, and take corresponding measures to solve them to ensure the stability of the civil engineering project structure. In the technical implementation, the team must carry out each step in strict accordance with the professional process, ensure the construction quality of the concrete cast-in-place pile, and control the quality of the project to prevent any accidents. Through reasonable construction technology, the concrete cast-in-place pile technology can effectively improve the overall stability of the deep foundation pit engineering, and ensure the smooth progress of the civil engineering project.

## 4. Construction of slope protection pile

To ensure the construction quality, the construction personnel should first carry out detailed site verification on the construction site, and make a feasible construction plan based on the site geological conditions and construction needs. In this process, the engineer in charge must fully master the construction technology and characteristics of the slope protection piles, and deeply understand the adaptability and performance of the piles under different construction environments, to ensure the safety and effectiveness of the supporting structure. Through the reasonable layout of the slope protection pile, the sliding and collapse of the pit wall can be effectively prevented, especially in unstable soil environments such as high water levels or soft soil layers. The slope protection pile plays a vital role in supporting it. The construction team should operate in strict accordance with the established supporting structure scheme to ensure that every link in the construction process is consistent with the design requirements, to ensure the smooth progress of the construction.

## 5. Construction technology of anchor bolt support

The anchor bolt support construction technology is widely used in deep foundation pit engineering and has good stability. This technique inserts the anchor rod deeply into the soil layer, which prevents the collapse and deformation of the foundation pit wall. In the actual construction process, it is necessary to accurately measure the site, and determine the layout position and quantity of the bolt, to ensure the rationality and safety of the supporting structure. The installation of the anchor rod not only needs to ensure that it is fixed firmly but also needs to strictly control its tilt angle and elevation to ensure the balanced distribution of its support force. The construction team should pay special attention to the accuracy of the drilling operation. If abnormal conditions are found, such as drilling deviation or soil instability, stop the operation immediately, conduct an on-site inspection, and adjust the technical scheme according to the specific problems [20].

## 6. Construction technology of soil nail wall

Soil nail wall construction technology is an important application method in deep foundation pit support, which is widely used in various soil environments. In the construction process, the design drawings of the project need to be carefully verified to ensure the reasonable layout of the drainage system to avoid water accumulation affecting the stability of the foundation pit soil. The design of a drainage system usually adopts a network format structure, which can effectively reduce soil erosion and enhance the bearing capacity of soil. During the installation of the large-diameter soil nail hole, the depth and position of the drilling hole must be strictly controlled to ensure that the soil nail hole is not affected by the surrounding environment and avoid the drilling deviation. Simultaneously, the construction team should ensure the quality of the soil nail material, especially the strength of the steel bar, to avoid rust or inferior materials, and affect the long-term stability of the soil nail wall. When welding the soil nail wall support, the construction personnel need to pay attention to the moderate mix ratio of the mortar, to ensure that it has enough bonding strength, and at the same time to pay attention to the combination strength of reinforcement and concrete. During the grouting operation, the grouting pressure and slurry fluidity must be accurately controlled to ensure that the cement slurry can fully penetrate the inside of the soil nail hole and form a solid support body. After grouting, the team shall check the grouting pipeline in time to remove impurities to ensure the smooth progress of subsequent operations. During the net operation, the construction team shall ensure that the wire mesh is welded firmly, select the appropriate drainage pipe material for installation, and conduct a quality inspection to ensure that the drainage function of the pipe meets the standard.

## 7. Pile row support technology

Pile row support technology provides the necessary support for the foundation pit through pile row to ensure safety in the construction process. Pile row can be divided into precast pile, slab pile, and cast-in-place pile, among which concrete cast-in-place pile becomes the most commonly used choice because of its good bearing capacity and adaptability. Generally, pile discharge technology is suitable for foundation pits ranging from 7 to 13 meters deep, and a detailed investigation of groundwater level, soil conditions, and other factors is required before construction. In some special circumstances, such as the requirements of the site conditions, the design scheme of a double-layer concrete cast-in-place pile may be adopted, and the construction sequence needs to be strictly controlled to ensure the coordination and stability between the pile foundations. The key point of pile row support lies in the layout density of the pile foundation. The drilling and piling operation must be rigorous to ensure that each pile can effectively withstand the pressure of the surrounding soil and prevent the collapse of the foundation pit. In the construction process, special attention should be paid to noise control, and reasonable selection of construction time, to avoid bringing unnecessary trouble to the surrounding residents. By taking noise prevention and control measures, the environmental protection of pile discharge technology can be effectively improved.

## 8. Epilogue

Deep foundation pit construction involves complex soil quality and hydrological conditions. Against this background, the application of various support technologies, such as reverse arch walls, concrete cast-in-place piles, and anchor bolt support, has gradually become an important means to ensure construction quality and safety. With the continuous development of technology, new construction methods are constantly introduced. However, the progress of technology does not mean that the accumulation of traditional experience can be ignored, especially the supporting technology in extreme environments, which needs to be flexibly adjusted according to the actual situation. The development of deep foundation pit construction technology should pay attention to the innovation of technology, but also strengthen the comprehensive consideration of environment and safety, and promote the integration of green construction concepts, to provide more efficient solutions for urban construction.

## Disclosure statement

The author declares no conflict of interest.

## References


[1] Yang X, 2024, Application of Deep Foundation Pit Construction Technology in Civil Engineering Construction. Popular Science, 45(3): 38–40.

[2] Qin J, 2024, Exploring the Application of Deep Foundation Pit Support Technology in Civil Engineering Housing Construction. Residential Industry, 2024 (3): 49–51.

[3] Duan H, 2016, Application Analysis of Deep Foundation Pit Supporting Construction Technology in Civil Engineering. Commodity and Quality, 000(027): 236.

[4] Hong J, 2024, Analysis of the Construction Technology of Earthwork Excavation of Deep Foundation Pit in Civil Engineering. Journal of Taiyuan City Vocational and Technical College, 2024(3): 46–48.

[5] Teng J, 2019, On the Application of Deep Foundation Pit Supporting Construction Technology in Civil Engineering. Building materials Decoration, 2019(9): 100–101.

[6] Hou M, 2024, Research on the Construction Technology of Deep Foundation Pit Support for Super High-Rise Buildings. Residential and Real Estate, 2024(11): 104–106.

[7] Ni H, 2017, Analysis of the Application of Deep Foundation Pit Construction Technology in Civil Engineering. Civil Engineering Technology and Design, 2017(14): 386.

[8] Zhang J, 2023, Analysis of the Application of Deep Foundation Pit Construction Technology in Civil Engineering. Sichuan Cement, 2023(8): 137–139.

[9] Peng J, 2023, Discussion on the Application of Deep Foundation Pit Construction Technology in Civil Engineering. Outdoor Equipment, 2023(3): 145–147.

[10] Liu Y, 2023, Discussion on Technical Quality Control of Building Civil Engineering. Volkswagen Standardization, 2023(4): 24–26.

[11] Yang L, 2023, Research on Key Technology of Oblique Alternating Combination Pile in Deep Large Foundation Pit Support. Engineering and Construction, 2023(4): 1219–1221.

[12] Wang X, Qiu L, Shen W, et al., 2023, Deformation Analysis of Multiring Beam Support in Deep Foundation Pit of Soft Soil. Low-temperature Building Technology, 2023(9): 67–70.

[13] Shang K, 2019, On the Application of the Construction Technology of Deep Foundation Pit Support in Civil Engineering. Doors and Windows, 2019(2): 45–46.

[14] Gan J, 2024, Application of Deep Foundation Pit Support Construction Technology in Construction Engineering.

Theoretical Research on Urban Construction, 2024(20): 139–141.
[15] Zhong XJ, 2023, Application of Foundation Pit Support Technology in Construction and Civil Engineering Construction. China Science and Technology Journal Database Industry A, 2023(1): 68–70.
[16] Zou Z, 2018, Application of Slope Support Technology in Civil Engineering Construction. Engineering Technology Research, 2018(2): 47–48.
[17] Chen Z, 2019, The Role of Deep Foundation Pit Support Construction Technology in High-Rise Buildings in Civil Engineering. Building Materials and Decoration, 2019(5): 14–15.
[18] Hu Z, 2023, Application Research on Deep Foundation Pit Support Technology in Civil Engineering Housing Construction, 2023(36): 15–17.
[19] Lu Z, 2023, Analysis of the Key Technology for the Design and Construction of a Deep Foundation Pit in a Complex Environment. Kehai Story Expo, 2023(9): 40–42.
[20] Wu W, 2023, Analysis on Slope Support Technology Based on Civil Engineering Construction. Sichuan Building Materials, 2023(9): 155–157.

Journal of Architectural Research and Development, 2025, Volume 9, Issue 1
https://ojs.bbwpublisher.com/index.php/JARD
Online ISSN: 2208-3537
Print ISSN: 2208-3529

# Research Progress on Earthquake Collapse Resistance of Reinforced Concrete Frame Structures

**Haibing Liu** [1,2], **Junqi Lin**[1,2]*, **Jinlong Liu**[1,2]

[1]Institute of Engineering Mechanics, China Earthquake Administration, Harbin 150080, China
[2]Key Laboratory of Earthquake Engineering and Engineering Vibration, China Earthquake Administration, Harbin 150080, China

***Corresponding author:*** Junqi Lin, linjunqi2024@126.com



**Abstract:** With the development of modern society, people put forward higher requirements for building safety, which makes the construction project face new challenges. Reinforced concrete frame structure as a common engineering type, although the construction technology has been relatively mature, but its earthquake collapse ability still needs to be strengthened. This paper analyzes the specific factors that affect the seismic collapse ability of reinforced concrete frame structure, summarizes the previous research results, and puts forward innovative application of fiber-reinforced polymer (FRP) composite materials, play the role of smart materials, improve the isolation and energy dissipation devices, etc., to promote the continuous optimization of reinforced concrete frame structure design, and show better seismic performance.

**Keywords:** Reinforced concrete frame structure; Seismic performance; Collapse; Research status

**Online publication:** February 13, 2025

## 1. Introduction

At present, as a common form of building structure, the seismic collapse performance of reinforced concrete frame structure has attracted much attention. It is of great significance to improve the safety of buildings in earthquakes by deeply exploring the factors that affect the collapse resistance of the structure.

## 2. Factors affecting collapse resistance

### 2.1. Structural design parameters

#### 2.1.1. Column-to-beam stiffness ratio analysis

Jizhi *et al.* put forward the design concept of "strong column and weak beam," thinking that the beam-column linear stiffness ratio is the key factor affecting the flexural stiffness of reinforced concrete frame structures with bending moment resistance, and put forward the limit setting values for different seismic grades. When the beam-column linear stiffness ratio is less than the limit setting value, the beam-hinge mechanism can be realized. In the experiment, ⅓ scale models of two 3-hole, 3-story reinforced concrete frame structures are constructed, and a series of nonlinear dynamic analyses are carried out for the numerical models that do not conform to or conform to the linear stiffness ratio limits of beam-columns by low reciprocating load tests. Based on the test results, it can be seen that the column area of the structure with large beam-column linear stiffness is more susceptible to earthquake damage, resulting in increased energy consumption of the structure. Therefore, the factor of beam-column linear stiffness ratio should be considered comprehensively when optimizing the seismic design of reinforced concrete frame structures [1]. By studying the isolation effect of a 15-story reinforced concrete building under the change of beam-column stiffness ratio,

Chun adjusted the vibration period between the superstructure and the isolation layer to adjust the beam-column stiffness ratio. When the isolation period was 2.5 times longer than the natural vibration period of the undisturbed structure, the beam-column stiffness ratio was relatively small, and the damage to the reinforced concrete building structure was reduced by about ⅓. This shows that reducing the stiffness ratio of the beam to column by increasing the safety of the superstructure is beneficial to strengthening the seismic resistance of reinforced concrete frame structures [2].

Chen *et al.* believed that in the seismic response analysis of reinforced concrete frame structures, due to the large stiffness of the beam-column joint area, a certain rigid region needs to be set in the construction process, and the rigid region will directly affect the seismic response ability of the structure. Moreover, different rigid region setting methods are compared based on the fiber finite element method of the flexibility method, to determine a more appropriate stiffness ratio of the beam-column. Effectively guarantee the earthquake resistance of reinforced concrete frame structure and reduce post-earthquake damage [3].

#### 2.1.2. Different beam-column connection types and effects

By analyzing the influence on the seismic performance of reinforced concrete frame structures under the new flexible connection and energy-dissipating connection modes of beam-columns, Holley *et al.* used finite element software to conduct static push nappe analysis and elastoplastic time history analysis and compared the damage mechanism under horizontal earthquake action and seismic performance under dynamic load. Based on the test results, it can be seen that when the rigid beam-column connection is adopted, the bolts at the connection joints are damaged, and the frame beams are seriously damaged. When flexible connections and energy-consuming connections are used, the connection bolts are kept in good condition. In addition, compared with the flexible connection mode, the damage state of the main structure under horizontal earthquake is lighter, and the displacement response of the beam-column energy-dissipating connection mode is reduced by 24.8%, 32.9%, and 36.5% compared with the flexible connection mode [4].

Sun *et al.* used different beam-column connection methods to compare and analyze the whole process of deformation and failure of reinforced concrete frame structures under earthquake action, to analyze the influence of beam-column connection methods on the seismic performance of structures. According to the research results, the relative displacement between the wall panel and the beam-column will occur when the card connection method is given by the atlas, but the L-shaped card can play a certain restraint role. When the beam and column are connected by the existing installation process of the enterprise, the wall panel and the main frame have good integrity from the beginning of the loading, and the loading stage has a great contribution to the lateral stiffness and lateral bearing capacity of the structure, but the wall panel has an out-of-plane deflection in the later stage. This shows that the two kinds of beam-column connection have their advantages and disadvantages, and the beam-column connection should be optimized reasonably [5].

Cheng *et al.* believed that the connection of beam-column joints of prefabricated reinforced concrete structures is very important. By innovatively constructing prefabricated partial steel-reinforced concrete frame structures and setting steel bones in the connection area of components and the core area of beams and columns, the bearing capacity of the frame structures is enhanced, which is three times that of traditional reinforced concrete specimens. Moreover, the degradation of bearing capacity and stiffness is slower, and the seismic performance is superior. It inspires the optimization of beam-column connection mode of reinforced concrete frame structures [6].

#### 2.1.3. Floor system design considerations for seismic resistance

Nguyen believed that in reinforced concrete frame structures, the variation of floor parameters would affect the stiffness of beam-column joints, and thus affect the seismic collapse performance of the frame structures. When the floor stiffness is increased, it is beneficial to increase the restraint ability of the beam, and reduce the deflection of the beam, to avoid the excessive deflection of the beam after the earthquake, resulting in the deformation and damage of the frame structure.

Therefore, in the reinforced concrete frame structure, to improve its seismic resistance, it is necessary to strengthen the rigidity of the floor system, thereby enhancing the bearing capacity and rigidity of the beam, rationally planning the size and scale of the floor, and then ensuring the safety and reliability of the frame structure [7]. Xu found that the buildings with reinforced concrete frame structures were seriously damaged by earthquake damage statistics. After analyzing the failure mechanism, he proposed to further improve the seismic design of the floor system, strengthen the seismic performance of the frame structure through diversified measures and methods, make the building have stronger deformation resistance and stability, and strengthen the building quality of reinforced concrete frame structure [8].

### 2.2. Material properties

#### 2.2.1. Concrete strength, ductility, and high-performance varieties

Wang *et al.* believed that compared with ordinary concrete, reactive powder concrete has higher toughness, strength, and significant application value. By studying the long-term performance and durability of reactive powder concrete, such as impact resistance, fatigue resistance, chloride ion resistance, and other indicators, the latest research results are reviewed and proposed in the design of reinforced concrete frame structures. Reactive powder concrete should be used to replace traditional concrete, thereby strengthening the seismic performance of the structure, resisting the damage caused by earthquakes with high-quality concrete, and promoting the continuous optimization of reinforced concrete frame structures [9].

In addition to reactive powder concrete, the selection of concrete materials with higher performance should consider the section height and steel ratio. The section height and steel ratio have the greatest impact on the damage to steel-reinforced high-strength concrete (SRHSC) beams, and the section size and axial compression ratio have the greatest impact on the damage to SRHSC columns, which lays a foundation for the application of concrete materials in the seismic design of frame structures. Moreover, some studies have shown that based on the concept of "strong column and weak beam," it should be combined with the strength and ductility of concrete to select a more appropriate strength grade of concrete, thus ensuring the seismic performance of the frame structure.

#### 2.2.2. Steel reinforcement characteristics and bond behavior

Zheng *et al.* proposed that steel bar corrosion is formed by the chemical reaction of iron elements on its surface with oxygen and water. Proper corrosion can enhance the surface roughness of steel bars, and then strengthen the mechanical occlusion between concrete and steel bars to form higher bonding properties. However, excessive corrosion will lead to loose corrosion products on the surface of steel bars, resulting in a decline in the bonding strength between steel bars and concrete. In this paper, the bond strength and bond stress-slip constitutive relation of the corroded steel bars are analyzed by analyzing the change of bond property of the corroded steel bar. It is suggested that the research on the bonding properties under the splitting failure mode should be strengthened, and the prediction model of bonding force should be built based on the width of the rust expansion crack, to better control the corrosion strength of steel bars. The bond between reinforcement and concrete can be guaranteed, and the seismic resistance of reinforced concrete frame structures can be improved [10].

Zhou researched the bonding properties of corroded reinforced concrete members and found that the volume of steel bars will increase after corrosion, resulting in splitting effect stress in concrete. This results in a significant decrease in the bond property of steel bars. Therefore, the finite element method was used to conduct simulation calculation, analyze the degradation mechanism of the bond properties of corroded reinforced concrete members, find out the specific influencing factors, and provide inspiration for the design optimization of reinforced concrete frame structures, to strengthen its seismic performance [11].

#### 2.2.3. Long-term material degradation factors and impacts

To investigate the influence of construction joints on the seismic resistance of reinforced concrete frame structures, Wu conducted a nonlinear time-history analysis with the new model. According to the research results, with the extension of the use time of the building, the construction material will degrade, resulting in the continuous expansion of the construction joint, and the construction joint will increase the displacement of the top of the frame structure, resulting in the change of the displacement distribution between the layers, and further aggravate the local response of key components, resulting in the decline of the seismic performance of reinforced concrete frame structures. Therefore, it is necessary to optimize construction materials and processes, minimize the width of construction joints, and reduce the adverse impact on the seismic resistance of reinforced concrete frame structures [12].

According to the linear damage theory, Zhang *et al.* built the damage index calculation model of concrete and reinforced concrete materials, combined with the weighted coefficient, and calculated the damage index of materials, reinforced concrete components, floors, and frame structures more accurately and efficiently, providing an effective basis for targeted optimization of materials and better resistance to earthquake damage. Ensure the high-quality development of reinforced concrete frame structures [13].

## 3. Strengthening and retrofit strategies

### 3.1. Fiber-reinforced polymer (FRP) composites in retrofit

To strengthen the seismic collapse ability of reinforced concrete frame structure, fiber-reinforced polymer (FRP) composite materials should be flexibly used to further strengthen the beam and column joints, strengthen the axial bearing capacity of the frame structure, and better resist earthquake damage.

Firstly, because FRP has good strength and stiffness, it can effectively restrain the lateral deformation of reinforced concrete columns and significantly improve the axial bearing capacity of columns. For example, in the seismic reinforcement project of old teaching buildings, the use of carbon fiber reinforced polymer (CFRP) to strengthen the columns can effectively improve the ultimate bearing capacity of concrete columns and enhance the stability of the overall structure under earthquake action.

Secondly, under the repeated action of earthquakes, FRP-confined concrete columns can produce more plastic hinges, increase the energy dissipation capacity of the structure, avoid brittle failure of the column, and the structure has better deformation and energy dissipation capacity under strong earthquakes.

Thirdly, compared with the traditional strengthening method, FRP material is light in weight, simple in construction, does not require large construction equipment and wet operations, can greatly shorten the construction period, reduce the impact on the use of building functions, strengthen the earthquake collapse capacity of the frame structure at the same time, and increase the economic benefits of the building [14]. Fourthly, the construction personnel should paste FRP strips or adopt FRP stirrup on the side of the beam, to significantly improve the shear-bearing capacity of the beam. For example, in the reinforcement of bridge structure, the stirrup made of aramid fiber reinforced polymer (AFRP) is used to replace part of the traditional steel stirrup, further improve the shear strength of the beam, and effectively improve the failure mode of the beam under the strong shear force caused by the earthquake, to avoid the sudden collapse of the structure due to shear failure.

### 3.2. Smart materials and their potential use in strengthening

In the seismic collapse optimization of reinforced concrete frame structure, the positive role of smart materials should be played to further strengthen the intelligent level of frame structure, and real-time monitoring of structural health status, to ensure the structural performance, improve its seismic resistance, and avoid continuous collapse.

Firstly, the construction personnel should introduce the shape memory alloy (SMA) material, which has a strong self-resetting ability, and apply it to the reinforced concrete frame structure node, which can strengthen the self-resetting ability of the frame structure, so that the connector can restore the initial state after the earthquake, reduce the residual deformation of the structure, and then ensure the recovery of the frame structure after the earthquake.

Secondly, the construction personnel should introduce advanced piezoelectric materials and combine them with intelligent control elements to form an efficient intelligent damper, which automatically adjusts the damping size based on the vibration of the structure to further strengthen the safety of the building.

Then, in the design of reinforced concrete frame structure, the application of magnetorheological fluid (MRF) should be strengthened, the MRF device should be applied in the supporting members, and the stiffness of the support can be automatically adjusted according to the intensity of ground vibration and the response of the structure so that the structure can maintain good seismic performance and improve the collapse resistance of the structure.

### 3.3. Base isolation and energy dissipation devices for existing structures

Designers should improve the internal components of the reinforced concrete frame structure, improve the isolation and energy dissipation devices, further strengthen the seismic ability of the structure, and effectively prevent collapse.

Firstly, in the design of the frame structure, the application of rubber isolation bearings should be improved, the material and process of the isolation bearings should be optimized, the mechanical properties should be maintained, the isolation effect of the structure should be sustained, and reliable, the seismic energy should be consumed and isolated through its deformation, and the direct effect of seismic forces on the superstructure should be reduced [15].

Secondly, the designer should optimize the metal yield energy dissipation device, adopt mild steel dampers, quickly enter the yield state, consume a lot of seismic input energy, and significantly reduce the seismic response of the main structure. Designers should also connect the energy-consuming device with the frame structure, not change the original structure form, and better strengthen the seismic performance of the structure, thereby improving the safety of the building.

## 4. Summary

To sum up, factors such as beam-column stiffness ratio, beam-column connection mode, seismic design of floor system, concrete performance, reinforcement bonding force, and material aging will significantly affect the seismic resistance of reinforced concrete frame structures. Therefore, it is necessary to study these influencing factors in detail, and actively introduce new technologies, new processes, and new materials to promote the continuous optimization of reinforced concrete frame structure.

## Disclosure statement

The author declares no conflict of interest.

## References


[1] Su J, Liu B, Xing G, et al. Influence of Beam-to-Column Linear Stiffness Ratio on Failure Mechanism of Reinforced Concrete Moment-Resisting Frame Structures[J]. Advances in Civil Engineering, 2020, 2020(1): 9216798.

[2] Chun Y, Hur M, 2015, Effects of Isolation Period Difference and Beam-Column Stiffness Ratio on the Dynamic Response of Reinforced Concrete Buildings. International Journal of Concrete Structures and Materials, 9(4): 439–451.

[3] Chen L, Feng Y, 2012, Influence of Stiffness Zone on Seismic Performance of Reinforced Concrete Frame Structures. Industrial Building, 42(09): 75–78.

[4] He L, Chong X, Sha H, et al., 2024, Research on Seismic Performance of Reinforced Concrete Frame Structure of External UHPC Curtain Wall with Different Connection Modes. Earthquake Research, 47(01): 94–104.

[5] Sun J, Li B, Meng C, et al., 2019, Siding with Beam-Column Connection Mode Between the Structure Seismic Performance Influence [J]. Journal of Building Structures, 49(08): 16–21.

[6] Cheng W, Song Y, Wang J, 2015, Experimental Study on Seismic Performance of Joints in Beams and Columns of Prefabricated Partial Steel-Reinforced Concrete Frames. Journal of Dalian University of Technology, 55(02): 171–178.

[7] Nguyen SH, Tran QV, Nguyen HQ, 2019, Influence of Parameters Reinforced Concrete Floor to Stiffness of Beam—Columns Connector in Composite Structures. International Journal of Innovative Technology and Exploring Engineering (IJITEE), 8(10): 3071–3075.

[8] Xu Kaiming, 2012, Seismic Damage Analysis and Research on Seismic Measures of Reinforced Concrete Frame Structure Houses. Science and Technology Vision, 2012(17): 191–193.

[9] Wang K, Lin J, Yang W, et al., 2017, Research Progress on Long-Term Properties and Durability of Reactive Powder Concrete. Concrete, 2017(11): 27–30 + 34.

[10] Zheng S, Yang J, Zheng Y, et al., 2020, Review on Bond Slip Performance of Corroded Reinforced Concrete. Materials Reports, 34(S2): 1221–1226.

[11] Zhou J, 2016, Study on the Degradation of Bonding Properties of Corroded Reinforced Concrete Members. Housing and Real Estate, 2016(36): 290–291.

[12] Yu J, Liu X, Liang X. The influence of construction joint on the seismic behavior of reinforced concrete frame structure[J]. Advances in Structural Engineering, 2017, 20(7): 112 5-1138.

[13] Zhang Y, Chen J, Du X, et al., 2015, Research on Material-Based Damage Model of Multi-Storey Reinforced Concrete Frame Structures. Building Structures, 45(06): 7–13.

[14] Del Rey Castillo E, Griffith M, Ingham J. Seismic behavior of RC columns flexurally strengthened with FRP sheets and FRP anchors[J]. Composite Structures, 2018, 203: 382-395.

[15] Orfeo A, Tubaldi E, Muhr A H, et al. Mechanical behaviour of rubber bearings with low shape factor[J]. Engineering Structures, 2022, 266: 114532.

Journal of Architectural Research and Development, 2025, Volume 9, Issue 1
https://ojs.bbwpublisher.com/index.php/JARD
Online ISSN: 2208-3537
Print ISSN: 2208-3529

# Study of Chilled Water Storage System in Subway Engineering: A Case Study of a Subway Station in Guangzhou

**Cen Li***

China Railway Design Corporation, Southwest Jiaotong University, Tianjin 300142, China

***Corresponding author:** Cen Li, licen1992@yeah.net



**Abstract:** Based on the distribution of cooling load at a subway station and the peak-valley electricity price in Guangzhou, a chilled water storage system is reserved in the ample space above the station's distribution area. This study proposes a design scheme and operational strategy for a chilled water storage system suitable for subway engineering, based on calculating the cooling load and designing a chilled water storage system in a subway station. Additionally, it proposes calculation coefficients of hourly cooling load suitable for subway engineering and convenient for estimation of hourly cooling load. Furthermore, an economic analysis is conducted by combining hourly cooling load with time-of-use electricity prices. This study provides a reference for the design and application of chilled water storage systems in subsequent subway projects.

**Keywords:** Chilled water storage; Subway station; Hourly cooling load; Peak-valley electricity price

**Online publication:** February 13, 2025

## 1. Introduction

The transportation sector has become the dominant user of energy consumption and carbon emissions in China, with the continuous enhancement of urbanization level and the diversification of transportation logistics and travel demands [1]. In 2020, the Chinese government announced at the United Nations Assembly, its commitment to achieving carbon peak by 2030 and carbon neutrality by 2060. Urban rail transit, as a crucial component of urban public transportation, is widely regarded as a significant means to alleviate traffic congestion and achieve energy conservation and emission reduction due to its characteristics of high speed and large capacity. According to statistics, as of 2023, 59 cities in China had opened 338 urban rail transit lines, with a total operating line length of 11,224.54 km. In the same year, the total passenger traffic reached 29.466 billion trips, with a total electricity consumption of 24.977 billion kWh [2]. The ventilation and air conditioning system, as a crucial component of energy consumption and environmental protection, accounts for approximately 25%–35% of the total energy consumption in subways [3], and in humid and hot regions such as Guangzhou, this proportion can even reach 40% [4–6].

The rapid increase in air conditioning load has become the primary cause of seasonal power shortages, leading to a widening peak-valley difference in the power grid and compromising grid safety. Cold storage technology takes advantage of sensible heat, latent heat, or the heat of chemical reaction during the phase change of a working medium to store cold energy [7]. Specifically, during periods of low electricity demand, the cold produced by a chiller unit is stored in a cold storage device, and during periods of high electricity demand, the cold is retrieved from the device to meet the user's needs [8]. On the one hand, it can reduce the peak load on the power grid, achieve the goal of "peak load shifting," [9] and improve the efficiency and stability of the grid. On the other hand, it can leverage the difference in peak and valley electricity prices to generate considerable economic benefits for users [10].

In the 1930s, cold storage technology was first applied in large and medium-sized buildings such as factories and theaters in the United States [11]. China introduced cold storage technology in the 1990s, and currently, over a thousand cold storage projects have been built and put into use [12]. Researchers have extensively explored the theory and practice of cold storage technology [13]. However, failure cases of cold storage applications are not uncommon, especially in special fields such as subway engineering construction.

Currently, the design process and calculation methods for cold storage in subway engineering remain unclear. The calculation of cooling load serves as a crucial basis for the design of the cold storage system. In the early stage of design, the coefficient method is commonly used to estimate the hourly cold load on the design day, to construct the cold storage system, and to obtain approximate parameters. However, there is currently a lack of default coefficients for subway stations [14]. Additionally, the cold storage time in subway stations is shorter than that in general buildings, and equipment rooms require continuous cooling 24 hours a day [15]. The current load calculation methods cannot accurately reflect the actual load distribution characteristics of subway stations, and the typical hourly load cannot fully represent the actual load distribution throughout the year, resulting in significant deviations between calculated results and actual data.

In response to the aforementioned issues, this paper systematically investigates the design methods and calculation procedures suitable for chilled water storage systems in subway stations. By adopting a partial load storage cooling approach, the chiller unit stores cold water while supplying cooling during valley electricity pricing periods, while during peak electricity pricing periods, priority is given to supplying cooling from the cold water storage tank, with any insufficient cooling capacity being supplied by the chiller unit. A monthly load coefficient model and an hourly load coefficient model have been established. A method combining hourly cooling capacity with time-of-use electricity pricing is adopted to calculate the static investment recovery period during the whole air-conditioning season, providing an economic analysis of the chilled water storage scheme for subway stations.

## 2. Methods and case study

### 2.1. Project overview

The project is located in Guangzhou, China. It involves the construction of an underground two-level island platform station. The total length of the station is 423 m, with a standard section width of 23.5 m. The total area of the station is 24,899 m$^2$. The station hall above the track area possesses ample space, which is suitable for the consideration of implementing chilled water storage technology applications.

### 2.2. Conventional water system design scheme

The design cooling load of the station is 1,369 kW, with a large system design cooling load of 768 kW and a small system cooling load of 601 kW. The conventional water system design scheme uses a primary pump variable flow system. The supply/return water temperature for the chilled water system is calculated at 7°C/14°C, while the supply/return water temperature for the cooling water system is calculated at 32°C/37°C.

## 2.3. Water cooling storage system design scheme

Currently, the primary cold storage media used in air conditioning systems include water, ice, and eutectic salts. Compared to the other two cold storage systems, the chilled water storage system boasts a relatively lower initial investment and more lenient requirements for terminal equipment. It can utilize conventional chiller units, offering high operational efficiency. However, its disadvantage lies in the smaller volumetric heat capacity, necessitating a larger footprint for the cold water storage tank [16]. Given the substantial cooling demand of this subway station and the ample space available in the station hall above the track area, it is suitable to adopt a chilled water storage system. In this project, the liquid level in the expansion tank and the cold water storage tank can be designed to exceed the highest point of the chilled water system's water pipes during the cold storage process. Taking into account the need to minimize the impact on the structural load-bearing capacity of the station, heat exchange losses, and economic considerations, the high-position cold water storage tank open-loop direct supply system scheme is selected [17,18].

## 2.4. Water cooling storage system load calculation

The ventilation and air conditioning system in the public area of subway stations (large system) primarily consists of seven components: heat dissipation and moisture dissipation from passenger flow, fresh air load of the ventilation and air conditioning system, heat dissipation from lighting, elevators, ticket machines, and communication equipment, heat dissipation and moisture dissipation from the station maintenance structure, fresh air infiltration load at station entrances and exits, and other loads caused by ventilation in the station tunnels [19]. The ventilation and air conditioning system in subway station equipment and management rooms (small system) is influenced by factors such as equipment heating capacity, fresh air load of the ventilation and air conditioning system, number of staff, heating capacity of lighting equipment, heat dissipation and moisture dissipation from walls [20]. Currently, designers have conducted in-depth research on the design cooling load of subway stations and have formed a relatively mature calculation model.

Given that the design cooling load for the large system is 768 kW, the design cooling load for the personnel management room system is 136 kW, and the design cooling load for the equipment management room system is 465 kW, the air conditioning season spans from March to November. The station operates from 06:00 to 00:00 (midnight).

(1) Step 1: Calculation of design cooling load

$$Q_s = Q_d + Q_x \quad (1)$$

In **Equation (1)**: $Q_s$ = Design cooling load, kW; $Q_d$ = Design cooling load of the large system, kW; $Q_x$ = Design cooling load of the small system, kW. Where $Q_d$ is calculated based on existing design methodologies, taking into account factors such as the civil engineering conditions of the station, indoor and outdoor air calculation parameters, and forecasted long-term peak passenger flow volumes; $Q_x$ is calculated using **Equation (2)**.

$$Q_x = Q_{xr} + Q_{xs} \quad (2)$$

In **Equation (2)**: $Q_x$ = Design cooling load of the small system, kW; $Q_{xr}$ = Design cooling load for personnel management rooms, kW; $Q_{xs}$ = Design cooling load for equipment management rooms, kW. Where $Q_{xr}$ and $Q_{xs}$ are calculated are conducted based on existing design methodologies, taking into account factors such as the environmental requirements of personnel management rooms, the heat dissipation and operational environment requirements of equipment management rooms, and indoor and outdoor air calculation parameters.

In this case, $Q_s = 768 + 136 + 465 = 1{,}369$ kW.

(2) Step 2: Calculation of monthly load factor

$$K_{m(n)} = \frac{Q_{m(n)}}{\max(Q_{m(n)})} \tag{3}$$

In **Equation (3)**: $K_{m(n)}$ = Monthly load factor, where $n$ is the month of the air conditioning season; $Q_{m(n)}$ = Monthly cooling load, kW, where $n$ is the month of the air conditioning season. Where $Q_{m(n)}$ is calculated based on the average temperature and humidity of each month during the air conditioning season, utilizing existing design methodologies. Calculations are conducted based on the station, the results are shown in **Table 1**.

**Table 1.** Monthly load factor estimation table

| Month | 1 | 2 | 3 | 4 | 5 | 6 | 7 | 8 | 9 | 10 | 11 | 12 |
|---|---|---|---|---|---|---|---|---|---|---|---|---|
| $K_{m(n)}$ | 0.26 | 0.33 | 0.44 | 0.63 | 0.82 | 0.94 | 1.00 | 0.99 | 0.89 | 0.69 | 0.48 | 0.31 |

Note: According to data from the Central Meteorological Observatory of China, the monthly average temperature and humidity in Guangzhou over 30 years (1991–2020)

Stations in other regions may refer to or make adjustments based on these data.

(3) Step 3: Calculation of hourly load factor

$$K_{td(t)} = \begin{cases} \frac{Q_{td(t)}}{\max(Q_{td(t)})} & (t_s \le t \le t_e) \\ 0 & (t_e < t < t_s) \end{cases} \tag{4}$$

In **Equation (4)**: $K_{td(t)}$ = Hourly load factor of the large system, where $t$ is the time; $Q_{td(t)}$ = Hourly cooling load of the large system, kW, where $t$ is the time; $t_s$ = Station start operation time; $t_e$ = Station end operation time. Where $Q_{td(t)}$ is calculated based on typical daily passenger flow, outdoor air calculation parameters, and other information according to existing design methodologies. The hourly load factor for the large system is calculated based on the station, the results are shown in **Table 2**.

**Table 2.** Hourly load factor estimation table

| Moment | 0–5 | 6 | 7 | 8 | 9 | 10 | 11 | 12 | 13 | 14 | 15 | 16 | 17 | 18 | 19 | 20 | 21 | 22 | 23 |
|---|---|---|---|---|---|---|---|---|---|---|---|---|---|---|---|---|---|---|---|
| $K_{td(t)}$ | 0 | 0.64 | 0.88 | 0.91 | 0.80 | 0.81 | 0.82 | 0.81 | 0.81 | 0.85 | 0.86 | 0.86 | 1 | 0.96 | 0.78 | 0.76 | 0.76 | 0.72 | 0.62 |

Note: Based on the calculations conducted at a station in Guangzhou, stations in other regions may refer to or make adjustments based on these data

$$K_{txr(t)} = \begin{cases} 1 & (t_s \le t \le t_e) \\ 0 & (t_e < t < t_s) \end{cases} \tag{5}$$

In **Equation (5)**: $K_{txr(t)}$ = Hourly load factor for personnel management room systems, where $t$ is the time; $t_s$ = Station start operation time; $t_e$ = Station end operation time.

$$K_{txs(t)} = 1 \tag{6}$$

In **Equation (6)**: $K_{txs(t)}$ = Hourly load factor for equipment management room systems, where $t$ is the time. For this case, $K_{txr(t)} = \begin{cases} 1 & (6 \le t \le 24) \\ 0 & (0 < t < 6) \end{cases}$; $K_{txs(t)} = 1$.

(4) Step 4: Calculation of hourly cooling load for each month

$$Q_{z(n,t)} = K_f \times K_{m(n)} \times \left(K_{td(t)} \times Q_d + K_{txr(t)} \times Q_{xr} + K_{txs(t)} \times Q_{xs}\right) \tag{7}$$

In **Equation (7)**: $Q_{z(n,t)}$ = Hourly cooling load, kW, where $n$ is the month of the air conditioning season and $t$ is the time; $Q_d$ = Design cooling load of the large system, kW; $Q_{xr}$ = Design cooling load for personnel management rooms, kW; $Q_{xs}$ = Design cooling load for equipment management rooms, kW; $K_f$ = Additional coefficient considering ineffective capacity and cooling losses of the cooling storage device, generally taken as 1.05 to 1.1; $K_{m(n)}$ = Monthly load factor, where $n$ is the month of the air conditioning season; $K_{td(t)}$ = Hourly load factor of the large system, where $t$ is the time; $K_{txr(t)}$ = Hourly load factor for personnel management room systems, where $t$ is the time; $K_{txs(t)}$ = Hourly load factor for equipment management room systems, where $t$ is the time. In this case, taking 08:00 on a certain day in June as an example, $Q_{z(6,8)} = 1.05 \times 0.94 \times (0.91 \times 768 + 1 \times 136 + 1\times465) =$ 1,282.98 kW.

(5) Step 5: Calculation of daily cooling load

$$Q_{d(n)} = \sum_{t=0}^{t=23} Q_{z(n,t)} \tag{8}$$

In **Equation (8)**: $Q_{d(n)}$ = Daily cooling load, kWh, where $n$ is the month of the air conditioning season; $Q_{z(n,t)}$ = Hourly cooling load, kW, where $n$ is the month of the air conditioning season and $t$ is the time. In this case, taking a certain day in June as an example, $Q_{d(6)} = \sum_{t=0}^{t=23} Q_{z(6,t)}$ = 24,536.03 kWh.

(6) Step 6: Calculation of daily cold storage capacity of the chiller units

$$Q_{g(n)} = \sum_{t=t_{g1}}^{t=t_{g2}} (Q_s - Q_{z(n,t)}) \tag{9}$$

In **Equation (9)**: $Q_{g(n)}$ = Daily cold storage capacity of chiller units, kWh, where $n$ is the month of the air conditioning season; $Q_{z(n,t)}$ = Hourly cooling load, kW, where $n$ is the month of the air conditioning season and $t$ is the time; $t_{g1}$ = Start time of the valley electricity pricing; $t_{g2}$ = End time of the valley electricity pricing. In this case, taking a certain day in June as an example, $Q_{g(6)} = \sum_{t=0}^{t=7} (1369 - Q_{z(6,t)})$ = 5,859.71 kWh.

(7) Step 7: Calculation of cooling capacity of the cooling storage tank

$$Q_x = \min\,(Q_{g(n)}) \tag{10}$$

In **Equation (10)**: $Q_x$ = Cooling capacity of the cooling storage tank, kWh; $Q_{g(n)}$ = Daily cold storage capacity of chiller units, kWh, where $n$ is the month of the air conditioning season. In this case, $Q_x = \min(Q_{g(n)}) = Q_{g(7)} =$ 5,534.67 kWh.

(8) Step 8: Calculation of the cool storage rate

$$i = \frac{Q_x}{\max\,(Q_{d(n)})} \tag{11}$$

In **Equation (11)**: $i$ = Cool storage rate; $Q_{d(n)}$ = Daily cooling load, kW, where $n$ is the month of the air conditioning season. In this case, $i = \frac{Q_x}{\max\,(Q_{d(n)})} = \frac{Q_x}{Q_{d(7)}} = \frac{5534.67}{26102.16}$ = 21%.

(9) Step 9: Calculation of effective volume of the cooling storage tank

$$V = \frac{3600 \times Q_x}{\eta \times \rho \times c \times \Delta t} \tag{12}$$

In **Equation (12)**: $V$ = Effective volume of the cooling storage tank, m³; $Q_x$ = Cooling capacity of the cooling storage tank, kWh; $\eta$ = Ratio of actual output to theoretically available energy during the energy storage period, generally taken as 0.85 to 0.90; $\rho$ = Density of water, kg/m³; $c$ = Specific heat capacity of water, kJ/(kg·K); $\Delta t$ = Temperature difference between supply and return water, °C, generally not less than 7°C. In this case, $V = \frac{3600 \times Q_x}{\eta \times \rho \times c \times \Delta t} = \frac{3600 \times 5534.67}{0.85 \times 1000 \times 4.2 \times 7}$ = 797.31 m³.

(10) Step 10: Calculation of hourly cooling capacity of chiller units for each month

The chilled water storage system operation strategy involves storing cold during the valley electricity pricing period, releasing cold during the peak and flat electricity pricing periods, with priority given to releasing cold during the peak electricity pricing period.

(i) Cold storage stage (valley electricity pricing period)

$$Q_{j(n,t)} = \begin{cases} Q_s \ (if Q_x \geq \sum_{t=g1}^{t} (Q_s - Q_{z(n,t)})) \\ \max\{Q_x - \sum_{t=t_{g1}}^{t=t-1} (Q_s - Q_{z(n,t)}), 0\} + Q_{z(n,t)} \ \ (if Q_x < \sum_{t=t_{g1}}^{t} (Q_s - Q_{z(n,t)})) \end{cases} \quad (13)$$

In **Equation (13)**: $Q_{j(n,t)}$ = Hourly cooling capacity of chiller units, kW, where $n$ is the month of the air conditioning season and $t$ is the time, $t_{p1} < t < t_{p2}$ ; $Q_x$ = Cooling capacity of the cooling storage tank, kWh; $Q_s$ = Design cooling load; $Q_{z(n,t)}$ = Hourly cooling load, kW, where $n$ is the month of the air conditioning season and $t$ is the time; $t_{g1}$ = Start time of the valley electricity pricing; $t_{g2}$ = End time of the valley electricity pricing.

(ii) Cold release stage (peak electricity pricing period)

$$Q_{j(n,t)} = \begin{cases} 0 \ (if Q_x \geq \sum_{t=t_{f1}}^{t} Q_{z(n,t)}) \\ Q_{z(n,t)} - \max\{Q_x - \sum_{t=t_{f1}}^{t=t-1} Q_{z(n,t)}, 0\} \ \ (if Q_x < \sum_{t=t_{f1}}^{t} Q_{z(n,t)}) \end{cases} \quad (14)$$

In **Equation (14)**: $Q_{j(n,t)}$ = Hourly cooling capacity of chiller units, kW, where $n$ is the month of the air conditioning season and $t$ is the time, $t_{p1} < t < t_{p2}$ ; $Q_x$ = Cooling capacity of the cooling storage tank, kWh; $Q_{z(n,t)}$ = Hourly cooling load, kW, where $n$ is the month of the air conditioning season and $t$ is the time; $t_{f1}$ = Start time of the peak electricity pricing; $t_{f2}$ = End time of the peak electricity pricing.

(iii) Cold release stage (flat electricity pricing period)

$$Q_{j(n,t)} = \begin{cases} 0 \ (if Q_x \geq \sum_{t=t_{f1}}^{t=t_{f2}} Q_{z(n,t)} + \sum_{t=t_{p1}}^{t} Q_{z(n,t)}) \\ Q_{z(n,t)} - \max\{Q_x - \sum_{t=t_{f1}}^{t=t_{f2}} Q_{z(n,t)} - \sum_{t=t_p}^{t=t-1} Q_{z(n,t)}, 0) \ \ (if Q_x < \sum_{t=t_{f1}}^{t=t_{f2}} Q_{z(n,t)} + \sum_{t=t_{p1}}^{t} Q_{z(n,t)}) \end{cases} \quad (15)$$

In **Equation (15)**: $Q_{j(n,t)}$ = Hourly cooling capacity of chiller units, kW, where $n$ is the month of the air conditioning season and $t$ is the time, $t_{p1} < t < t_{p2}$ ; $Q_x$ = Cooling capacity of the cooling storage tank, kWh; $Q_s$ = Design cooling load; $Q_{z(n,t)}$ = Hourly cooling load, kW, where $n$ is the month of the air conditioning season and $t$ is the time; $t_{f1}$ = Start time of the peak electricity pricing; $t_{f2}$ = End time of the peak electricity pricing; $t_{p1}$ = Start time of the flat electricity pricing; $t_{p2}$ = End time of the flat electricity pricing.

**Table 3.** Time-of-use electricity prices

| Time period | Electricity price (RMB/kWh) |
|---|---|
| Valley electricity price: 00:00–08:00 | 0.28 |
| Peak electricity price: 10:00–12:00; 14:00–19:00 | 1.17 |
| Flat electricity price: 08:00–10:00; 12:00–14:00; 19:00–00:00 | 0.70 |

In this case, it has been found that similar projects in Guangzhou which are proposed to implement a time-of-use electricity pricing system in the future by investigation, time-of-use electricity prices are shown in **Table 3**.

(i) Cold storage stage (valley electricity pricing period)

Taking 07:00 on a certain day in June as an example, $Q_{j(6,7)} = max\{5534.67\text{-}\sum_{t=t_0}^{t=6}(1369\text{-}Q_{z(6,t)}),0\}+Q_{z(6,7)}$ 1,260.24 kWh.

(ii) Cold release stage (peak electricity pricing period)

Taking 10:00 on a certain day in June as an example, $Q_{j(6,10)} = 0$ kWh.

(iii) Cold release stage (flat electricity pricing period)

Taking 13:00 on a certain day in June as an example, $Q_{j(6,13)} = Q_{z(6,13)} - max\,(5513.2 - \sum_{t=10}^{t=11} Q_{z(6,t)} - \sum_{t=14}^{t=18} Q_{z(6,t)} - \sum_{t=12}^{t=12} Q_{z(n,t)}, 0) = 1{,}207.18$ kWh

The effect of the chilled water system for each month can be ascertained by calculation. The effect of the chilled water system for June is shown in **Figure 1**.


**Figure 1.** The effect of the chilled water system in June

(11) Step 11: Calculation of static payback time

$$C_s = \sum_{n=1}^{n=12} \{ \sum_{t=0}^{t=23} ( \frac{Q_{z(n,t)}}{K_f \times COP} \times C_{(t)}) \times N_{(n)} \} \tag{16}$$

In **Equation (16)**: $C_s$ = Annual electricity cost of the conventional design scheme, RMB; $Q_{z(n,t)}$ = Hourly cooling load, kW, where $n$ is the month of the air conditioning season and $t$ is the time; $K_f$ = Additional coefficient considering ineffective capacity and cooling losses of the cooling storage device, generally taken as 1.05 to 1.1; $COP$ = Coefficient of performance of the chiller unit; $C_{(t)}$ = Time-of-use electricity price, RMB; $N_{(n)}$ = Number of days in the air conditioning season month, where $n$ is the month of the air conditioning season. In this case, $C_s = \sum_{n=1}^{n=12} \{ \sum_{t=0}^{t=23} ( \frac{Q_{z(n,t)}}{1.05 \times 5} \times C_{(t)}) \times N_{(n)} \}$ = 818,600 RMB.

$$C_x = \sum_{n=1}^{n=12} \{ \sum_{t=0}^{t=23} ( \frac{Q_{j(n,t)}}{COP} \times C_{(t)}) \times N_{(n)} \} \tag{17}$$

In **Equation (17)**: $C_s$ = Annual electricity cost of the chilled water storage scheme, RMB; $Q_{j(n,t)}$ = Hourly cooling capacity of chiller units, kW, where $n$ is the month of the air conditioning season and $t$ is the time; $COP$ = Coefficient of performance of the chiller unit; $C_{(t)}$- Time-of-use electricity price, RMB; $N_{(n)}$ = Number of days in the air conditioning season month, where $n$ is the month of the air conditioning season. In this case, $C_x = \sum_{n=1}^{n=12} \{ \sum_{t=0}^{t=23} ( \frac{Q_{j(n,t)}}{5} \times C_{(t)}) \times N_{(n)} \}$ = 596,400 RMB.

$$A = \frac{C_c}{C_s - C_x} \tag{18}$$

In **Equation (18)**: $A$ = Static investment payback period, years; $C_c$ = Initial investment in the chilled water storage system, RMB; $C_s$ = Annual electricity cost of the conventional design scheme, RMB; $C_x$ = Annual electricity cost of the chilled water storage scheme, RMB. In this case, the initial investment for this scale of chilled water storage system is estimated to be 1,500,000 RMB by investigation. $A = \frac{150}{81.86 - 59.64}$ = 6.75 years.

## 3. Conclusion

This study presents the design methods and calculation steps for a chilled water storage system applicable to subway stations comprehensively and systematically for the first time, based on a subway station in Guangzhou. The monthly and hourly load coefficient models have been established by adopting a partial load storage cooling approach. Furthermore, the estimation tables for monthly and hourly load coefficients suitable for subway engineering have been proposed based on actual project cases, filling the gap in hourly load coefficients for subway station-type buildings and making the estimation of hourly loads in subway stations more convenient and accurate. The calculations determined the required volume of the cooling storage tank for this project is 797.31 $m^3$, the cooling storage rate of this project is about 21%, and the effect of the chilled water system for each month has been analyzed. The static payback time is calculated by combining hourly cooling capacity with time-of-use electricity pricing throughout the entire air conditioning cycle, making economic analysis of the chilled water storage system more accurate. The calculation shows that the static payback time of the chilled water storage system in this project is approximately 6 years.

## Funding

This work is supported by the Science and Technology Development Project of China Railway Design Corporation (Project No. 2024CJ0401).

## Disclosure statement

The author declares no conflict of interest.

## References

[1] Lulu Z, Qiong T, 2023, Research on the Effectiveness of Urban Low-Carbon Transportation under the Construction of Dual-Carbon Goals Based on the Perspective of Fuzzy Evaluation. Journal of Highway and Transportation Research and Development (English Edition), 17(3).

[2] China Urban Rail Transit Association, 2024, Annual Statistical and Analysis Report of Urban Rail Transit in 2023. China Urban Rail Transit Association, 2024(3): 1, 46.

[3] Zhu J, Sun Z,2015, New Perspectives on Subway Ventilation and Air Conditioning Systems. HVAC, 45(7): 1–5, 27.

[4] Zhang J, Tan Z, Tan M, et al., 2020, Investigation and Analysis of the Current Operation Status and Energy Consumption of Subway Ventilation and Air Conditioning Systems. Installation, 2020(4): 52–55.

[5] Su Z, Li X, 2021, Research on the Principle Model and Simplification of Sub item Energy Consumption in Subway Stations. HVAC, 51(09): 18–23.

[6] Cao H, 2022, Research on Energy Consumption Prediction and Energy saving Measures of Subway Ventilation and Air Conditioning System. Enterprise Technology and Development, 2022(11): 128–130.

[7] Zhang X, 2006, Air Conditioning Cold and Heat Storage Technology. Dalian Maritime University Press, Dalian.

[8] Jia Y, 2018, Analysis of Water Storage Cooling Systems Based on Actual Measurements and Research on Water Storage Tanks, thesis, Xi'an University of Engineering.

[9] Li Y, 2014, Benefit Analysis of Water Storage Cooling in Peak Shaving and Valley Filling. Demand Side Management of Electric Power, 16(02): 30–33.

[10] China Academy of Building Research, 2012, Code Description of Civil Building Heating, Ventilation, and Air Conditioning Design Standard GB50736-2012. China Building Industry Press, 2012: 172–175.

[11] Jan V, Michael B, 2012, Cost Optional Analysis and Load Shifting Potentials of Cold Storage Equipment. Energy and Buildings, 49: 226–234.

[12] Sun ZY, 2015, Energy & TES situation in China. China, Japan and Korea TES Workshop and Expert Meeting, Korea.
[13] Xu W, Sun Z, Li J, et al, 2016, Investigation and Analysis of Cold Storage Engineering Applications in China. HVAC, 46(7): 75–80.
[14] China Academy of Architectural Design and Research Co. Ltd., 2022, Unified Technical Measures for HVAC Design of Civil Buildings 2022. China Architecture&Building Press, Beijing.
[15] Zhu M, Chen L, 2023, Application of Water Storage Cooling Technology in Energy Conservation of Subway Stations. Energy Conservation, 42(05): 58–60.
[16] Parson R, 2008, ASHRAE Handbook. S50 SI-Thermal Storage. Atlanta (USA): ASHRAE Inc., 2008: 50.4.
[17] Ren J, Wu X, 2013, Design and Construction Debugging Analysis of Open Water Storage Air Conditioning System. HVAC, 43(10): 83–85.
[18] Chen L, 2016, A Preliminary Discussion on Open and Closed Systems. Building Thermal Energy Ventilation and Air Conditioning, 35(01): 60–63.
[19] Wu W, Peng J, Liu Y, et al., 2010, Discussion on Air Conditioning Design for Public Areas of Subway Platform Screen Doors. Refrigeration and Air Conditioning, 10(6): 94–101.
[20] Zhu P, Ding D, Xu L, 2008, Dynamic Simulation and Analysis of Air Conditioning Loads in Subway Small Systems. HVAC, 38(11): 21–24.

Journal of Architectural Research and Development, 2025, Volume 9, Issue 1
https://ojs.bbwpublisher.com/index.php/JARD
Online ISSN: 2208-3537
Print ISSN: 2208-3529

# Study on the Correlation Between the Preservation Status of Mountain Ancient Buildings, Wind Environment, and Protection Methods — A Case Study of the Rock Temples on Wudang Mountain

**Jin Xu, Chen Gaonan Wang, Yansong Wang***

School of Urban Design, Wuhan University, Wuhan 430072, China

***Corresponding author:** Yansong Wang, yzwys201@163.com



**Abstract:** The preservation condition of historical buildings is closely related to their ventilation environment. This study focuses on the rock temples in Wudang Mountain, specifically comparing the ventilation conditions of Yinxian Rock and Huayang Rock. The following conclusions are drawn: (1) The main wind direction at Yinxian Rock aligns with its orientation, which is an easterly wind, while Huayang Rock experiences a westerly wind, deviating from its southwestern entrance; (2) Huayang Rock has significantly lower wind speeds compared to Yinxian Rock, with minimal airflow; (3) The surrounding environment of Huayang Rock features steep terrain, dense tree cover, and the presence of railings and other structures that impede wind entry into the cave, whereas Yinxian Rock is surrounded by fewer trees and has a flat terrain; (4) In terms of cave morphology, Yinxian Rock is completely open on the east side, while Huayang Rock's opening accounts for only half of its area and is not directly aligned with the rock temple. In summary, Huayang Rock's ventilation environment is inferior to that of Yinxian Rock, leading to more severe pathologies. It is inferred that Huayang Rock's preservation issues are closely related to its poor ventilation environment. Therefore, improving its ventilation conditions is crucial for preventive conservation. Using environmental simulation, this study compares the ventilation conditions of Huayang Rock under different wind directions and speeds, identifies the two most ideal scenarios, and proposes several feasible solutions.

**Keywords:** Wudang Mountain rock temple; Architectural issues; Natural ventilation; Preventive conservation

**Online publication:** February 12, 2025

## 1. Introduction

Wudang Mountain, a famous Taoist holy site in China, is located in Danjiangkou City, Hubei Province. The mountain is home to a large number of brick and stone buildings, representing the most traditional and concentrated brick and stone surface building groups in China. Currently, there are more than twenty rock temples with their main structures still preserved, most of which face challenges in access and maintenance for protection and management. Continuous environmental impacts have had a negative effect on them, causing various degrees of damage that are becoming more severe. Due to the scarcity of relevant literature on Wudang Mountain's rock temples and the inadequacy of analysis on their brick and stone buildings, there is a lack of specific interpretation of the causes of their architectural issues and research on protective measures [1]. This has led to a delay in timely protection and accelerated the severity of their architectural issues. Currently, domestic researchers such as Wang Zi have explored the mechanism of "water" on the architectural issues of Wudang Mountain's brick and stone buildings, and Wang Chengnan *et al.* have further analyzed that the main cause of the peeling phenomenon in Wudang Mountain's rock temples is the water-rock interaction [2,3]. However, other environmental factors affecting the architectural issues have not been fully explored, and there is almost no research on the correlation between the architectural issues of Wudang Mountain's rock temples and the wind environment. Regarding natural ventilation of stone cultural relics, Wang Jiangli *et al.* have explored the airflow movement patterns and ventilation control methods in Mogao Caves through a series of natural ventilation tests and Zhou Baofa *et al.* have also analyzed the influencing factors and control measures of natural ventilation in Maijishan Grottoes [4–8]. However, due to the unique characteristics and environmental conditions of Wudang Mountain, its natural ventilation differs from these cases.

Yinxian Rock and Huayang Rock are two rock temples on Wudang Mountain that have high research and protection value. Yinxian Rock is located north of the Five Dragon Palace, in Lujiazhai Village, under Yinxian Peak. Many accomplished Taoist practitioners, such as the famous alchemists Yin Xi and Yin Gui, once lived and practiced here in secrecy, giving Yinxian Rock its long-standing reputation. The rock cave faces east, and there are five brick and stone halls inside, forming a "pin" shaped layout centered around the main hall, as shown in **Figure 1**. Huayang Rock, also one of the thirty-six rocks of Wudang Mountain, is located more than 200 m away from the Five Dragon Palace, facing southwest opposite to Yunmu Rock. Surrounded by trees, there is only one stone hall inside the rock, as shown in **Figure 2**. According to records, the construction of the stone halls in both rock temples dates back to the Ming Dynasty [9]. Under the same climatic conditions, the altitude of the two rocks is also similar, with Yinxian Rock at 604.5 m and Huayang Rock at 647.8 m. Both use a mixture of brick and stone as building materials, and their architectural features and construction techniques are basically the same [10]. However, there is a significant difference in their degree of damage.

**Figure 1.** Yinxian Rock

**Figure 2.** Huayang Rock

The preservation status of cultural relic buildings is closely related to the micro-environmental conditions in which they are located [11]. For stone cultural relics in damp areas, the ventilation environment is an important indicator that affects the surface deterioration [12]. As the wind speed increases, the heat exchange on the building surface also increases, with the convective heat exchange on the windward side being greater than that on the leeward side, leading to an increase in the surface temperature of the building and stronger evaporation of water from the bricks and stones [13]. A good ventilation environment can remove moisture from the building surface, reducing some architectural issues caused by water.

In the Wudang Mountain area, where the east wind is the predominant wind direction, Yinxian Rock and Huayang Rock face almost opposite directions, so their wind exposure conditions will also be different. To further explore the relationship between the ventilation environment of the two rocks and the difference in the degree of architectural issues they suffer, this paper compares the ventilation conditions of Yinxian Rock and Huayang Rock in terms of wind direction, wind speed outside the cave, the surrounding environment of the building, and the shape of the cave. The analysis reveals that the ventilation environment of Huayang Rock is relatively poor compared to Yinxian Rock. Through real-time environmental monitoring and data analysis of the wind direction and speed in front of the two caves, it is found that the main wind direction at Yinxian Rock is easterly, while at Huayang Rock it is westerly, and the monitored wind speed at Huayang Rock is much lower than that at Yinxian Rock.

Theoretical analysis of the cave shape and surrounding environment shows that the terrain around Yinxian Rock is flat with few trees, while the opposite is true for Huayang Rock. The east side of Yinxian Rock is completely open, favoring wind exposure, while the opening area of Huayang Rock is only about half of its facing side. To find an ideal ventilation effect for Huayang Rock and improve its current ventilation status, this paper roughly simulates the ventilation situation of Huayang Rock under different wind directions and speeds through environmental simulation. It is found that the better ventilation effect for Huayang Rock occurs with a south or southwest wind, with wind speeds of around 5 m/s and 10 m/s, respectively. Based on this, several implementable operations are proposed, providing a scientific basis and theoretical foundation for the preventive protection of Huayang Rock in the future.

## 2. Comparison of architectural issue conditions and ventilation environments between Yinxian Rock and Huayang Rock

Comparing the architectural issue conditions of Yinxian Rock and Huayang Rock, significant differences in the degree of architectural issue were observed at the same height of approximately 90 cm on the Xumizuo (a type of stone pedestal in traditional Chinese architecture). The west side of the Xumizuo in Huayang Rock Temple showed large areas of powdery peeling, while the east side exhibited considerable erosion and defects. The south side had a relatively minor degree of architectural issue, but there were still some signs of powdery peeling and erosion [14]. On the other hand, when examining the main hall's altar table and the northeast and southwest side halls of Yinxian Rock, and comparing the same Xumizuo areas, it was found that there was almost no peeling, only a small amount of weathering erosion [10]. From this, it can be roughly inferred that the degree of architectural issue suffered by Yinxian Rock is less severe than that of Huayang Rock.

(a) (b)

(i) (ii) (iii)

**Figure 3.** Photographs of architectural issues on the two rocks (a) Yinxian Rock (b) Huayang Rock

The surface integrity damage suffered by the Xumizuo of Huayang Rock can be roughly divided into six types: defects, powdery peeling, layered peeling, massive peeling, erosion, and hole-like weathering, as shown in **Figure 3(b)**. Among them, peeling is the most significant architectural issue that causes the greatest degree of damage to the rock temple. Its mechanism is mainly due to water-rock interaction, which primarily involves the hydration and expansion of clay minerals and the dissolution of soluble minerals in the rock temple's stone material [3]. The widespread presence of moisture accelerates the formation of peeling architectural issues in the rock temple, and the wind environment is one of the important factors that affect the amount of water residue on the building surface.

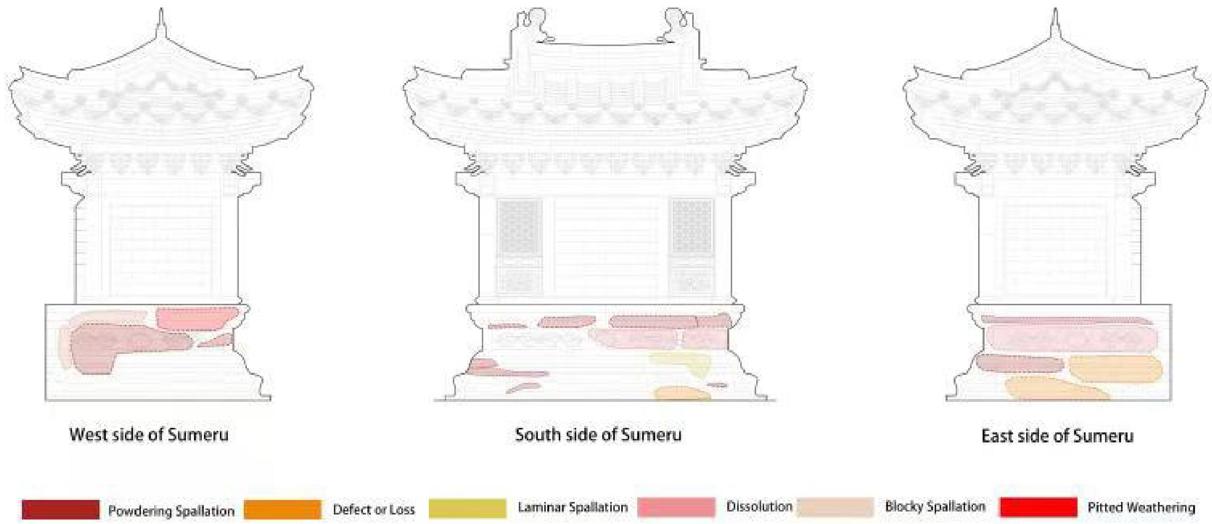


**Figure 4.** Cloud map of main architectural issues on the Xumizuo of Huayang Rock

To explore the correlation between the differences in architectural issues of the two rocks and their ventilation environments, it is necessary to understand the external ventilation conditions of the buildings and the reasons that affect their ventilation. It is known that natural ventilation is divided into three modes: wind pressure ventilation, thermal pressure ventilation, and combined wind and thermal pressure ventilation [15]. Wind pressure ventilation is related to the indoor and outdoor wind speeds. When the internal wind speed is constant, the greater the outdoor wind speed, the larger the wind pressure difference formed, and the better the ventilation effect. Thermal pressure ventilation is caused by air flow due to differences in air density resulting from temperature differences between indoor and outdoor air and height differences between inlet and outlet. To increase thermal pressure ventilation, while utilizing the temperature difference between indoor and outdoor air, it is necessary to create upper and lower openings to allow airflow to enter from the bottom and exit from the top.

The ventilation situation of rock temples can be analogized to the principle of architectural ventilation, treating the caves as buildings with a single-side opening. The wind exposure outside the rock temple buildings can be considered as the ventilation conditions inside the caves, and the outdoor wind speed can be regarded as the wind speed inside the caves [16]. Since there is no height difference between the inlet and outlet of the single-side opening of the rock temples, the natural ventilation mode of the two rock temples is basically wind pressure ventilation. The factors that affect wind pressure ventilation include external factors such as wind speed outside the cave and the surrounding environment, as well as internal factors such as the opening of the cave and its own shape. For rock temple buildings, the temperature changes inside the caves can be ignored, so it is only necessary to investigate the wind speed changes outside the caves. The following sections will compare the ventilation environments of Yinxian Rock and Huayang Rock in terms of wind direction and speed outside the caves, the surrounding environment of the caves, and the openings and shapes of the caves.

## 2.1. Wind direction and speed

Wind speed and direction are two fundamental characteristics of natural wind and the main factors influencing the ventilation environment. To measure the environmental data of the two rocks, we used outdoor weather station monitors to observe the changes in the surrounding environment of the two rocks and record data in real time. The models are shown in **Table 1** below. The test indicators include air temperature and humidity, gas concentration, illumination, ultraviolet (UV) intensity, as well as wind force, speed, and direction. Sampling was done at 10-minute intervals to capture instantaneous values. This article will focus on three indicators: wind force, speed, and direction.

**Table 1.** Monitor models and measurement ranges

| Measurement variable | Instrument brand & model | Instrument accuracy | Sampling interval (min) |
|---|---|---|---|
| Wind direction | JianDaRenKe Weather Station &RS-QXZ | ± 45° | 10 |
| Wind speed | JianDaRenKe Weather Station &RS-QXZ | ± 0.1 m/s | 10 |
| Wind force | JianDaRenKe Weather Station &RS-QXZ | Level 1 | 10 |

Instruments were placed on the sides of the air intakes of two rock temples to detect their overall environmental conditions, as shown in **Figure 5(a)** and **Figure 5(b)**. Data collected over four months from November 2022 to February 2023 were analyzed. Due to signal issues, some data were missing. Therefore, days with complete data for both temples were selected as the sample size for this analysis, ensuring at least ten days of data per month. This data volume is sufficient and representative, allowing for the derivation of general patterns. The following analysis is based on this dataset.

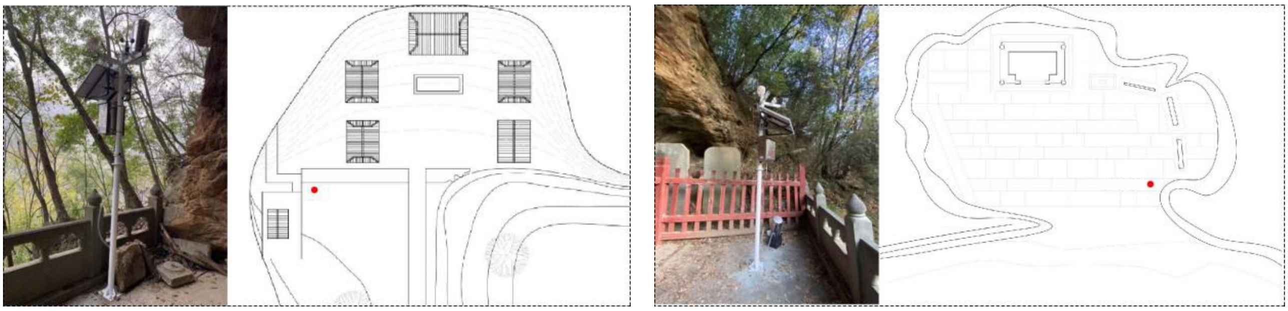

(a) (b)

**Figure 5.** Locations of meteorological stations at (a) Yinxian Rock and (b) Huayang Rock

As a reference, this paper selects meteorological station data from Mount Wudang over the same four-month period, with indicators including dd (wind direction at 10–12 m above ground level within 10 min before observation, compass bearing), ff (average wind speed at 10–12 m above ground level within 10 min before observation, m/s), and ff3 (maximum gust wind speed at 10–12 m above ground level between two observations, m/s). These indicators were monitored every three hours, daily. The collected data were then compared with the monthly average and maximum wind speeds, overall wind force distribution, and wind direction distribution at Yinxian Rock and Huayang Rock.

As shown in **Figure 6(a)** and **Figure 6(b)**, the average and maximum wind speeds at both rock temples are significantly lower than those at the local area, with Yinxian Rock having noticeably higher wind speeds than Huayang Rock. The four-month overall average wind speed at Yinxian Rock is approximately 0.17 m/s, while that at Huayang Rock is about 0.01 m/s, and Mount Wudang records around 1.8 m/s. It is worth noting that Huayang Rock experienced an almost windless environment in November, with average monthly wind speeds remaining stable between 0.01 and 0.02 m/s over the four months. Both rocks showed a monthly increasing trend in wind speed from November to February. The monthly average maximum wind speed at Mount Wudang stabilized at around 5.25 m/s, whereas Yinxian Rock demonstrated a clear upward trend, ranging from 1.9 m/s to 3.6 m/s. In contrast, Huayang Rock recorded only 0.1 m/s in November, stabilizing at approximately 1.5 m/s for the following three months.

**Figure 7** illustrates the wind force distribution at Mount Wudang and the two rocks. The wind force range at Mount Wudang spans from 0 to 5, with grades 1, 2, and 3 predominating and distributed relatively evenly, accounting for about 93%. Grades 0, 4, and 5 are less frequent. The wind force range at Yinxian Rock and Huayang Rock is limited to grades 0 to 3 (based on the "Wind Force Grade" national standard released in June 2012 in China, which divides wind force into 13 grades, with 0 being the minimum and 12 being the maximum). Yinxian Rock mostly experiences grades 0 and 1 winds, with few occurrences of grade 2 and only one day reaching grade 3. Huayang Rock, on the other hand, frequently encounters grade 0 winds, with limited days of grades 1 and 2 winds.

**Figure 8** depicts the wind direction frequency. According to the figure, the prevailing winds at Mount Wudang are primarily eastern winds, with northeast and southeast winds being the most frequent. There are also some northwest and southwest winds, and among the cardinal directions, the east wind is the most prevalent, while other directions are less common, with the west wind significantly less frequent than the east. Yinxian Rock also exhibits a dominant east wind, followed by northeast and southeast winds, with a certain amount of north wind and fewer occurrences of other directions. In contrast, the main wind direction at Huayang Rock is west, with the west wind being the most frequent, followed by northwest and southwest winds, and all other directions are rare.

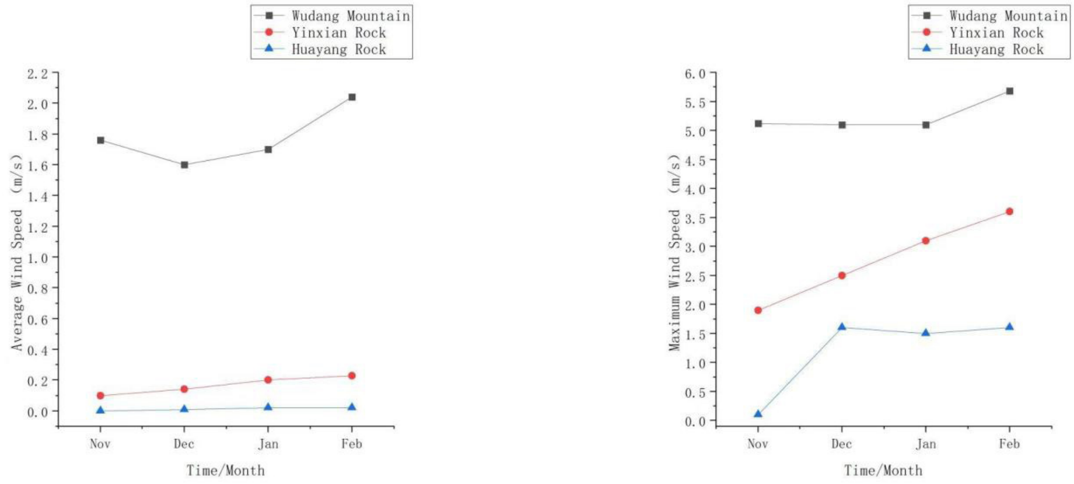


(a) (b)

**Figure 6.** Comparison of wind speeds at Yinxian Rock, Huayang Rock, and Mount Wudang, (a) Average wind speed and (b) Maximum wind speed

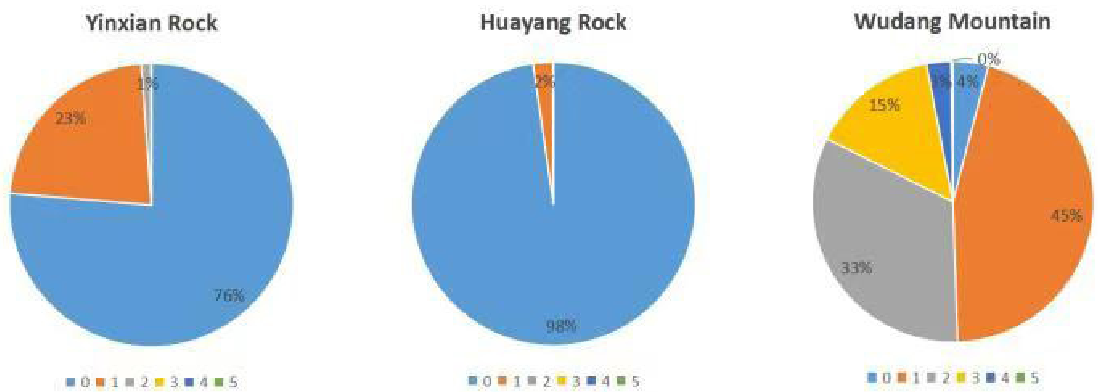


**Figure 7.** Statistical comparison of wind force at Yinxian Rock, Huayang Rock, and local area of Mount Wudang

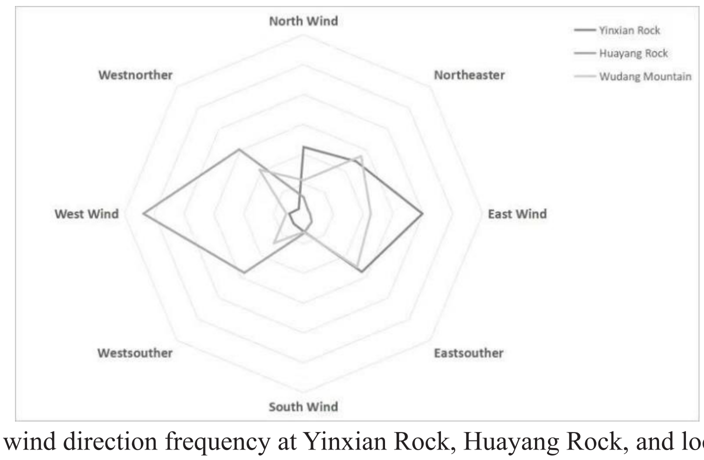


**Figure 8.** Comparison of wind direction frequency at Yinxian Rock, Huayang Rock, and local area of Mount Wudang

Based on the comparison charts above, it is evident that there are significant differences in the wind environments of Yinxian Rock and Huayang Rock. Both the average and maximum wind speeds at Huayang Rock are much lower than those at Yinxian Rock. The dominant wind directions also differ between the two rocks, with Yinxian Rock's primary wind direction aligning with the local prevailing wind, while Huayang

Rock exhibits the opposite trend. Simultaneously, the micro-environmental climates of Yinxian Rock and Huayang Rock deviate considerably from the local climate of Mount Wudang. This divergence is reflected in the much lower wind speeds at the entrances of the two rocks compared to the average wind speed in the local area of Mount Wudang, and the more uniform distribution of wind force.

## 2.2. Surrounding environment and cave formation

Factors contributing to the ventilation differences between the two rocks also include the surrounding environment, cave formation, and orientation of openings. Yinxian Rock is situated in a flat area with minimal obstruction from trees, and its ceiling is raised, allowing wind from various directions to flow into the cave. Additionally, Yinxian Rock's dimensions, including a height of 11.05 m, a width of 23.7 m, and a depth of 12.8 m, result in a total volume of approximately 1,676 $m^3$ (roughly half of a cube), making it a relatively large cave. The temple inside the cave maintains a certain distance from the cave walls, facilitating the formation of positive and negative pressure differences, as illustrated in **Figure 9(a)**.

On the other hand, Huayang Rock is located on a slanted hillside surrounded by trees, with its entrance partially blocked by trees overhead. The addition of stone and wooden railings at the entrance also serves to block some external wind. Huayang Rock's dimensions, consisting of a height of 3.5 m, a width of 7.4 m, and a depth of 5.1 m, yield a total volume of approximately 132 $m^3$ (resembling a cube), indicating a smaller cavity, as shown in **Figure 9(b)**. Moreover, the back of the temple structure is tightly pressed against the cave wall, making it difficult for wind to pass through the narrow space and establish a stable airflow circulation. This aspect significantly impacts the ventilation conditions within Huayang Rock.

(a)

(b)

**Figure 9.** Overviews of the two rock temples (a) Yinxian Rock (b) Huayang Rock

The orientation of the cave openings and the prevailing wind direction together influence the magnitude of the wind direction projection angle. The wind direction projection angle is the angle between the wind direction projection line and the normal line of the building wall. For these two temples, the wall direction corresponds to the direction perpendicular to the opening. It is known that the ventilation volume is related to the wind direction projection angle. A smaller wind direction projection angle results in a larger ventilation volume through the opening. As the wind direction projection angle increases, the wind speed inside the cave decreases, which is not conducive to ventilation [17]. The orientation of Yinxian Rock's cave faces east (91° clockwise from the true north), aligning with its prevailing wind direction. Therefore, theoretically, most of the wind can blow directly into the temple's opening, with a wind direction projection angle close to zero, achieving maximum ventilation, as shown in **Figure 10(a)**. This allows the wind to form a complete circulation path inside the cave.

On the other hand, the orientation of Huayang Rock's cave is roughly southwest (212° clockwise from the true north), which deviates from its prevailing west wind, resulting in a reduced ventilation volume due to the wind direction projection angle, as illustrated in **Figure 10(b)**. When the west wind blows into the cave, it is difficult for the wind to flow into the areas on both sides of the temple, creating two windless zones.

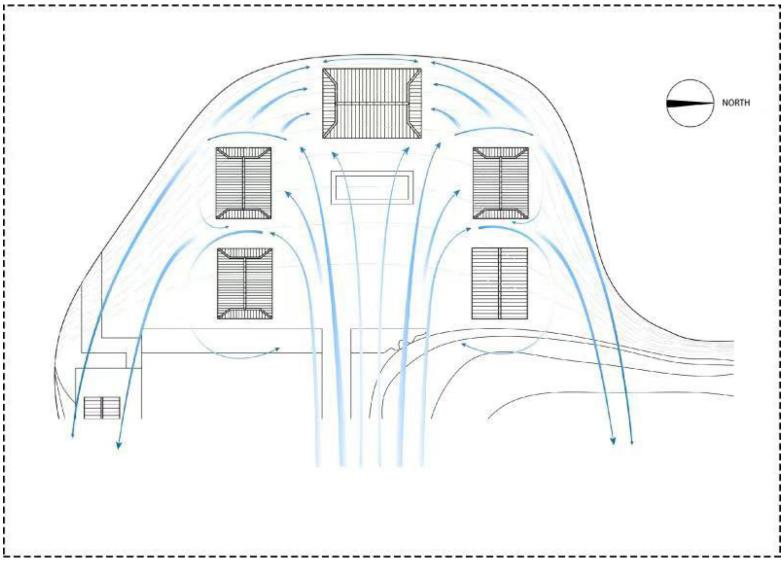


(a)

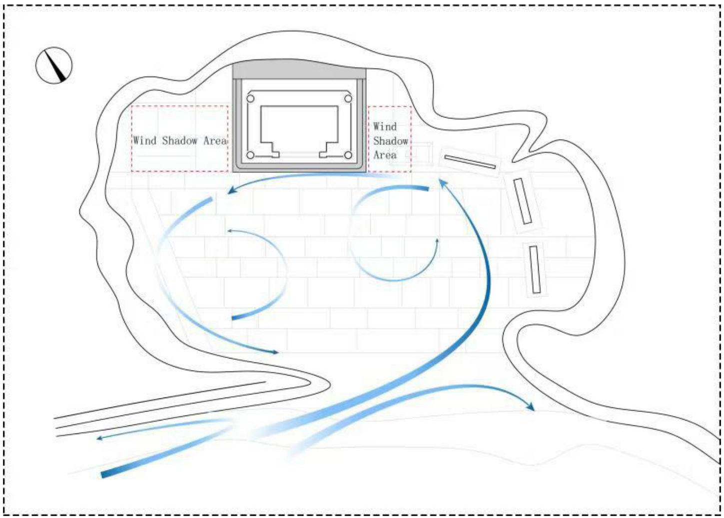


(b)

**Figure 10.** Schematic diagram of wind circulation inside (a) Yinxian Rock and (b) Huayang Rock

In summary, after comparing factors affecting the ventilation environment, such as wind direction and speed, surrounding environment, and cave opening formation, between the two temples, it can be concluded that Huayang Rock's ventilation environment has many disadvantages compared to Yinxian Rock in various aspects. To improve its poor ventilation environment and slow down the damage rate of the temple, the following section will adopt numerical simulation of the wind environment to simulate the ventilation conditions of Huayang Rock when subjected to winds from different directions and magnitudes. By varying the wind direction and speed, we aim to find an ideal ventilation effect, providing methodological support for future preventive protection plans.

## 3. Numerical simulation of wind environment in Huayang Rock

Wind speed provides a direct indication of the ventilation status within an environment. Additionally, a larger wind pressure difference suggests better wind pressure ventilation within the temple [17]. The wind vector diagram illustrates the amount of ventilation and the internal movement path of the wind. These three indicators can collectively assess the general ventilation conditions of the temple's microenvironment within the cave. The simulation software used in this paper is PHOENICS, which can simulate the instantaneous values of wind speed, direction, and pressure at various points on a plane for buildings and environments, presenting clear and intuitive graphical results. Considering local environmental data, these instantaneous values represent the average of hourly calculation results. For the PHOENICS settings, the template is selected as FLAIR, the energy equation focuses on temperature, the turbulence model is Chen-Kim KE, and the profile type is Power Law. Wind speed and direction are set according to simulation requirements, while the temperature parameter is set to 20°C without considering the influence of solar radiation. The environmental wind speed settings are based on local meteorological data from November 1, 2022, to February 28, 2023.

### 3.1. Ventilation conditions of Huayang Rock under different wind directions

Since the general orientation of Huayang Rock is southwest, there are four types of winds that can flow into the cave entrance: northwest wind, west wind, southwest wind, and south wind. The remaining directions are similar to the temple's orientation and have a minimal impact, so they are not considered. When testing different wind directions, the wind speed is set to 2 m/s, which is more in line with the site environment [17]. **Figure 11** shows that the wind pressure generated when the wind direction is southwest is the highest, with approximately 1.51 Pa at the entrance, and the pressure difference with the rock wall is also the largest among the four wind directions. Therefore, its wind pressure ventilation conditions are the best, which aligns with theoretical expectations. The west wind follows, and the northwest wind has the smallest pressure difference, almost zero, indicating the poorest wind pressure ventilation conditions.

Regarding wind speed, it is evident that the south wind environment produces the highest wind speeds. The highest wind speeds within the temple are located at the entrance and the southwest corner of the building, where the building's preservation status is also the best. The wind speeds for the other three wind directions are relatively low, consistent with actual measurements. Surprisingly, the wind speed around the rock wall in a southwest wind environment directly facing the temple opening is the lowest, contradicting theoretical expectations. Since Huayang Rock experiences less south wind in actual measurements, but the wind speed blown into Huayang Rock under the south wind is the highest among the four wind directions, increasing south wind could be considered.

The wind direction vector diagram reveals that the northwest wind does not blow into the cave. The cave's formation in Huayang Rock alters the wind direction, preventing it from flowing into the cave. More winds from the southwest and south directions flow into the cave, with the southwest wind being the most prominent. Based on wind pressure difference, wind speed, and ventilation volume, it can be generally inferred that under the same wind speed, the temple experiences the best ventilation effects from the south and southwest winds.

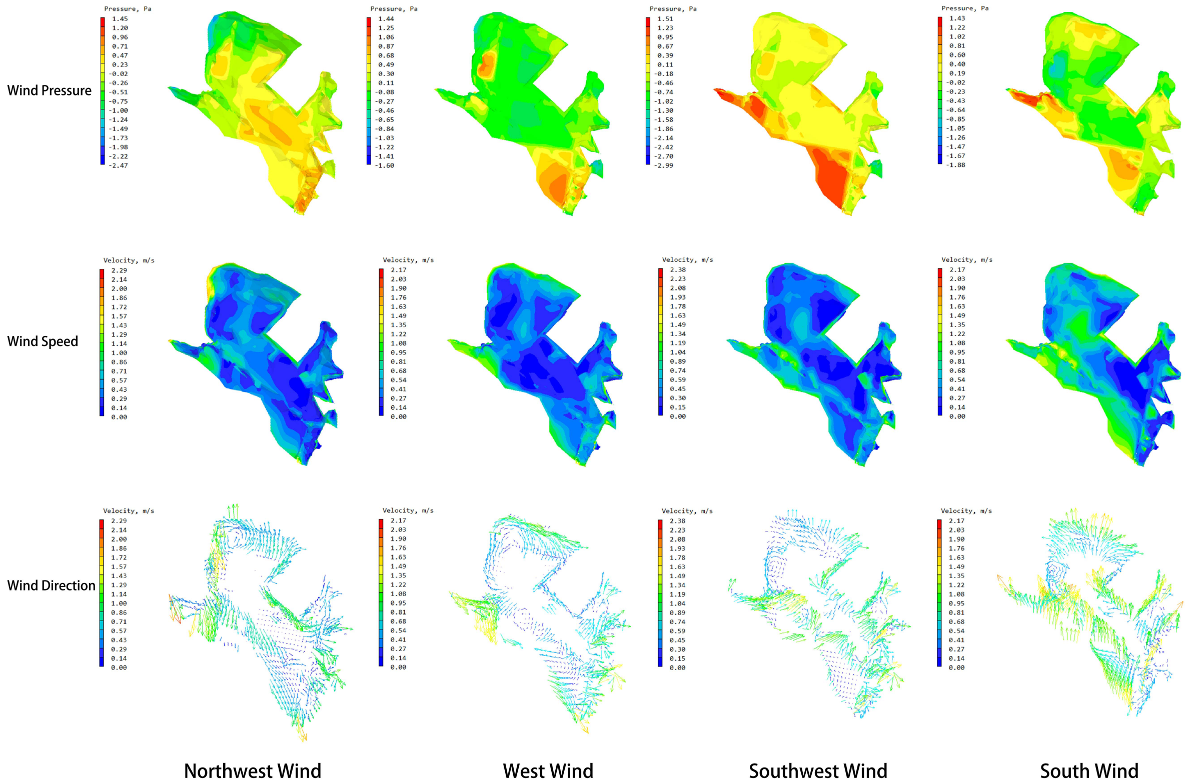


**Figure 11.** Comparison of different wind directions at 2 m/s wind speed

## 3.2. Ventilation conditions at different wind speeds under south and southwest winds

Wind speed is not necessarily better when it is higher. Although wind can reduce moisture on building surfaces, excessively strong winds can also increase the probability of weathering, so an appropriate wind speed is crucial to achieve the best effect. Based on the above conclusions, this study selected south and southwest winds to simulate the ventilation effects of Huayang Rock under these wind directions at different wind speeds. The wind speeds were set to 2 m/s, 5 m/s, and 10 m/s, representing the range from a breeze to a light breeze and then to a moderate breeze. The simulation results of internal wind pressure, wind speed, and wind vector diagrams were compared to determine which range of wind speeds could achieve better ventilation effects.

The figures show that when Huayang Rock is subjected to south winds of different strengths, the distribution of wind pressure and wind speed inside the cave does not undergo significant changes as the wind speed increases, except for numerical increases. The wind vector diagram reveals a vortex wind area in front of the rock temple and the cave entrance at a wind speed of 5 m/s, which disappears when the wind speed increases to 10 m/s. Overall, among the three scenarios, the ventilation conditions are best at a wind speed of 5 m/s, with an average internal wind speed of 2–3 m/s, which is an ideal situation.

Similarly, the simulation results for southwest winds at 2 m/s, 5 m/s, and 10 m/s are shown in the figures. It can be seen that the distribution of wind pressure at a wind speed of 5 m/s is different from the other two conditions. The wind pressure difference between the front of the cave and the front of the rock temple decreases, and the increase in wind pressure at the front of the rock temple becomes larger, without forming a positive and negative pressure difference. At 10 m/s, the wind pressure in this area changes from positive to negative, and the area close to the rock wall becomes positively pressurized, with wind blowing from the rock wall to the cave entrance. A large difference in wind pressure is formed between the cave entrance and the front of the rock temple, with the red area ranging from 32 Pa to 38 Pa and the green area ranging from -11 Pa to -5 Pa. The wind pressure ventilation is greatly improved in the area front of the south facade of the rock temple, and the wind pressure on both sides of the rock temple also becomes negative, with wind blowing from the rock wall to both sides of the rock temple.

In terms of wind speed, it can be observed that as the wind speed increases, the wind speed inside the cave does not increase significantly as it does under south wind conditions. When the wind speed reaches 5 m/s, the average wind speed inside the cave remains around 0–2 m/s, which is not ideal. When the wind speed increases to 10 m/s, except for a significant increase in wind speed in the southwest corner of the building, the wind speed on the three sides of the rock temple building actually decreases.

From the wind vector diagrams under the three conditions, it can be seen that when the wind speed is also 5 m/s, a small area of wind vortex forms in front of the rock temple, and there is a significant rebound of wind speed. When the wind speed reaches 10 m/s, similar to the south wind situation, more wind blows into the cave, but the vortex area in front of the cave disappears, and a new vortex forms in the southeast corner of the cave entrance. Overall, the ventilation effect is best when the wind speed is 10 m/s under southwest winds, which corresponds to a moderate breeze.

The above analysis indicates that Huayang Rock has better ventilation effects when subjected to southwest and south winds. Under south wind conditions, when the wind speed is 5 m/s, a more pronounced circulating wind can form in front of the rock temple. The best ventilation effect is achieved when the southwest wind speed is 10 m/s, creating a wind pressure ventilation effect where wind flows from positive to negative pressure on all three sides of the rock temple.

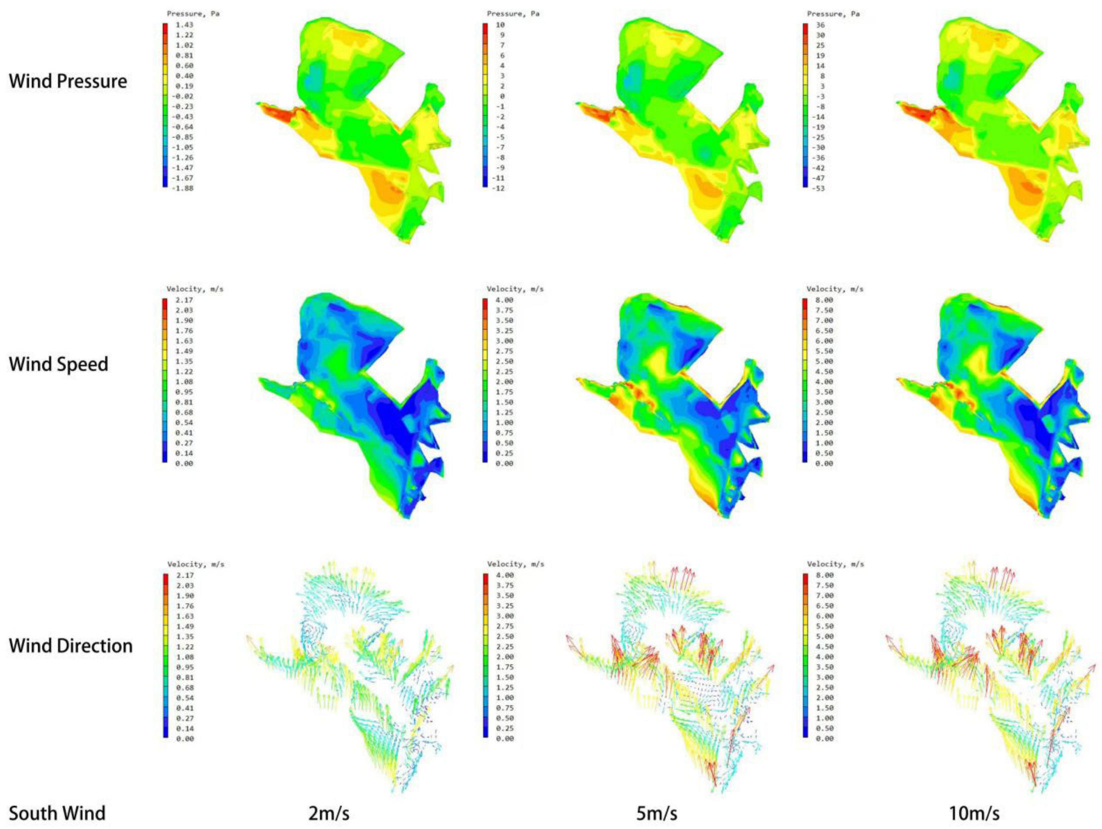


**Figure 12.** Comparison of different wind speeds under south wind direction

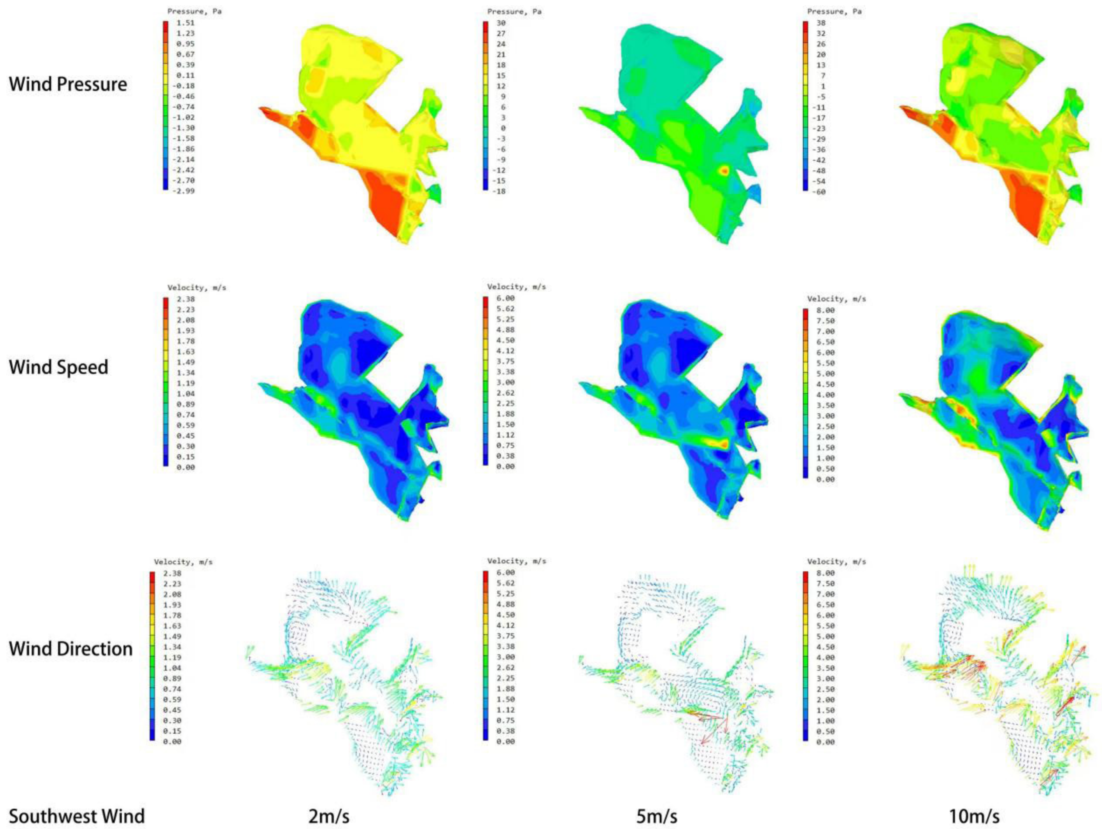


**Figure 13.** Comparison of different wind speeds under southwest wind direction

# 4. Concept of preventive protection plan

After simulating the wind environment of Huayang Rock under different wind directions and speeds and identifying several favorable scenarios, we hope to achieve similar effects through implementable solutions, providing a generally feasible direction for the preventive protection of Huayang Rock in the future. Preventive protection methods for cultural relic buildings are mainly divided into active and passive measures. For Huayang Rock, which has a poor ventilation environment, active measures for wind pressure ventilation mainly include active air supply and extraction, such as using mechanical equipment like blowers to increase the wind speed within the building's microenvironment.

Passive regulation refers to methods that can achieve physical environmental control without the intervention of mechanical equipment. Compared to active regulation, this approach is less likely to cause secondary damage to cultural relics, so it can be prioritized for intervening and regulating the environment of Huayang Rock. One method is to appropriately remove environmental obstacles that block Huayang Rock, such as surrounding trees and stone railings, to reduce wind resistance. Another approach is to place windshields in front of the cave to alter the wind direction. Based on simulation results, the ambient wind can be largely converted into south and southwest winds to increase ventilation. This method is currently one of the most feasible options. Since the wind speed at the entrance of Huayang Rock is already low, merely changing the wind direction may not yield significant results. It is necessary to increase the overall wind speed before altering the direction to achieve more uniform wind distribution and optimal effects. Additionally, there is a more challenging method that involves greater intervention in the current environmental state, which is to seal the cave entrance, increase the temperature difference between the indoor and outdoor environments, or directly remove moisture from inside the cave to enhance the thermal pressure ventilation of Huayang Rock.

Considering the various aspects of Huayang Rock's wind environment that are unfavorable to the cave itself, it is necessary to intervene and regulate factors such as wind speed, wind direction, and environmental obstacles. A combination of active and passive measures, with active measures as the primary approach and passive measures as a complement, can achieve the best results through a multi-mode integrated approach.

## 5. Conclusion

This paper starts from observing the phenomenon of different architectural issue severities in two rock temples on Wudang Mountain: Yinxian Rock and Huayang Rock. It explores the correlation between the causes of the architectural issues and their environmental conditions. After comparing and monitoring the wind environments of the two rock temples, it concludes that the wind speed at Yinxian Rock is much higher than that at Huayang Rock, and its orientation aligns with the prevailing wind direction, which is eastward. On the other hand, Huayang Rock faces southwest, deviating from the prevailing westerly wind. By analyzing their surrounding environments and cave formations, it is determined that Huayang Rock has a poorer ventilation environment compared to Yinxian Rock.

To improve the inadequate ventilation at Huayang Rock, microenvironment wind pressure, wind speed, and wind vector diagrams were simulated under different wind directions and speeds. Several scenarios with better ventilation effects were identified, specifically when the wind speed is 5 m/s from the south and 10 m/s from the southwest. Based on these findings, several general directions for preventive protection are proposed.

This paper primarily considers wind environmental factors in analyzing the causes of architectural issues in the two rock temples, while neglecting other potential influencing factors such as humidity and carbon dioxide concentration. Additionally, the simulation conditions are relatively idealized and may not fully reflect the actual situation. Future research will incorporate more possible environmental factors and introduce more realistic variables into the environmental simulation, aiming to closely approximate the real environmental conditions and enhance the accuracy and feasibility of the simulation results.

## Funding

Supported by the National Natural Science Foundation of China (Grant No. 52278042) for the research on "Architectural issue mechanisms and defense of architectural heritage under harsh environments - Taking the rock temples of Wudang Mountain as an example."

## Disclosure statement

The authors declare no conflict of interest.

## References

[1] Huang K, 2018, Thoughts on Several Issues of Stone Cultural Relics Protection. Chinese Cultural Heritage, 04: 4–12.

[2] Wang Z, 2020, Analysis of the Architectural issue Mechanism and Potential Hazards of "Water" on the Brick and Stone Architectural Heritage of Wudang Mountain, thesis, Huazhong University of Science and Technology.

[3] Wang C, Chen M, Wang Y, 2023, Surface Flaking Mechanism of Stone Components of Ancient Building Complex in Wudang Mountain, China. Construction and Building Materials, 399: 132611.

[4] Wang J, Yan Z, Wang X, et al., 2015, Experimental Study on Natural Ventilation of Caves in Mogao Grottoes, Dunhuang. Journal of Xi'an University of Architecture and Technology (Natural Science Edition), 47(05): 712–716.

[5] Wang J, Yan Z, Wang X, et al., 2015, Research on Natural Ventilation Test of Mogao Grottoes. Dunhuang Research, 04: 121–126.

[6] Wang J, Yan Z, 2020, Research on the Mechanism of Air Exchange Inside and Outside the Caves of Mogao Grottoes in Dunhuang. Building Science, 36(02): 140–147.

[7] Wang J, 2016, Research on Ventilation Regulation and Control Technology of Mogao Grottoes in Dunhuang, thesis, Xi'an University of Architecture and Technology.

[8] Zhou B, 2021, Analysis and Research on Natural Ventilation Characteristics of Maijishan Grottoes, thesis, Xi'an University of Architecture and Technology.

[9] Zhu J, 2005, Collection of Hubei Architecture: World Cultural Heritage—Ancient Building Complex of Wudang Mountain. China Architecture & Building Press, Beijing.

[10] Liu Z, 2020, Research on the Architectural Features and Genesis Analysis of the Brick and Stone Hall of Yinxian Rock in Wudang Mountain, thesis, Huazhong University of Science and Technology.

[11] Song S, Wang D, Tian M, et al., 2022, Research on the Influence of Atmospheric Environment on the Architectural issue Mechanism of Stone Cultural Relics Sites. Journal of North China University of Science and Technology (Natural Science Edition), 2022, 44(03): 86–93.

[12] Liu J, 2019, Research on the Architectural issues of Brick Cultural Relic Buildings in the Southeast Coastal Area, thesis, Harbin Institute of Technology.

[13] Wan L, 2018, Research on the Mechanism of Cracking Architectural issues in Cultural Relic Buildings Under Dry and Wet Climate Environments, thesis, Huazhong University of Science and Technology.

[14] Wang J, Chen J, Wang L, et al., 2022, Research on the Architectural issues and Types of Grotto Temples in China. Southeast Culture, 04: 25–32.

[15] Zhang K, 2016, Research on Wind Environment Design of Green Industrial Buildings, thesis, Suzhou University of Science and Technology.

[16] Ye C, 2018, Analysis of Effective Ventilation in Single-Sided Naturally Ventilated Buildings Driven by Wind Pressure, thesis, Wuhan University of Technology.

[17] Hao M, Xu D, 2019, Discussion on Passive Natural Ventilation Design Methods for Green Buildings. Ju She, 28: 118.

[18] Meng Y, 2022, Research on Physical Environment Control Technology of Longmen Grottoes Based on Weathering Mechanism of Cultural Relics, thesis, Xi'an University of Architecture and Technology.

[19] Li Y, 2003, Technologies of Inducing, Guiding, and Creating Winds in Natural Ventilation of Buildings. Architectural Knowledge, 04: 17–20.

**Publisher's note**

Bio-Byword Scientific Publishing remains neutral with regard to jurisdictional claims in published maps and institutional affiliations.

# Innoscience research

## Integrated Services Platform of International Scientific Cooperation

Innoscience Research (Malaysia), which is global market oriented, was founded in 2016.Innoscience Research focuses on services based on scientific research. By cooperating with universities and scientific institutes all over the world, it performs medical researches to benefit human beings and promotes the interdisciplinary and international exchanges among researchers.

Innoscience Research covers biology, chemistry, physics and many other disciplines. It mainly focuses on the improvement of human health. It aims to promote the cooperation, exploration and exchange among researchers from different countries. By establishing platforms, Innoscience integrates the demands from different fields to realize the combination of clinical research and basic research and to accelerate and deepen the international scientific cooperation.

### Cooperation Mode

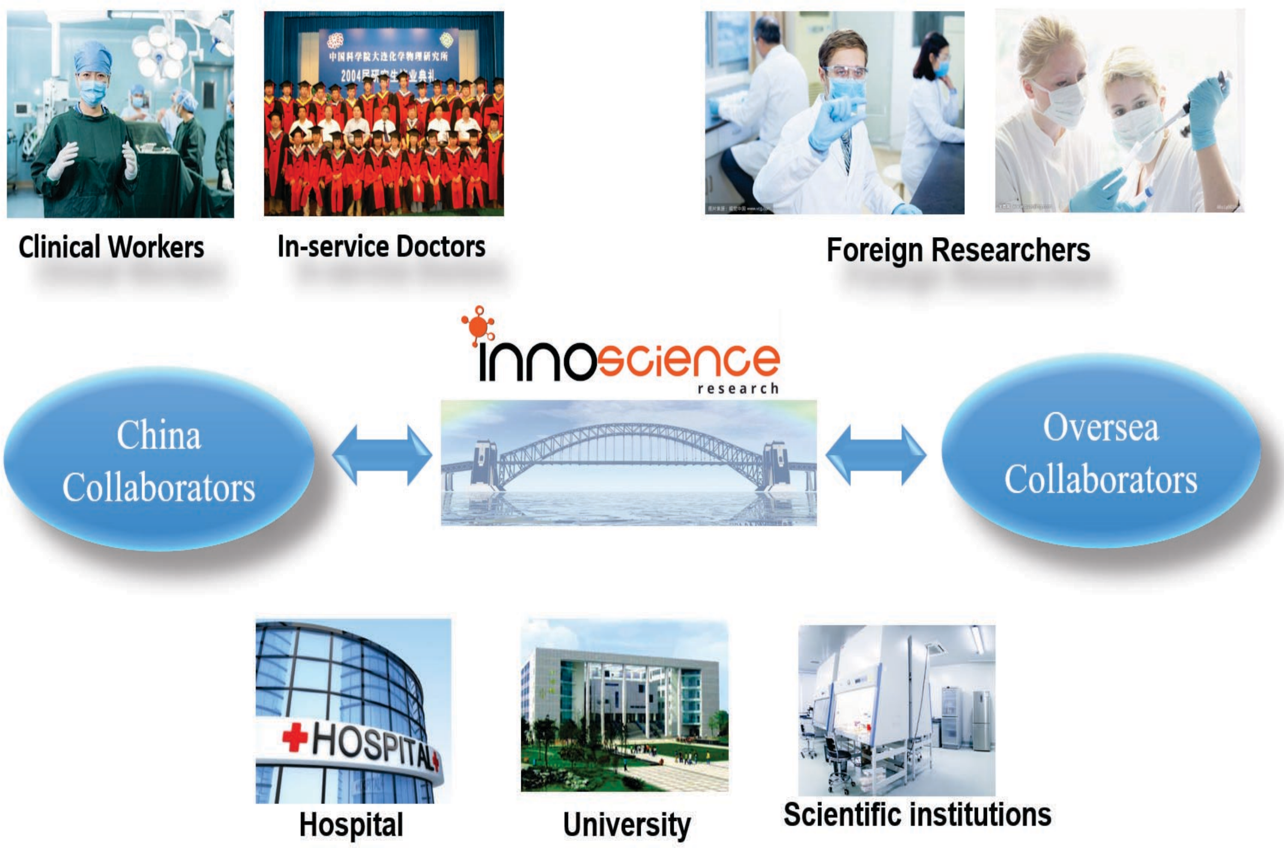

# OUR JOURNALS


The *Journal of Architectural Research and Development* is an international peer-reviewed and open access journal which is devoted to establish a bridge between theory and practice in the fields of architectural and design research, urban planning and built environment research.

Topics covered but not limited to:

- Architectural design
- Architectural technology, including new technologies and energy saving technologies
- Architectural practice
- Urban planning
- Impacts of architecture on environment

*Journal of Clinical and Nursing Research (JCNR)* is an international, peer reviewed and open access journal that seeks to promote the development and exchange of knowledge which is directly relevant to all clinical and nursing research and practice. Articles which explore the meaning, prevention, treatment, outcome and impact of a high standard clinical and nursing practice and discipline are encouraged to be submitted as original article, review, case report, short communication and letters.

Topics covered by not limited to:

- Development of clinical and nursing research, evaluation, evidence-based practice and scientific enquiry
- Patients and family experiences of health care
- Clinical and nursing research to enhance patient safety and reduce harm to patients
- Ethics
- Clinical and Nursing history
- Medicine

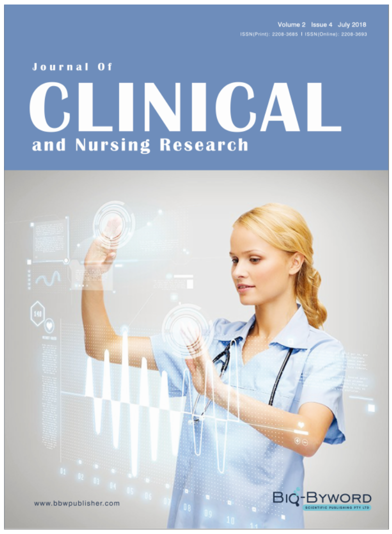



*Journal of Electronic Research and Application* is an international, peer-reviewed and open access journal which publishes original articles, reviews, short communications, case studies and letters in the field of electronic research and application.

Topics covered but not limited to:

- Automation
- Circuit Analysis and Application
- Electric and Electronic Measurement Systems
- Electrical Engineering
- Electronic Materials
- Electronics and Communications Engineering
- Power Systems and Power Electronics
- Signal Processing
- Telecommunications Engineering
- Wireless and Mobile Communication